THE MECHANISM OF ACTION OF A NEW CLASS OF NUCLEOSIDE ANALOGUES TARGETING GASTROINTESTINAL TUMOURS

Laura Collins

A thesis submitted to the Faculty of Graduate and Postdoctoral Studies in partial fulfillment of the requirements for the degree of

MASTER OF SCIENCE

In Biochemistry with Specialization in Human and Molecular Genetics

Faculty of Medicine

University of Ottawa

Ottawa, Canada

Abstract

Gastrointestinal malignancies such as liver and pancreatic cancers are the deadliest due to late detection and drug resistance. Nucleoside analogues, like Gemcitabine, are the conventional therapy despite their little impact on survival and off-target toxicity. A novel class of nucleoside analogues able to evade drug resistance mechanisms has been developed by the Guindon group and biologically screened in our lab. Some of these proprietary molecules were further equipped with a lipoate moiety designed to target cancer cell metabolism. LCB2151 and LCB2179 have emerged as the lead molecules in this class, with an IC_{50} of 10-15 μM in the Gemcitabine-resistant human pancreatic (Capan-2 & Panc-1) cancer cell lines. The focus of this project is deciphering the cellular mechanisms activated by LCB2151 in these pancreatic cancer lines. A series of biased molecular approaches, like gene expression profiling, and unbiased large throughput proteomic and metabolomics analyses were applied to identify potential targets and affected pathways. Results collectively show that LCB2151 evades drug resistance mechanisms, increases pro-apoptotic markers and impairs mitochondrial respiration as early as 6 hours posttreatment. Furthermore, MS/MS analyses reveal that LCB2151 alters the levels of several metabolites in the central carbon metabolism pathway and identifies the citric acid cycle enzyme α-ketoglutarate dehydrogenase as a potential molecular target of LCB2151. Understanding the exact mechanism of action of our lead molecule along with extensive testing on murine cancer models, will surely pave its way to clinical testing and evaluation.

Acknowledgements

Firstly, I would like to thank Dr. Mona Nemer for accepting me into her lab. She is a source of inspiration both personally and professionally. I am forever grateful for the past seven years of working with her team that have shaped the rest of my life.

My sincere appreciation to the Guindon Lab, who has designed and synthesized the fascinating drugs that I have the privilege to test. My special thanks to Dr. Yvan Guindon for all his guidance throughout this project.

I am grateful to Ariana Rostami and Claudia Teran who together have created the biochemical foundation of my research project. To Claudia Teran specifically, for teaching me the techniques to move forward.

I am deeply thankful to Dr. Wael Maharsy for his invaluable guidance, mentorship, and for correcting my thesis. He had a positive outlook no matter the situation and always encouraged me to reach for my academic goals.

I would also like to thank the entire Nemer Lab Family, past and present. From the day I walked in the lab as an undergrad, they have always made me feel welcome and at home. My gratitude goes to Dr. Hiba Komati, Dr. Wael Maharsy, Dr. Georges Kanaan, Janie Beauregard, Dr. Lara Gharibeh, Jamie Whitcomb, Massy Sh-Hassani, Mathieu Joyal, Alice Lau and Megan Fortier. I wish them all a lifetime of health and happiness.

Heartfelt thanks go to my parents, brother and Caesar. They understand that this means more than a thesis to me and none of it would be possible without their unconditional love and support.

Table of Contents

List of Figures

List of Tables

Abbreviations

^{18}F-FDG	2-[^{18}f]Fluoro-2-Deoxy-D-Glucose	LA	Lipoic Acid
5-fU	5-Fluorouracil	MAPK	Mitogen-Activated Protein Kinase
ABC	ATP-Binding Cassette	MRM	Multiple-Reaction Monitoring
ADP	Adenosine Di-Phosphate	MRNA	Messenger RNA
AMPK	Adenosine Monophosphate-Activated Kinase	MRP1/2	Multidrug Resistance-Associated Protein 1/2
ATP	Adenosine Tri-Phosphate	MS	Mass Spectrometry
CDA	Cytidine Deaminase	NA	Nucleoside Analogue
cDNA	Complementary DNA	NAD	Adenine Dinucleotide
Co-A	Coenzyme A	NADPH	Nicotinamide Adenine Dinucleotide Phosphate
COXIV	Cytochrome C Oxidase	NBMPR	Nitrobenzylthioinosine
CPI-613	6, 8-Bis(Benzylthio)Octanoic Acid	NOD-SCID	Nonobese Diabetic/Severe Combined Immunodeficiency
DCA	Dichloroacetate	OCR	Oxygen Cnosumption Rate
dCK	Deoxy-Cytidine Kinase	OGDH	2-Oxoglutarate Dehydrogenase, E1
dCTP	Deoxycytidine Triphosphate	oxphos	Oxidative Phosphorylation
DEPC	Diethyl Pyrocarbonate	PAL	Photoaffinity Labelling
dFdC	2′-Deoxy-2′,2′-Difluorocytidine (Gemcitabine)	PanIN	Pancreatic Intraepithelial Neoplasia
DLD	Dihydrolipoamide Dehydrogenase, E3	PAP	Photoaffinity Probe
DLST	Dihydrolipoamide Succinyl Transferase, E2	PC	Pancreatic Cancer
DMEM	Dulbecco's Modified Eagle's Medium	PDAC	Pancreatic Ductal Adenocarcinoma
DNA	Deoxy-Nucleic Acid	PDH	Pyruvate Dehydrogenase Complex
DNTP	Deoxy-Nucleotide Tri-Phosphate	PDK	Pyruvate Dehydrogenase Kinase
ECAR	Extracellular Acidification Rate	PEG	Polyethinol Glycol
EDTA	Ethylenediaminetetraacetic Acid	PET	Positron Emission Tomography
EGTA	Egtazic Acid	PFK-1	Phosphophructokinase-1
ETC	Electron Transport Chain	PFK-2, PFKFB3	Phosphofructokinase-2
F1,6BP	Fructose 1,6-Bisphosphate	PPP	Pentose Phosphate Pathway
F2,6BP	Fructose-2,6-Bisphosphate	QPCR	Quatitative Polymerase Chain Reaction
F6P	Fructose-6-Phosphate	RIPA	Radioimmunoprecipitation Assay
FDA	Food and Drug Administraion (USA)	RNA	Ribonucleic Acid
Gem	Gemcitabine	ROS	Reactive Oxygen Species
GI	Gastrointestinal	RR	Ribonucleotide Reductase
GSH	Glutathione	RT-PCR	Reverse Transcription-Polymerase Chain Reaction
GSSG	Glutathione Disulfide	SDS	Sodium Dodecyl Sulfate
HCC	Hepatocellular Caricnoma	SOD	Superoxide Dismutase
hENT1	Human Equilibrative Nucleoside Transporter	TCA	Tricarboxylic Acid
HuR	Hu Antigen R	UPLC	Ultrahigh-Performance Liquid Chromatography
IPMN	Intraductal Papillary Mucinous Neoplasm	Wnt	Wingless/Integrated
KGDH	Alpha-Ketoglutarate Dehydrogenase Complex	3PO	3-(3-pyridinyl)-1-(4-pyridinyl)-2-propen-1-one

1. Introduction

1.1. Gastrointestinal Cancer

Cancer remains a serious health challenge in societies worldwide. Gastrointestinal (GI) tumours are one of the major causes of morbidity and mortality. Almost 30% of cancer incidence and 32% of cancer deaths worldwide are due to GI malignancies, both of which rise exponentially with age (Mislang et al., 2018). These tumours can originate anywhere in the GI tract from the esophagus to the rectum (Szucs and Jones, 2018). Of the GI cancers, carcinomas of the pancreas and liver are more likely diagnosed at later stages and have some of the lowest 5-year net survival estimates of 8% and 19% in Canada, respectively (Canadian Cancer Statistics 2018).

1.1.1. Hepatocellular Carcinoma

Hepatocellular carcinoma (HCC) is the deadliest of liver cancers. It is the fifth most common cancer in men, the ninth most common in women worldwide, and the second leading cause of cancer-related deaths (Torre et al., 2015). HCC has one of the highest mortality rates: high incidence ratios accompanied by the lowest 5-year overall survival rate among all cancers (Kamangar et al., 2006). The pathogenesis of HCC involves a complex interplay between genetic and environmental perturbations (Lee et al., 2017a). HCC incidence is largely correlated with rates of hepatitis B and C infections. Important causative factors include alcoholic and non-alcoholic steatohepatitis, associated with the development of chronic inflammation and cirrhosis (Kikuchi et al., 2014). Frequently altered oncogenic pathways in HCC are the canonical wingless/integrated (Wnt) signaling and cell cycle pathways. At the genetic level, *CTNNB1* and *TP53* mutations are present in 25-30% of HCCs (Zucman-Rossi et al., 2015).

Generally, GI cancer patients present in advanced stages when effective therapeutic options are limited (Jindal, 2018). HCC is more lethal and difficult to treat due to the scarring and inflammation associated with chronic liver disease (Lee et al., 2017a). As for most localized GI cancers, resection of the tumour is the preferred curative therapy. However, this is rarely an option due to the extent of the disease and liver dysfunction at diagnosis (Jindal, 2018; Szucs and Jones, 2018). Liver transplantation is another option for localized tumours but is avoided due to the chances of rejection and immunosuppression (Jindal, 2018). The prognosis for patients with advanced tumours is very poor and treatment with radiotherapy and chemotherapy does not significantly improve outcome. By this time the cancer is refractory to treatment, for which there is also associated toxicities (Lee et al., 2017a). Sorafenib is the main FDA approved targeted therapy for HCC despite the very low partial response rate of 2% and improvement in survival rate of only 3 months (Llovet et al., 2008).

1.1.2. Pancreatic Cancer

Pancreatic cancer (PC) is an even more aggressive disease characterized by delayed diagnosis, metastasis, resistance to therapy and high mortality (Di et al., 2018). It is the fourth leading cause of cancer-related deaths worldwide with an incidence close to 338,000 each year and the highest incidence in men in high-income countries (Roth and Berlin, 2018; Torre et al., 2015). In the USA alone, the American Cancer Society projected 43,090 estimated deaths for 2017 (Roth and Berlin, 2018). If the mortality rates continue this trajectory, PC will become the second leading cause of deaths from cancer by 2030, surpassing liver, breast, prostate and colorectal cancer (Rahib et al., 2014). The outcomes for pancreatic ductal adenocarcinoma (PDAC) have not changed for the last 40 years. The five-year survival rate remains under 10% which is among the lowest of solid cancer types (Amrutkar and Gladhaug, 2017; Kleeff et al., 2016; Siegel et al.,

2017). Less than 2% of patients survive more than 5 years and the median overall survival time is 4-6 months in patients with metastatic disease (Bilimoria et al., 2007; Siegel et al., 2014; Uccello et al., 2018).

1.1.2.1. Characteristics

Pancreatic cancer is derived from the glandular tissue of the pancreas. Almost 90% of pancreatic cancers are PDAC arising from the ducts of the pancreas (Kamisawa et al., 2016; Zijlstra et al., 2016). It can be either localized to the pancreas (local disease), locally advanced (confined to the area around the pancreas but involving adjacent structures such as lymph glands), or metastatic (spread to distant areas) (Roth and Berlin, 2018). A hallmark of PDAC is a poorly vascularized, dense and fibrous stroma that can account for nearly 90% of the tumour volume (Kadaba et al., 2013; Neesse et al., 2011). It is known to interact closely with the encapsulated malignant cells. Not only is the stroma difficult to penetrate by the immune system, but it also acts as a physical barrier for drug delivery (Dimou et al., 2012; Stromnes et al., 2014). A broad heterogeneity of genetic mutations in addition to the dense stromal environment contribute to tumour growth and dissemination (Kong et al., 2012; Nielsen et al., 2016). PDAC is associated with two main types of morphologically distinct precursors: pancreatic intraepithelial neoplasia (PanIN) and intraductal papillary mucinous neoplasm (IPMN). Progression of PanIN into invasive cancer is well characterized (Bardeesy et al., 2006; Kopp et al., 2012; Morris et al., 2010) and is paralleled by successive aggregation of genetic mutations (Kleeff et al., 2016; Oldfield et al., 2017). Early activation of K-Ras oncogene is found in 80-95% of PDAC patients by major hot spot mutations at *KRAS* codon 12 (G12D, G12V, and G12R) or other less frequent variants resulting in the development of PanIN (Biankin et al., 2012; Collisson et al., 2011; Hruban et al., 2000; Witkiewicz et al., 2015). Progression to higher grade lesions and then to invasive PDAC is

driven by subsequent acquisition of inactivating mutations in tumor suppressor genes *CDKN2A*, *TP53* and *SMAD4*/*DPC4* (Patra et al., 2017). Almost all PDAC patients carry one or more of these four frequently-mutated driver genes (Oldfield et al., 2017).

1.1.2.2. Diagnosis

Most patients have advanced disease when they are diagnosed with an extremely poor prognosis. Patients commonly present with vague, non-specific symptoms that consist of abdominal pain, weight loss and jaundice, which worsen over time and are generally identified too late. (Howard and Jordan, 1977; Warshaw and Castillo, 1992). Upon physical examination, another common sign is an enlarged liver present in fewer than half of patients (Chin et al., 2018). Extent of the disease is classified as localized (resectable), borderline resectable, locally advanced, and metastatic. A resectable tumour shares a boundary with the superior mesenteric vein or portal vein, but does not produce vein contour irregularity (Al-Hawary et al., 2014). Unfortunately, 80% of patients are diagnosed with metastatic or non-resectable disease (Jemal et al., 2010). With better neoadjuvant therapy, more patients will be classified as borderline and qualify for resection.

1.1.2.3. Treatment

Despite efforts to improve the treatment and outcome of PDAC patients, little progress has been made (Stathis and Moore, 2010; The Lancet, 2011). Surgical resection remains the only curative therapy offering prolonged survival, for which only 15-20% of patients are eligible (Krempien et al., 2006). The role of adjuvant chemotherapy in advanced PDAC is well established and currently remains the standard of care for these remaining cases (Roth and Berlin, 2018). Unfortunately, PDAC is one of the most chemoresistant cancers, and conventional therapies have little impact on the course of disease (Adamska et al., 2017). The aim of chemotherapy in the

metastatic setting is mainly for symptom control and survival prolongation with tolerable side effects (Uccello et al., 2018). The benefits of radiotherapy alone or in combination as a palliative treatment is usually uncertain (Sultana et al., 2007). Until recently, chemotherapeutic options were all single agents including Gemcitabine (Gem), 5-fluorouracil (5-FU) and capecitabine. Gem has been the standard first-line treatment for PDAC sine 1997, preferred for its modest survival advantage of up to 5.65 months and a more acceptable toxicity profile (Burris et al., 1997). Major limitations of Gem include high dosage, rapid inactivation in the blood, and development of chemoresistance (Maksimenko et al., 2015; Moysan et al., 2013). Nowadays, there are several more effective options that clinicians can consider of which Gem in combination with other cytotoxic agents is the predominant one. The MPACT trial demonstrated superior efficacy of combination of the stromal-targeting nanoparticle albumin-bound paclitaxel (nab-paclitaxel) plus Gem versus Gem monotherapy (8.5 vs 6.7 months) (Chantrill et al., 2015; Von Hoff et al., 2013). FOLFIRINOX is another standard combination of drugs that have proven to substantially increase survival in metastatic PDAC patients (prodige/accord trial)(Conroy et al., 2011). It comprises of 5-Fluorouracil (a pyrimidine analog acting in a similar way of Gem), Leucovorin (a folinic acid which acts to reduce its side effects), Oxaliplatin (a DNA repair inhibitor), and Irinotecan (a topoisomerase inhibitor which blocks DNA duplication). The slightly better outcomes of FOLFIRINOX compared to Gem (median overall survival of 11.1 vs 6.8 months) come at the cost of increased hematologic toxicity and fatigue, limiting it to patients under 75 years old with a good performance status (Gourgou-Bourgade et al., 2013).

1.2. Nucleoside Analogues in Cancer Therapy

Phosphorylated nucleosides are the building blocks of DNA and RNA. Nucleoside analogues (NAs) are anti-metabolite drugs that mimic their endogenous counterparts. Incorporation of NAs into deoxyribonucleic acid (DNA) or ribonucleic acid (RNA) interferes with chain lengthening in actively replicating cells. Over the past few decades, NAs have been used to treat a variety of cancers and most drugs share a common metabolic pathway.

1.2.1. Gemcitabine: Characteristics and Mechanism of Action

Gem or 2′-Deoxy-2′,2′-difluorocytidine (dFdC) is one of the most important nucleoside analogues in cancer therapy. It is a cytidine (pyrimidine) analogue with a unique spectrum of anti-proliferative activity (Adamska et al., 2018; Genini et al., 2000). Intracellular uptake of Gem, a hydrophilic prodrug, is mediated by the SLC29 family of integral membrane proteins termed human nucleoside transporters (Figure 1). Gem is known to be transported by five transporters, primarily by human equilibrative nucleoside transporter 1 (hENT1, *SLC29A1*) (Mackey et al., 1998). Once inside the cytoplasm, Gem is phosphorylated into Gem-monophophoryl (dFdCMP) by deoxycytidine kinase (dCK), which is considered the rate-limiting step in its activation. The molecule is subsequently di- and tri-phosphorylated to dFdCDP and dFdCTP, respectfully. The major active metabolite dFdCTP acts as a competitive substrate for endogenous deoxycytidine triphosphate (dCTP), allowing it to be incorporated and locked into DNA in a process called "masked chain termination". Polymerases are unable to proceed, and normal mechanisms of DNA repair are unable to remove Gem, thus inhibiting DNA synthesis and leading to cell death. Gem also possesses the unique ability to enhance its own activation, termed "self-potentiation". The dFdCDP metabolite inhibits the ribonucleotide reductase (RR), a regulatory enzyme for DNA synthesis that converts CDP to dCDP (Heinemann et al., 1990; Xu et al., 2006). Inhibition of RR

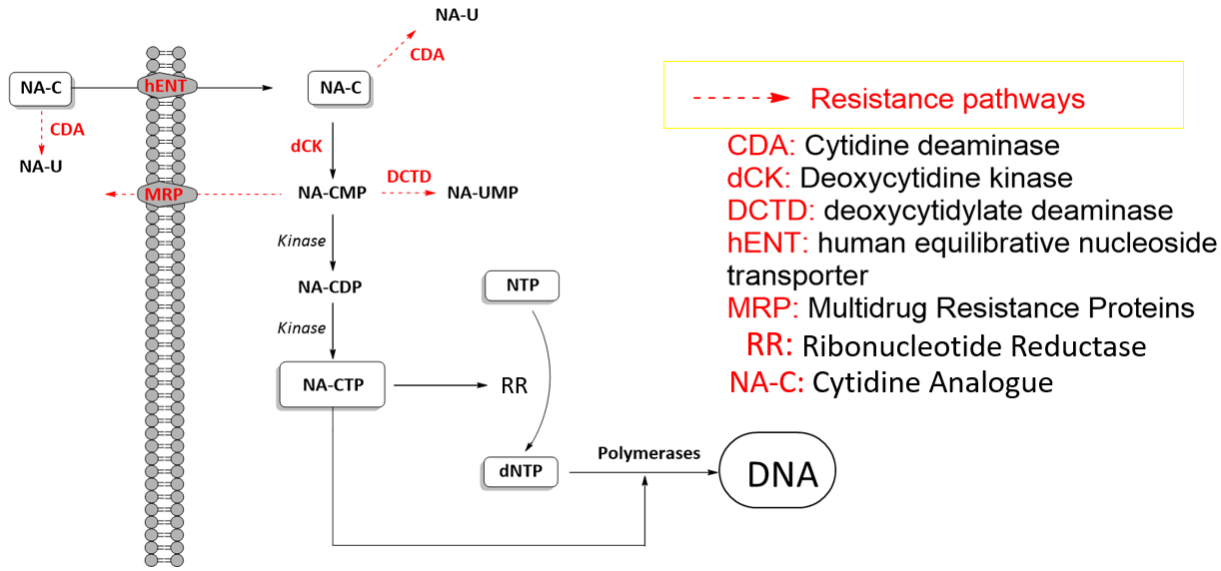

Figure 1. Nucleoside analogue metabolism and mechanisms of resistance. To act as antimetabolites, NAs first enter the cell through diffusion or with transporters. The first phosphorylation by dCK is rate-limiting. A second and third phosphorylation results in the formation of the di- and triphosphate metabolites which are converted to the deoxy metabolite using ribonucleotide reductase (RR). Resistance pathways result from a decrease and/or increase in various key enzymes.

depletes the pool of deoxyribonucleotides, favouring Gem incorporation into DNA (Heinemann et al., 1992). A positive feedback loop is created that increases the cytotoxicity of Gem.

1.2.2. Common Eide Effects and Toxicity of Antineoplastic Treatments

Rapid catabolism and development of cell resistance in the body pose as serious challenges for NA chemotherapy. Gem has low membrane permeability and once inside, most of Gem is inactivated by rapid deamination by cytidine deaminase (CDA) (Shipley et al., 1992). The other phosphorylated metabolites are also reduced by cellular 5′-nucleotidase or converted by deoxycytidylate deaminase and then rapidly cleared in the bloodstream. To compensate for these limitations, doses of Gem are high (about 1000 mg/m^2) and regularly must be increased, in turn generating severe toxicity and a narrow therapeutic index. Some side-effects include breathlessness, neutropenia, hepatoxicity, nausea and kidney failure (Galmarini et al., 2002; Moysan et al., 2013; Song et al., 2005). Lung toxicity has been reported with mortality rates at 20%. It tends to be quick in onset with an average onset of less than two months of Gem initiation, progressing quickly to respiratory failure (Sherrod et al., 2011). NA-induced replicative stress may not be specific to cancer cells either. In fact, rapidly dividing normal cells, including those in the bone marrow, gastrointestinal tract, and hair follicles, are often damaged by Gem as well resulting in myelosuppression, mucositis, and hair loss (Alexander et al., 2016; Galmarini et al., 2002; Song et al., 2005). Another unwanted scenario may be the accumulation of cells that incorporate NAs but survive therapy, potentially making tumours more aggressive. If these are not concerning enough, multi-agent regimens are associated with more severe cytotoxic side effects (Conroy et al., 2011). Despite these concerns, combination therapies with Gem are more likely to emerge as treatment of choice, especially for pancreatic cancer.

1.2.3. Recurrent Resistance Determinants to Nucleoside Analogues

Development of NA resistance is the main reason for the inefficacy of current treatments for pancreatic cancer. Pancreatic cells are most susceptible to Gem compared to any other anticancer agents however, most patients develop resistance within weeks of treatment initiation. In addition to the abundant fibrotic stroma surrounding the tumour being widely considered as a physical barrier to delivery of Gemcitabine, several resistance mechanisms have been reported and well-established (Kleger et al., 2014; de Sousa Cavalcante and Monteiro, 2014; Walker and Ko, 2014). Chemoresistance mechanisms in Gem treatment are associated with transport and metabolism and include reduced uptake, increased efflux, reduced activation or increased deactivation. The most studied mechanisms are the downregulation of hENT1 and of the rate-limiting enzyme dCK as well as upregulation of CDA and RR. Gem sensitivity can be predicted using a model based on the ratio of these parameters (Nakano et al., 2007) (Figure 1).

1.2.3.1. Nucleoside Transporters: Equilibrative Nucleoside Transporters and Multidrug-Associated Proteins

Specialized human equilibrative transporters (hENTs) are required for hydrophilic NAs like Gem to pass through the lipid bilayer of plasma membrane (Griffiths et al., 1997a, 1997b). hENT1 transports Gemcitabine with high affinity and low capacity (Mackey et al., 1999). Reduced hENT1 expression in cancer is a well-established phenomenon that leads to limited intracellular influx of Gemcitabine *in vitro* and *in vivo* (Mackey et al., 1998). Upregulation of hENT1 in cancer cell lines enhances the cytotoxic effect of Gem, while deficiency of hENT1 results in development of resistance to Gem (Achiwa et al., 2004; Mackey et al., 1998). Higher tumour expression of hENT1 in pancreatic cancer patients is associated with better overall survival compared to patients with low hENT1 expression (Morinaga et al., 2012; Spratlin et al., 2004). CO-101 a lipid-drug conjugate of Gem, was rationally designed to enter cells independently of hENT1. However, it

failed to demonstrate superiority over Gem in a population of metastatic pancreatic cancer patients with low hENT1 expression (Poplin et al., 2013).

Another major mechanism governing intracellular concentration of Gem in pancreatic cancer is the regulation of efflux. High expression of several multidrug-associated resistance proteins (MRPs) have been linked to poorer outcome in a variety of cancer types. MRPs are ATP-binding cassette (ABC) pumps in the plasma membrane that mediate the outflow of a large range of chemotherapeutics including Gem (Misra et al., 2005). Their normal function is to mediate transport of amphiphilic anions overexpressed in some types of cancers including pancreatic (Borst et al., 2000; Deeley and Cole, 1997; Miller et al., 1996). The ABCC family (MRP) consists of nine transporters, MRP1-9 (Gottesman et al., 2002). Of these, MRP-1 overexpression was found in human PDAC cell lines with the most frequent hotspot p53 mutations (Dhayat et al., 2015). Loss of proapoptotic wild-type p53 activity and overexpression of oncogenic mutant p53 lead to transcriptional activation of MRP-1, supporting its role in PDAC chemoresistance (Freed-Pastor and Prives, 2012; Wang and Beck, 1998). Another study in Capan-2 pancreatic cancer cell line found that MRP-1 plays a significant role in removal of Gem from Capan-2 cells. (Kohan and Boroujerdi, 2015). Discovery of MRP-1 in chemoresistance lead to its development into a drug target. Studies indicate that MRP-1 inhibitors could significantly elevate intracellular concentrations of chemotherapy drugs (Zhang et al., 2015b).

1.2.3.2. Expression of Deoxycytidine Kinase and Cytidine Deaminase

DCK is the rate-limiting enzyme of Gem's intracellular activation (Shipley et al., 1992). A clear correlation has been demonstrated between dCK levels and Gem sensitivity in both human and murine xenografts (Bergman et al., 1999; Haperen et al., 1994; Qin et al., 2009). Low pre-treatment levels of dCK tumour protein corresponds with a higher degree of Gem resistance in

pancreatic cancer patients and significantly decreased overall survival (Maréchal et al., 2010; Nakano et al., 2007; Ohhashi et al., 2008). Expression of dCK is considered stable even after development of resistance to Gem (Sebastiani et al., 2006). It has been reported that Gem-resistant human ovarian and pancreatic cancer cell lines show a loss of dCK mRNA and frequent inactivation of dCK (Ohhashi et al., 2008; Ruiz van Haperen et al., 1996). Knockdown of dCK in pancreatic cancer cell lines resulted in enhanced Gem resistance, while overexpression restored Gem sensitivity (Funamizu et al., 2010; Kroep et al., 2002; Saiki et al., 2012). It has been of interest to study the regulation of dCK to increase its analogue-activating activity. The expression and activity of dCK is enhanced by association with the RNA-binding stress-response protein Hu antigen R (HuR) (Costantino et al., 2009; Richards et al., 2010). Low HuR expression is reported to put patients at a seven-fold increased risk of cancer death compared to patients with high HuR levels (Costantino et al., 2009; Williams et al., 2010). The selective protein kinase inhibitor Masitinib also interacts with dCK to surprisingly activate the enzyme and sensitize Gem-refractory cancer cells when treated in combination. The resulting growth inhibition in human PDACs has been shown *in vitro* and *in vivo* (Humbert et al., 2010). A phase III trial of Masitinib plus Gem has even confirmed a survival benefit for advanced pancreatic cancer patients (Deplanque et al., 2015).

Deactivation of NAs is equally a contributor to chemoresistance. Major inactivation of Gem occurs through CDA via removal of the -NH2 group from pyrimidine (Shipley et al., 1992). The uracil metabolite dFdU is degraded, excreted out of the cell and is the only Gem metabolite found in urine of cancer patients (Abbruzzese et al., 1991). CDA levels are also found to correlate with clinical outcome as well as preclinical responses of cancer patients to Gem (Amrutkar and Gladhaug, 2017; Tibaldi et al., 2012). In this case high levels of CDA correspond to decreased overall survival. Several *in vitro* studies report that upregulation of CDA results in Gem resistance,

while lowering CDA levels restores Gem sensitivity (Eda et al., 1998; Funamizu et al., 2010; Weizman et al., 2014). Low levels of CDA mRNA were found in neuroblastoma cell lines highly sensitive to Gem and inhibiting CDA with tetrahydrouridine significantly increased Gem cytotoxicity in other human cancer cell lines (Eda et al., 1998; Funamizu et al., 2010; Ogawa et al., 2005). There is an urgent need to develop treatments that overcome the resistance caused by decreased activation and increased deactivation that current NA-based therapies face.

1.2.3.3. Expression of Ribonucleotide Reductase

Ribonucleotide reductase (RR) is among the most extensively studied molecular targets commonly associated with Gem resistance that is not directly related to its metabolism. Conversion of ribonucleotides to deoxynucleotides (dNTPs) by RR is essential for DNA synthesis and repair. RR is a holoenzyme that consists of two subunits: RR subunit M1 (RRM1) possesses a binding site for enzyme regulation and RR subunit M2 (RRM2) is involved in conversion activity. Gem (dFdCDP)-induced inhibition of RR (RRM2) is an important mechanism in the potentiation of Gem activity (Heinemann et al., 1990, 1992). However, high levels of RRM1 or RRM2 are associated with Gem resistance and correlate with a worse prognosis in pancreatic cancer patients (Amrutkar and Gladhaug, 2017; Aye et al., 2015). Increased expression of RRM1 was found in Gem-resistant cell lines of pancreatic, biliary, colon and non-small lung cancer, whereas in Panc-1 cell line, overexpression of both M1 and M2 subunits was necessary for development of resistance to Gem (Bergman et al., 2005; Davidson et al., 2004; Nakahira et al., 2007; Nakano et al., 2007; Wang et al., 2015). On the other hand, knockdown of M1 in MiaPaCa-2 could completely restore Gem sensitivity (Nakahira et al., 2007). As for M2, overexpression results in increased Gem resistance, while M2 knockdown leads to enhanced Gem sensitivity *in vitro* and in human cancer xenografts in mice models (Jonckheere et al., 2012).

1.2.4. Development of Novel Gemcitabine Derivatives

Chemical modification of nucleoside analogs began shortly after they were first approved for clinical use and novel chemotherapeutic agents are now being tested in many early phase trials. Numerous chemical modifications and encapsulation designs of the Gem molecule have been proposed to overcome three important determinants of resistance to Gem: downregulation of hENT1, downregulation and inactivation of dCK and deaminase-induced deactivation (Allain et al., 2012). Modifications of the Gem molecule are mainly based on prodrug and nanocarrier approaches that are aimed at improved bioavailability and efficacy (Amrutkar and Gladhaug, 2017). Resulting drugs have demonstrated their potential to improve clinical outcomes of the traditional Gem-based therapy (Hung et al., 2012; Moysan et al., 2013). Recent advances have been made in conjugating hydrophilic NAs to lipids. For instance, a group has conjugated Gem monophosphate to an amido-containing phospholipid moiety, producing the drug KPC34 (Pickin et al., 2009). KPC34 was designed to have dCK-independent activation and hENT1-free uptake with improved pharmacokinetics. *In vitro* and *in vivo* studies show that KPC34 is as effective or superior to Gem in treating several types of cancer (Pickin et al., 2009). Similarly, Neopharm synthesized a novel Gem-cardiolipin conjugate (NEO6002) that displayed higher antitumour activity in a pancreatic cancer mouse model and enhanced uptake and efficacy by prolonged release of Gem in various human PC cell lines (Ali et al., 2005; Chen et al., 2006). Another lipophilic prodrug, Gem-elaidic acid conjugate CP-4126 (CO-101) has been shown to be absorbed by cancer cells independent of hENT1 levels, yet in randomized phase II study CP-4126 was not superior to Gem with respect to survival in patients with metastatic PDAC and low hENT1 expression (Bergman et al., 2011; Poplin et al., 2013; Stuurman et al., 2013). To bypass the rate-limiting step in the Gem activation pathway catalyzed by dCK, monophosphate forms of Gem

have been developed (Wu et al., 2007). Screening a series of prodrugs identified NUC-1031 6f whose activation was less dependent on dCK than Gem and resistant to CDA-mediated degradation (McGuigan et al., 2011). A phosphoramidate ProTide moiety has since been added (ProTide 6f), which is currently under clinical development in a phase I/II study (Slusarczyk et al., 2014). Another example of an attempt to bypass inactivation of Gem is bio-conjugation with squalene, a natural and biocompatible lipid. The spontaneous formation of nanoparticles were able to overcome limitations to Gem in human pancreatic cancer cell lines. (Couvreur et al., 2008; Réjiba et al., 2011). This strategy was extended with the development of monophosphate prodrug SQ-dFdCMP nano-assemblies that displayed reduced tumour growth in xenograft mouse models of pancreatic cancer (Maksimenko et al., 2015). Altogether, chemical modifications of Gem show strong potential in overcoming resistance to cancer therapy.

1.2.4.1. Nucleoside Analogue Chemistry: Synthesis and Conformational Aspects

Existing approaches to synthesize modified nucleosides was limited by the natural pool of nucleosides and control of stereochemistry, which is particularly challenging. Dr. Guindon's medicinal chemistry group developed an novel acyclic methodology as a more efficient route for the formation of NAs, specifically those bearing an all-carbon stereogenic quaternary centers (Dostie et al., 2016). Their lab has since developed a series of novel NAs in search of new antimetabolites that may serve as anticancer agents. By varying the nucleobase and introducing various prodrugs and lipophilic carriers, the newly synthesized NAs are designed to circumvent the major known resistance pathways of cancer cells encountered by Gem (Figure 2). The base is protected with a lipophilic amide that will prevent deamination by CDA and will also allow hENT1-independent penetration in to the cell by passive transport. Next, the amide could be cleaved by proteases freeing the nucleoside. A monophosphate prodrug could then avoid the rate-

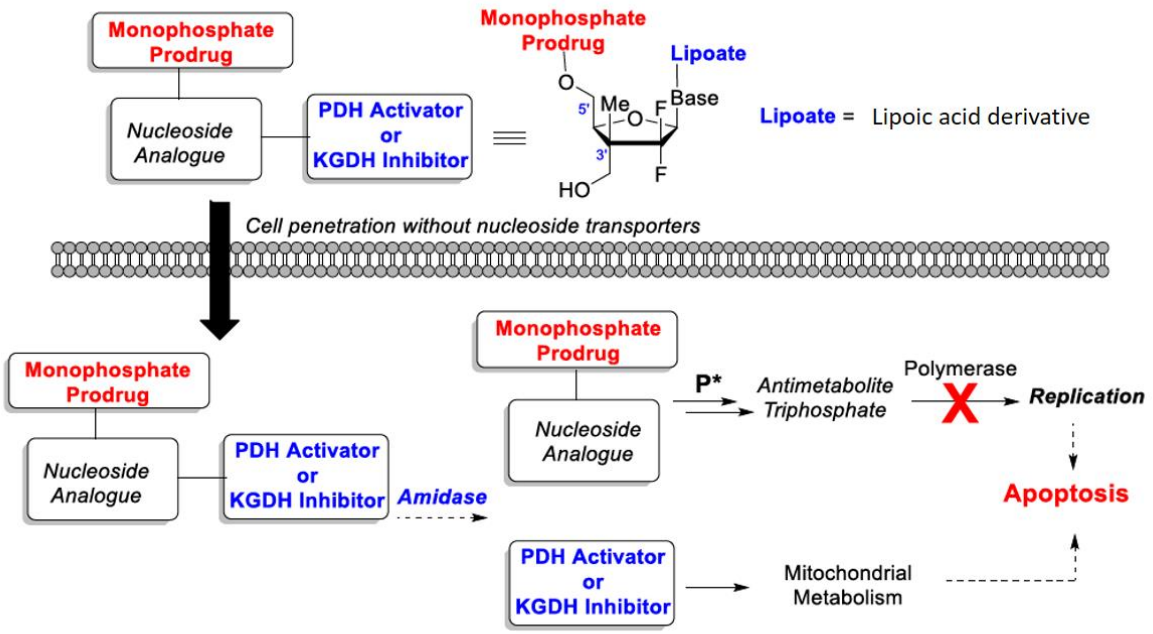

Figure 2. Summary of drug design rational. Our novel molecules consisting of a lipoate moiety attached to a nucleoside analogue. The resistance pathways (dCK or CDA) are overcome through installation of a phosphoramidate moiety (Monophosphate Prodrug) and the presence of lipoate chain. The released nucleoside analogue in the cell interferes with DNA replication, while the lipophilic attachment disrupts mitochondrial metabolism.

limiting step of activating phosphorylation by dCK (ex Sofosbuvir), while the lipophilic moiety could interfere with mitochondrial metabolism. Lastly, a stereogenic quaternary center at C2' or C3' of the furanose ring increases plasticity of the molecule and hinders the interaction with RR, which transforms NAs into different metabolites. In a collaborative effort, we have screened hundreds of molecules that has identified two bioactive lead molecules: LCB-2151 and LCB-2179 (Figure 3). Remarkably, both are the only known molecules to achieve 100% cell killing of Gem-resistant cell lines with or without *KRAS* mutation. The objective of my project is to elucidate their mechanisms of action to advance their development into the clinic.

1.3. Cancer Cell Metabolism

Glucose, the most widely available catabolite, can be metabolized multiple ways to generate adenosine triphosphate (ATP) and substrates for anabolic reactions involved in generating cellular components (Ahn and Metallo, 2015; Pietrocola et al., 2015). Either it can be metabolized through glycolysis to generate lactate in the cytoplasm or through glycolysis followed by further metabolism of pyruvate via the tricarboxylic acid (TCA) cycle and oxidative phosphorylation (oxphos) in the mitochondria (Martinez-Outschoorn et al., 2017) . Glycolysis with lactate production generates 2 moles ATP per mol glucose versus 36 moles ATP per mol glucose through mitochondrial oxphos (Vander Heiden et al., 2009). Cells frequently use both pathways, although typically one pathway dominates in a given cell, depending on nutrient availability (Goodwin et al., 2014; Sonveaux et al., 2008; Vander Heiden et al., 2009; Whitaker-Menezes et al., 2011). It is a thermodynamic trade-off between yield and rate of ATP production required by the cell. ATP is rapidly synthesized by glycolysis (100X faster than oxphos) but the yield is lower than synthesis by oxphos (Cox and Bonner, 2001). Under aerobic conditions, normal cells predominantly catabolize glucose through mitochondrial oxphos to generate ATP (Ahn and Metallo, 2015).

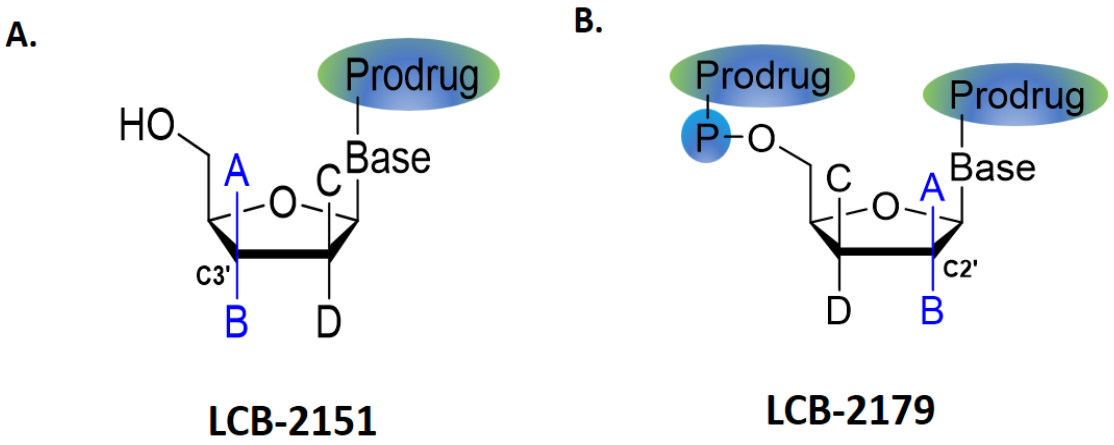

Figure 3. Structure of two lead prodrugs. A. LCB2151 is the lead molecule in the single pro-drug series, containing a lipophilic moiety. **B.** LCB2179 is the lead molecule in the dual pro-drug series, containing a lipophilic moiety and a phosphoramidate moiety (monophosphorylated prodrug).

Tumour cells are characterized by uncontrolled rapid proliferation. Compared to their normal counterparts, they require metabolic adjustments to fuel growth and division, exhibiting characteristic features in the way they utilize nutrients. This metabolic reprogramming has more recently been recognized as an essential hallmark of cancer and extensively reviewed in the major tumour types (Cairns et al., 2011; Christofk et al., 2008; Deberardinis et al., 2008; DeBerardinis et al., 2008; Hanahan and Weinberg, 2011; Vander Heiden et al., 2009). Cells within tumours can reprogram their metabolism to enhance glycolysis or oxphos. Glucose happens to be the most abundant energy source in the blood and is the substrate commonly used by tumour cells (Boroughs and DeBerardinis, 2015). Elevated aerobic glycolysis and reduced oxphos is therefore most observed metabolic reprogramming (Yu and Li, 2017). Elevated glycolysis relative to the surrounding tissue has been exploited for diagnostic imaging of tumours in the clinic by 2-[^{18}F]fluoro-2-deoxy-$\mathcal{D}$-glucose (^{18}F-FDG) positron emission tomography (PET) (Vander Heiden et al., 2009). Tumours also exhibit metabolic coupling, the transfer of catabolites from one compartment to another to overcome the metabolic stress imposed by a nutrient depleted environment. Overall, their metabolic flexibility allows tumours to generate ATP while maintaining reduction-oxidation (redox) balance and committing resources to biosynthesis of molecules such as nucleotides, lipids, as well as reduced nicotinamide adenine dinucleotide phosphate (NADPH) for macromolecular synthesis (Amelio et al., 2014). The commonly observed metabolic phenotype in cancer is induced by several factors including alterations in oncogenes and tumor suppressor genes. Onco-proteins and tumor suppressors such as the PI3K/Akt/mTOR signaling pathway, Myc, Ras, PTEN, hypoxia-inducible factor (HIF-1α) and p53, are involved in the regulation of this metabolic adaptation (Coller, 2014; Galluzzi et al., 2013; Jones and Schulze, 2012; Lu et al., 2015). They are responsible for changes in the expression levels of metabolic

enzymes, expression of alternative enzyme isoforms and mutations in genes encoding metabolic enzymes (Pavlova and Thompson, 2016). Although in many cases metabolic processes in cancer are similar to the ones in healthy tissues, metabolic phenotype of cells within tumours is distinct from that of their normal counterparts. There is less metabolic heterogeneity than variance in the genetic landscape of tumours, making metabolism-based therapies a more attractive anticancer strategy than treatment based on the complex and highly variable genetic profiles of tumours (Martinez-Outschoorn et al., 2017). Moreover, resistance to cell death is a hallmark of malignant cancers associated with altered metabolism. (Hanahan and Weinberg, 2011; Viale et al., 2014). The rational design of anticancer drugs targeting metabolic enzymes could be required to improve cancer-treatment outcomes by overcoming drug resistance (Elia et al., 2016; Galluzzi et al., 2013). In fact, these approaches have led to the development of several molecules that are now entering clinical trials (Kim et al., 2016).

1.3.1. Glycolysis, TCA Cycle and the Warburg Effect

The first to observe the elevated uptake of glucose that characterizes the majority of cancers was German physiologist Otto Heinrich Warburg (1883-1970) in 1927 (Vander Heiden et al., 2009; Warburg et al., 1927). The so called 'Warburg Effect' describes the ability of malignant cells to maintain elevated glycolytic rates in the presence of sufficient oxygen (Figure 4). This hypothesis seems counterintuitive for rapidly dividing cells. Why they choose a less efficient route to generate ATP has not been satisfactorily answered and the exact purpose of this metabolic adaptation remains unclear. What has been clarified is Warburg's initial assumption of defective non-functional mitochondria in cancer. For decades, mitochondria were a mere bystander of the oncogenic process. Today, we know that most cancer cells contain metabolically efficient mitochondria that are required to sustain high proliferation rates, to provide ATP and intermediate

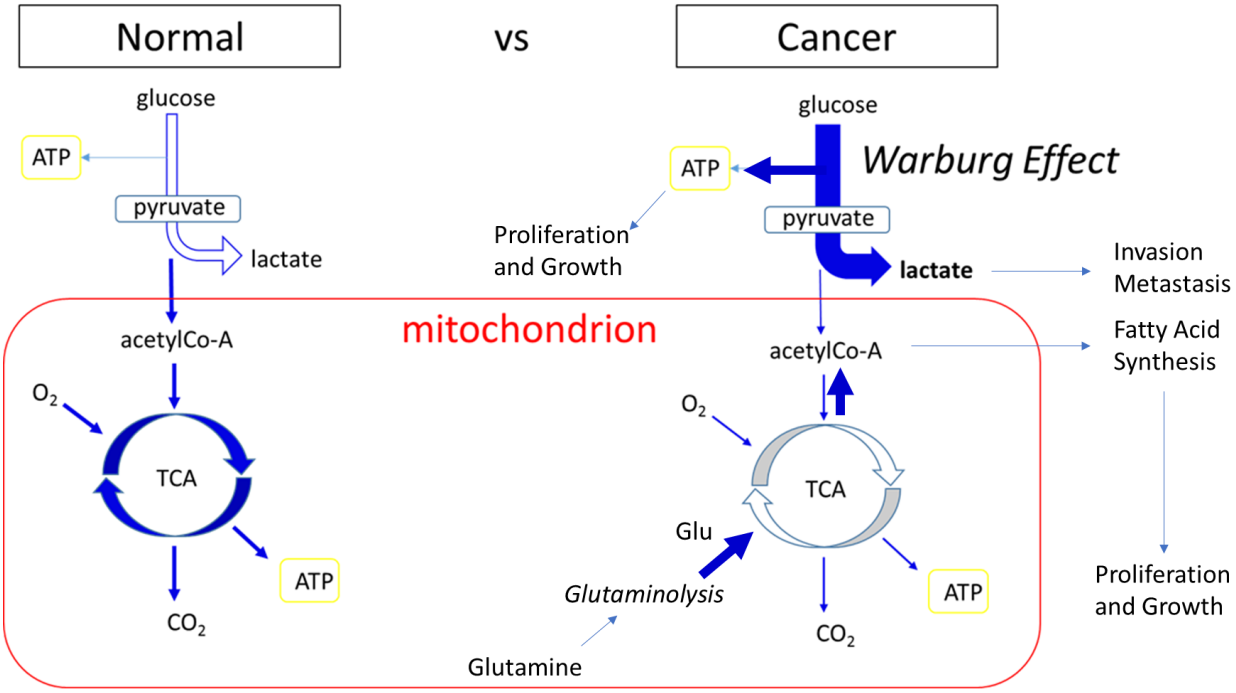

Figure 4. Altered Metabolism in Cancer. Cancer cells prefer to produce ATP by glycolysis, which is a less efficient pathway compared to oxidative phosphorylation, even under aerobic conditions. Glutamine metabolism is crucial for cancer cell growth via the generation of intermediate molecules in the tricarboxylic acid (TCA) cycle.

metabolites for anabolic reactions critical to cancer growth, with 10-15% of glucose carbons entering the TCA cycle (Hitosugi and Chen, 2014; Vander Heiden et al., 2009). Better known today as "aerobic glycolysis", it is clear that the metabolic reprogramming in cancer cells now goes beyond the Warburg effect to include increased flux through the pentose phosphate pathway (PPP), high glutamine consumption, reduction/oxidation (redox) imbalance and elevated rates of lipid biosynthesis (Chaiswing et al., 2014; Galluzzi et al., 2013; Schulze and Harris, 2012; Warburg, 1956; White, 2012). Even though ~85% of glucose carbon is excreted as lactate, the generation of acetyl-CoA from pyruvate remains critical for cancer growth. Pyruvate dehydrogenase complex (PDH) catalyzes pyruvate to acetyl-coA and is essential for converting glucose carbons into lipids and other TCA intermediates (Pardee et al., 2014a). There is a need for replenishing (anaplerosis) the TCA cycle with carbon sources other than glucose to fulfil these processes. Glutamine is another substrate for the bioenergetic pathways that support tumour growth. Together, increased glucose and glutamine consumption by tumours have been proposed to provide carbon and nitrogen precursors to sustain the biosynthesis of building blocks required for proliferation. Cells can utilize glutamine after its conversion to α-ketoglutarate that enters the TCA cycle via alpha-ketoglutarate dehydrogenase complex (KGDH) (Pardee et al., 2014a). It is predicted that simultaneous inhibition of PDH and KGDH would deprive cancer cells of their ability to metabolize carbon via the TCA cycle.

1.3.2. Key Metabolic Enzymes Involved

Most glycolytic enzymes are deregulated in cancer cells and play important roles in tumour progression. For instance, a number of studies correlate overexpression of the glucose transporter GLUT1 with increased glycolysis in cancer (Medina and Owen, 2002). There has been a rapidly growing interest in targeting glycolytic enzymes in cancer therapy. Drugs that target glycolytic

enzymes, are being studied in preclinical studies and even tested clinically, for example the GLUT1 inhibitor Silibinin (Deep and Agarwal, 2013; Galluzzi et al., 2013; Marchiq and Pouysségur, 2016; Ooi and Gomperts, 2015). Branching from glycolysis is the PPP that is required for the synthesis of ribonucleotides and NADPH (Stincone et al., 2015). Enzymes crucial for the diversion of glycolysis to PPP, such as phosphophructokinase-1 (PFK-1), have become emerging therapeutic targets as they are also upregulated in cancer cells (Lincet and Icard, 2015).

1.3.2.1. Phosphofructokinase-1

PFK-1 catalyses the rate-limiting conversion of fructose-6-phosphate (F6P) to fructose 1,6-bisphosphate (F1,6BP) in the third step of glycolysis. It plays a key regulatory role in controlling the node that determines the entry of metabolites into glycolysis or the associated PPP pathway (Mor et al., 2011). Shunting metabolism towards PPP leads to increased ribose-5-phosphate for the synthesis of nucleotides and of NADPH, which is essential for scavenging reactive oxygen species, preventing cancer cells from oxidative stress (Yi et al., 2012; Yu and Li, 2017). Mammalian PFK-1 contains two allosteric sites for its substrate ATP: the catalytic site and the inhibitory allosteric site. Hence, ATP exerts inhibitory effects on PFK-1 at different levels, depending on the metabolic state of the cell. When the ATP/ADP ratio is high, the inhibitory effect is elevated, which is also potentiated by other metabolites such as citrate and lactate (Costa Leite et al., 2007; Marcondes et al., 2010; Marinho-Carvalho et al., 2009). The most potent allosteric activator of PFK-1 is fructose-2,6-bisphosphate (F2,6BP), which is produced by phosphofructokinase-2 (PFK-2, PFKFB3). Affinity of PFK-1 for F6P increases upon binding of F2,6BP to PFK-1 and ATP-mediated inhibition of PFK-1 is lost (Deprez et al., 1997). PFK-2 is generally overexpressed in human cancers and has received attention recently as a therapeutic target (Clem et al., 2013; Yalcin et al., 2014). For example, inhibition of PFK-2 by 3-(3-pyridinyl)-

1-(4-pyridinyl)-2-propen-1-one (3PO) rapidly reduces glucose uptake, lactate secretion and intracellular ATP in leukemia cells (Clem et al., 2008). PFK-1 is also upregulated by activation of c-Myc oncogene, stimulating the Warburg Effect (Osthus et al., 2000). On the other hand, hypoxia induces glycosylation (O-GlcNAcylation at S529) of PFK-1 to inhibit enzymatic activity and redirect glucose flux towards PPP (Yi et al., 2012). Overall, blocking glycolysis affects oxphos by decreasing the concentration of pyruvate which integrates into the TCA cycle to produce ATP.

1.3.2.2. Pyruvate Dehydrogenase Complex

Pyruvate is the product of glycolysis that fuels mitochondrial oxygen consumption. In the mitochondria, pyruvate is oxidized by pyruvate dehydrogenase complex (PDH) to form acetyl co-A. Acetyl co-A can be oxidized to support ATP generation through oxphos, or its carbon can be diverted to anabolism (Martinez-Outschoorn et al., 2017). Considered the gatekeeper of pyruvate entry into the mitochondria, PDH is a huge complex with a core structure formed by more than 60 subunits including PDHA1 (E1), dihydrolipoyl acetyltransferase (E2), dihydrolipoyl dehydrogenase (E3), E3-binding protein (E3BP), pyruvate dehydrogenase kinase (PDK) and pyruvate dehydrogenase phosphatase (Patel and Roche, 1990). As the gatekeeper of pyruvate entry into the mitochondria, PDH regulation is especially well understood. It is one of four enzymes using lipoate as cofactor and its regulatory mechanisms are unique to this complex among the other lipoate enzymes (Kikuchi et al., 2008; Yeaman, 1989). Cyclic acylation/reduction of lipoate in the PDH complex modulates PDH activity by regulating the kinases (PDKs) that inactivate it. High levels of acyl and/or reduced lipoate (indicating high PDH saturation) stimulate PDKs to inactivate the E1α component of PDH via phosphorylation, blocking pyruvate entry into the complex (Roche et al., 2001). There are four PDKs and each has a distinct response to lipoate intermediates of PDH

(Roche and Hiromasa, 2007). PDKs are overexpressed in many cancers leading to inactivation of PDH (Hitosugi et al., 2011; Zachar et al., 2011). Pyruvate metabolism is being targeted in cancer therapy using modulators of the TCA cycle. Dichloroacetate (DCA), a pyruvate analogue and PDK-1 inhibitor stimulates PDH activity and suppresses tumour growth by shifting the Warburg phenotype to oxphos (Kinnaird and Michelakis, 2015; Velpula et al., 2013). Despite these results, current evidence shows that cancer cells retain functional mitochondria and the capacity for oxphos in spite of the Warburg effect (Bensinger and Christofk, 2012). Persistence of PDH activity is vital to cancer cell survival and was found to be essential for growth of lung tumours driven by oncogenic Ras in mice (Davidson et al., 2016). Inhibition of residual PDH activity rather than stimulation is another therapeutic angle to be considered.

1.3.2.3. Alpha-Ketoglutarate Dehydrogenase Complex

The need in cancer cells for biosynthetic intermediates leads to a TCA cycle functioning in a reverse mode, favouring tumour growth (Metallo et al., 2011; Mullen et al., 2011; Sun and Denko, 2014). To replenish the TCA cycle intermediates in support of anabolic processes, cancer cells rely on glutamine as an alternative carbon donor for lipid synthesis (DeBerardinis et al., 2007; Mullen et al., 2011). Glutamine is also important for synthesis of glutathione, an abundant antioxidant in cancer cells required for redox homeostasis and survival in response to oxidative stress (Martinez-Outschoorn et al., 2017). Glutamate from glutathione is a critical precursor for nonessential amino acids and increased activity of the enzymes involved is observed in cancer (DeBerardinis and Cheng, 2010; Weinberg et al., 2010). Lastly, transformed cells maintain the ability to metabolize glutamine oxidatively, accounting for the majority of ATP production under hypoxic condition (Altman et al., 2016; Fan et al., 2013; Son et al., 2013). Entry of glutamine-derived carbon into the TCA cycle is controlled by KGDH (DeBerardinis et al., 2008). Once

glutamine is converted to α-ketoglutarate (KG), KGDH catalyzes the oxidative production of succinyl-coA in the mitochondria. KG can also be carboxylated to isocitrate then citrate, which is transported to the cytoplasm for fatty acid synthesis (Han et al., 2016). KGDH consists of 3 types of subunits: 2-oxoglutarate dehydrogenase (OGDH, E1), dihydrolipoamide succinyl transferase (DLST, E2) and dihydrolipoamide dehydrogenase (DLD, E3) (Reed and Hackert, 1990). OGDH is the rate-limiting component for the overall enzymatic reaction (Huang et al., 2003). LA is bound to the DLST subunit that acts as a cofactor in transesterification reaction producing succinyl-Co-A and DHLA, the reduced form of lipoic acid (LA). DLD catalyzes the restoration of oxidized LA (Reed and Hackert, 1990). In contrast to PDH, KGDH is not regulated by phosphorylation but rather primarily by allosteric processes to adjust mitochondrial metabolism through energy status sensing (Strumilo, 2005). Its activity is finely regulated by levels of ATP, ADP, inorganic phosphate (Pi) and by the reduced nicotinamide adenine dinucleotide (NADH)/NAD+ ratio, where low energetic conditions have a stimulating effect. Succinyl Co-A, Ca+, ROS and variations in mitochondrial pH appear to also be involved in the control of KGDH activity (Vatrinet et al., 2017a). Intriguingly, KGDH can both sense and generate ROS. Increased ROS levels inhibit KGDH function via modification of LA bound to E2. The E3 subunit is the site of superanion production that causes generation of a thiyl radical on the reduced lipoic acid bound to E2, to ultimately undergo self-inactivation under high NADH conditions (McLain et al., 2011; Starkov et al., 2004). Inhibition of KGDH (OGDH/E1) suppresses cancer cell growth and inhibition of glutamine metabolism increased the sensitivity of cancer cells to chemo- and radiotherapy by increasing oxidative stress (Izaki et al., 2008; Li et al., 2015a, 2015b; Mullen et al., 2014; Sun and Denko, 2014). These findings lend support for further investigation of KGDH as a therapeutic target in resistant cancers.

1.4. Role of Mitochondrial Biogenesis in Cancer

It is now clear that mitochondria play a key role in all steps of oncogenesis. (Lu et al., 2015; Vyas et al., 2016). Not only are they a major source of ATP, mitochondria also have the ability to provide building blocks for anabolism via anaplerosis, the capacity to produce ROS and hold a central position in regulated cell death signalling. In view of the vital role of mitochondrial function in sustaining cancer cell survival, mitochondrial metabolism now stands out as a promising target for the development of novel antineoplastic agents. Drugs targeting mitochondrial oxidative stress are currently being explored. Reactive Oxygen Species (ROS) are primarily generated as by-products during mitochondrial electron transport chain (ETC) and regulate key cellular processes such as cell death, invasiveness and metabolism. ROS at low levels can promote proliferation, but elevated ROS production causes oxidative stress, which can include lipid peroxidation, DNA damage and protein oxidation, leading to cell death (Martínez-Reyes et al., 2016). Cancer cells have enhanced antioxidant systems to maintain ROS homeostasis in high oxidative stress environments (Cairns et al., 2011; Sun et al., 2013). NADPH is produced via the PPP and is central to the ability of cancer cells to control ROS by re-generating antioxidants such as glutathione (Fan et al., 2014; Scarbrough et al., 2012). Redox signaling is extensively studied in altered tumor cells. For example, Ras-driven cancer cells with a heightened antioxidant system, including stimulation of the NADPH-generating PPP, are among the most difficult to treat and there is also evidence for redox-dependent changes associated with malignancy-related metabolic alteration in breast cancer development (Schafer et al., 2009; Watson, 2013). Considering that cancer cells, with tightly regulated redox homeostasis, are more vulnerable to excessive ROS levels than normal cells, disruption of redox balance and mitochondrial function by promoting oxidative stress is an attractive therapeutic strategy to eradicate vulnerable cancer cells (Trachootham et al., 2009).

1.4.1. Lipoic Acid in Cancer

The short-chain fatty acid alpha-lipoic acid (LA) is an endogenous disulfide compound synthesized *de novo* in the mitochondria, where it serves as an essential cofactor for mitochondrial enzymes that are key to maintaining TCA carbon flow (Ziegler et al., 1995). Specifically, LA is covalently bound as a lipoamide to DLAT and DLST subunits of the PDH and KGDH complexes, respectively. It contains two sulfur atoms and either can exist in higher oxidation states (Dwivedi et al., 2014; Mignini et al., 2013). LA and its reduced counterpart dihydro lipoic acid (DHLA) form a potent redox couple (Durand and Mach, 2013). LA is synthesized in the liver and other tissues with high metabolic activity such as the heart and kidneys and is found in every cell (Akiba et al., 1998; Yamada et al., 2011). Both water and fat soluble, LA crosses biological membranes easily, reaching all parts of the cell. In humans, LA is primarily metabolized by S-methylation and ß-oxidation (Teichert et al., 2003). In addition to its catalytic roles, LA occupies a unique position in cancer biology. A number of studies have demonstrated that LA and derivatives thereof are capable of antitumor activity *in vitro* and *in vivo*, while non-transformed primary cells are hardly affected (Jeon et al., 2016; Sen et al., 1999). The mode of cell death was further characterized and revealed the intrinsic apoptosis that is p53-independent (Dörsam et al., 2014). Further studies show evidence that LA is able to generate ROS, contributing to LA-induced cell death in lung, breast, colon and ovarian cancer cells (Dozio et al., 2010; Kafara et al., 2015; Moungjaroen et al., 2006; Trivedi and Jena, 2013). In addition, LA was found to activate adenosine monophosphate-activated kinase (AMPK) in various tissues, which inhibits cancer cell proliferation (Li et al., 2015c; Park et al., 2008). Altogether, LA triggers apoptotic cell death, likely initiated by increased ROS production and is associated with p53 activation and deregulation of the ratio between anti-/pro-apoptotic factors (Simbula et al., 2007). The anticancer effects of LA seem to require high

mM concentration ranges to be induced (Gruzman et al., 2004). In contrast to antineoplastic agents used in cancer chemotherapy, LA does not damage DNA, but targets mitochondria. When tested in combination with hydroxycitrate and with Gem chemotherapy, LA improves effectiveness against pancreatic tumor development (Guais et al., 2012). This *in vivo* data suggests a possible advantage in using a combination of treatment targeted at lipoate-dependent cancer metabolism with classical chemotherapy.

1.4.2. Lipoic Acid Derivatives in Cancer Therapy

LA is difficult to apply in clinical use as it is easily oxidized and unstable (Hiratsuka et al., 2013). Lipoate analogs have been explored as improved chemotherapeutic agents that selectively disrupt mitochondrial metabolism of cancer cells. With variable substituents on the carboxyl group or disulfide bonds, LA analogues show notable anticancer activities and low toxicity. (Gruzman et al., 2004). To provide a few examples of LA analogues in action, the zinc complex of reduced lipoamide DHL-TauZnNa inhibited the proliferation of HT-29 cells *in vitro* and *in vivo* and a substituted lipoamide 17m showed antitumour activity in a xenograft model using S180 mouse sarcoma cells (Hiratsuka et al., 2013; Zhang et al., 2010).

1.4.3. CPI-613: Mechanism of Action, Clinical Status and Limitations

The most promising member of a novel class of anti-cancer lipoate derivatives is currently 6, 8-bis(benzylthio)octanoic acid (CPI-613). Structurally similar to lipoate, CPI-613 strongly disrupts mitochondrial metabolism with selectivity for tumour cells in various cancer cell lines and in human cancer (lung & pancreatic) xenograft models (Lee et al., 2014). Multiple redundant cell death pathways, including apoptosis, are induced by CPI-613. Malignant cell death is preceded by ATP depletion and AMPK activation, but not in normal cells (Pardee et al., 2014a; Zachar et al., 2011). The regulatory targets of this agent are KGDH and PDH, each through distinct mechanisms

(Stuart et al., 2014; Zachar et al., 2011). Collectively, these two complexes control that majority of carbon flux through the TCA cycle and are differentially regulated in cancer cells. In contrast to recently described agents that attempt to upregulate PDH function, CPI-613 may kill cancer cells by hyper-stimulation of tumour-specific PDH regulatory processes. Inhibition of PDH correlates with stimulation of PDKs and lipoate-responsive regulatory phosphorylation of the E1α subunit of PDH. CPI-613 also attacks the second lipoate-containing, mitochondrial enzyme complex, KGDH by a redox mechanism selectively in tumour cells (Stuart et al., 2014) . A burst of ROS generated by the E3 subunit is induced, inactivating KGDH via redox modification of the endogenous lipoate residues of the E2 subunit. Taken together, this single drug simultaneously attacks two essential tumor mitochondrial metabolic enzymes, behaving as a 'cocktail of one'. The drug was well tolerated in Phase I trials in patients with hematologic malignancies but showed no efficacy in a phase II study in patients with relapsed or refractory small-cell lung cancer who have failed 1st line chemotherapy (Lycan et al., 2016; Pardee et al., 2014a). Further clinical trials are currently running with CPI-613 to (a) assess its side effects and best dose when administered together with chemotherapy (FOLFIRINOX) in patients with metastatic pancreatic cancer and to (b) monitor its safety and efficacy in patients with advanced and/or metastatic solid tumors (Alistar et al., 2017).

1.4.4. The Potential of Nucleoside Analogues with a Lipoate Moiety

Targeting multiple metabolic pathways simultaneously through combination therapy might be a novel anticancer approach. LA derivatives are likely to synergize with, and compliment current chemotherapy drugs, most of which interfere with DNA replication to limit tumour growth, especially considering that LA itself was shown to potentiate the killing effects of the anticancer drug 5-FU (Dörsam et al., 2014). In review, LCB2151 and LCB2179 are novel molecules

combining nucleoside analogues bearing all carbon quaternary centers with lipoate-derived adducts. They are designed to target two critical pathways for cancer cells: i) proliferation, via the antiproliferative effect of the nucleoside analogue and ii) mitochondrial metabolism, via the lipoate adduct. We selected a lipophilic carrier derivative of CPI-613 as the lipoate adduct. The structure of CPI-613 was modified to block β-oxidation and aromatic para-oxidation to increase the potency of our analogues. Early screening of this series of analogs led to the most active compound, LCB2151.

1.5. Objective, Hypothesis and Aims

Objectives: To decipher the mechanisms of action of newly developed nucleoside analogues that have shown great cytotoxic potency in various pancreatic and hepatic cancer cell lines.

Hypothesis: Strategically designed proprietary nucleoside analogues can overcome cancer cell resistance mechanisms and interfere with cancer cell metabolism, resulting in higher specificity and efficacy than the current pancreatic anticancer therapies.

Aims:

a) Characterize structure-activity relationship of lead molecules in human cancer cell lines
b) Measure global drug-induced changes in cellular pathways of treated cancer cells
c) Validate potential molecular targets and key pathways involved in the mechanism of action

2. Materials and Methods

2.1. Cell Culture

HepG2, Capan-2 and BxPC-3 cell lines were obtained from the American Type Culture Collection (ATCC). Panc-1 cell line was obtained from Dr. John Bell's Lab. HepG2 was cultured in Eagle's Minimum Essential Medium (ATCC); Capan-2 was cultured in McCoy's 5A Medium (ATCC); BxPC-3 was cultured in RPMI 1640 (ATCC); and Panc-1 was cultured in Dulbecco's Modified Eagle Medium (DMEM). All growth media were supplemented with 10% fetal bovine serum and 2% penicillin/streptomycin. When confluent, cells were washed twice with 1X Phosphate-Buffered Saline (PBS), detached from the bottom of the plate with 0.05% trypsin, centrifuged at 500g for 5 minutes at room temperature to remove the trypsin and cell pellet was resuspended in the appropriate growth medium to be passaged. The cells were kept in a humidified chamber at 37˚C with 5% CO_2.

2.2. Growth Inhibition Determination

Cells were plated in 96-well plates at a density of 10,000 cells/well in 100ul of media. Media was replaced after a 24 hour incubation and cells were treated in triplicate with increasing concentrations of drug. All wells contained the same final amount of DMSO vehicle. The plates were then incubated for 96 hours in a humidified chamber at 37˚C with 5% CO_2. Cell viability was measured using the CellTiter-Glo® 2.0 Assay (Promega, WI) by quantitation of ATP present in each well. Each plate is incubated at room temperature for 30 minutes before addition of 100ul of reagent to each well. The plates were covered in aluminum foil and placed on a rotator for 10 min. Readings were done in a GloMax® luminometer (Promega, WI). Each well was corrected over

the vehicle-treated wells and the average of each treatment was calculated. Growth inhibition curves were generated using the program GraphPad (Prism).

2.3. Consecutive Treatments

After 24 hours of incubation, the cells were treated in triplicates with increasing concentrations of Gemcitabine or vehicle and incubated for 96 hours. Media was changed, and remaining cells were re-treated with LCB2151 10μM, Gemcitabine 0.2μM or vehicle. After 48 hours, well viability as measured using Celltiter-Glo® 2.0 Assay (Promega, WI) as previously described.

2.4. Cell Entry Determination

After 24 hours incubation, media was replaced for Panc-1 cells with media containing 10μM of human equilibrative nucleoside transporter inhibitor S-(4-Nitrobenzyl)-6-thioinosine (NBMPR, Sigma N2255) or vehicle. Cells were immediately treated in triplicates with increasing concentrations of LCB2151, LCB2179, Gemcitabine or vehicle. The plates were then incubated for 96 hours in a humidified chamber at 37˚C with 5% CO_2. Cell viability was measured and analyzed as previously described.

2.5. Drug Activation Determination

Two small interfering RNAs (siRNAs) targeting independent sequences of human DCK (siDCK) gene were designed and synthesized by Sigma. Panc-1 cells were plated in a 6-well plate at a density of 500,000 cells/well. After 24h, cells were transfected with siDCK using Lipofectamine RNA iMAX (Invitrogen) according to manufacturers recommendations at final concentrations of 10nM and 20nM. After 24 hours cells were collected to measure mRNA levels of *DCK* (see Quantitative RT-PCR of methods section 2.6). Non-targeting siRNA was used as a control. Protein levels of dCK were measured after 24 and 42 hours of the same treatments (see

protein extraction and western blot method) with anti-dCK 1/1000 (Abcam, ab96599). Transfection was carried out with siDCK set1 or scramble at 0.5pmol/well. After 24 hours, cells were treated in triplicate with increasing concentration of LCB2151, LCB2179, Gem or vehicle. 24 hours later, cell viability was determined and analyzed.

2.6. RNA Extraction & Quantitative RT-PCR

Capan-2 and BxPC-3 cells were plated in 6-well plates at a density of 5x10^5 cells/well. After 24 hours of incubation, media were changed, and cells were treated with LCB2151 15 µM, LCB2179 15 µM, Gem 1 µM or vehicle for a total of 4 replicates per condition. At 6 or 18 hour time points, wells were washed twice with PBS 1X before scraped and collected with 500mL TRIzol (Thermo Fischer Scientific). 200uL of chloroform was added to each tube, vortexed for 15 seconds and let to sit at room temperature for 2 minutes. Samples were spun at 12,000g for 15 minutes at 4°C. The top phase was transferred to a new tube and equal volumes of isopropanol were added. Samples were shaken 10 times before sitting at room temperature for 10 minutes. Samples were spun at 12,000g for 10 minutes at 4°C. Supernatant was discarded, and pellet was washed with 75% ethanol three times, spun at 8,000g for 5 minutes at 4°C each wash. The final pellet was resuspended in 25mL Diethyl Pyrocarbonate (DEPC)-treated water. RNA concentration and quality were determined using Nano-Drop ND Spectrophotometer (NanoDrop). cDNA was generated using QuantiTect Reverse Transcription kit (Qiagen). mRNA levels were quantified by QPCR in Rotorgene 6000 apparatus (Corbett). The reactions were performed in duplicate for each sample using the RotorGene SYBR Green PCR Kit (Qiagen, 205310). Gene expression was normalized against the internal reference gene *RNPS1*. Results were expressed as fold change relative to cells treated with vehicle, which was set as 1 for each gene. The sequences of the specific primers are detailed in Table 1.

Table 1. List of Oligo Sequences for QPCR.

Gene	Sense	Antisense
ABCC1	ACTTCGTTCTCAGGCACATC	TGATCCGAAATAAGCCCAGG
ABCC2	TCATCGTCATTCCTCTTGGC	ACGGATAACTGGCAAACCTG
SLC29A1	ATGAAGTAACGTTCCCAGGTG	CCACTCTATCAAAGCCATCCTG
CDA	AAGGGTACAAGGATTTCAGGG	ACAATATACGTACCATCCGGC
RRM1	ACCGCCCACAACTTTCTAG	CCAGTAGCCCGAATACAACTC
DCK	GTTGGTTTTCAGTGTCCTATGC	TTTATCTTCAAGCCACTCCAGAG
BID (isoform 1)	TGACCACATCGAGCTTTAGC	ATTAACCAGAACCTACGCACC
BIK	CTGGGTCTGGCTTTCATCTAC	CTGTTCGCAGGACACCC
BAX (isoform alpha)	AAGTCCAATGTCCAGCCC	GACATGTTTTCTGACGGCAAC
BBC3 (isoform 1)	CGACCTCAACGCACAGTAC	CCTAATTGGGCTCCATCTCG
DIABLO (isoform 1)	TTGGTCTTTCAGAGATGGCAG	GTGATTCCTGGCGGTTATAGAG
ENDOG	CCCCACCTCAACCAGAATG	ATTTCCCATCAGCCTCTGTC
TP53	TCATCCAAATACTCCACACGC	GCCATCTACAAGCAGTCACAG
MCL1	AAGGACAAAACGGGACTGG	ATATGCCAAACCAGCTCCTAC
XIAP	GGGTCTTCACTGGGCTTC	GCACGGATCTTTACTTTTGGG
BCL2	TTGTGGCCTTCTTTGAGTTCGGTG	GGTGCCGGTTCAGGT ACTCAGTCA
BCLXL	GTGGAAAGCGTAGACAAGGAG	CTGCATTGTTCCCATAGAGTTC
NFKB1	GAACCACACCCCTGCATATAG	GCATTTTCCCAAGAGTCATCC
CXCL1	CATCCAAAGTGTGAACGTGAAG	GTCACTGTTCAGCATCTTTTCG
CDKN1A	GGCGTTTGGAGTGGTAGAA	TGTCACTGTCTTGTACCCTTG
CCND2	ACTTGTGATGCCCTGACTG	ACTTGGATCCGTCACGTTG
CCNE1	TCTTGAGCAACACCCTCTTC	TTCTTGTGTCGCCATATACCG
CCNE2	CTGCCTTGTGCCATTTTACC	GTCTTCAGCTTCACTGGACTAG
SOD1	TGTGGCCGATGTGTCTATTG	GCGTTTCCTGTCTTTGTACTTTC
NCF2	AGGTAGTTGCAGGGAACAAG	CGTGTGCTATTTGGGTTTGTG
UCP2	TCCTGAAAGCCAACCTCATG	GGCAGAGTTCATGTATCTCGTC
BECN1	AAGAGGTTGAGAAAGGCGAG	TGGGTTTTGATGGAATAGGAGC

2.7. Assessing Mitochondrial Function

Panc-1 cells were seeded (4x10^4 cells/well) into 24-well assay plates (Seahorse Bioscience) and grown over night. Cells were treated with 15 µM LCB251, 15 µM LCB2179, 0.75 µM Gemcitabine or vehicle and incubated at 37 °C. At 6 hours cells were washed and DMEM culture media was replaced with Seahorse assay buffer (bicarbonate-free DMEM, 5 mM D-glucose, 4 mM L-glutamine, 1 mM sodium pyruvate; pH 7.4) and incubated in a non-CO_2 incubator at 37 °C for 45 minutes. The sensor cartridge was hydrated with XF calibrant solution one day prior to experiment and left in a non-CO_2 incubator at 37 °C overnight. Oxygen consumption rate (OCR) measurements were determined using a Seahorse XF24 Extracellular Flux Analyzer (Seahorse Bioscience, Agilent Technologies) before and after sequential injections of the following inhibitors: 2 ug/ml oligomycin (Sigma-Aldrich), 1 µM FCCP (Sigma-Aldrich), and 1 µM antimycin A (Sigma-Aldrich). Cells were lysed with 50 µL of 0.5N NaOH to conduct protein quantification determination (Bradford assay). Rates were normalized to the protein content in each well.

2.8. Capacity of the Glycolytic Pathway

Panc-1 cells were seeded (4x10^4cells/well) and treated with similar concentrations of LCB2151, LCB2179 and Gemcitabine. Wells were washed, and DMEM culture medium was replaced with assay medium (DMEM supplemented with 1mM L-glutamine, pH 7.4) and incubated in a non-CO_2 incubator at 37 °C for 45 minutes. The sensor cartridge was hydrated with XF calibrant solution one day prior to experiment and left in a non-CO_2 incubator at 37 °C overnight. Extracellular acidification rate (ECAR) was measured by a XF24 extracellular flux analyzer (Seahorse Bioscience, Agilent Technologies). Glucose (10mM); Oligomycin (1 µM) and 2 deoxyglucose (50mM) were sequentially injected into each well in accordance with the

manufacturer's standard protocol for the Glycolysis Stress Test (Agilent Seahorse XF). Cells were lysed with 50 µL of 0.5 N NaOH to conduct protein quantification determination (Bradford assay). Rates were normalized to the protein content in each well.

2.9. Detection and Quantification of Total Glutathione Ratios

Panc-1 cells were plated (1x10^6cells/well), incubated overnight and then treated with LCB2151 (10,15,20 µM), LCB2179 (10,15,20 µM), Gemcitabine (0.5, 1, 2 µM) or vehicle for 2 and 6 hours. Cells were lysed and measurements of total and reduced glutathione levels were carried out in parallel on separate plates using the GSH/GSSG-Glo™ luminescence based kit (Promega, V6611), according to the manufacturer's instructions. The luminescence signal was recorded with the GloMax luminometer (Promega). The GSH/GSSG ratio was calculated using the formula provided by the manufacturer. GSSG contribution to the total glutathione concentration was multiplied by two and this value was subtracted from total glutathione amount to generate the GSH concentration in the samples. Readings were normalized to vehicle-treated wells.

2.10. Detection of Hydrogen Peroxide

Panc-1 cells were treated with Gemcitabine (1 µM) or vehicle for 6 hours. ROS level was detected through the measurement of H_2O_2 in the cells, according to the non-lytic instructions of the ROS-Glo™ H_2O_2 Assay luminescence-based kit (Promega, G8820). The luminescence signal was recorded with the GloMax luminometer (Promega). Cells were then lysed, and cell viability was measured. All readings were normalized to amount of ATP, and then treated wells were normalized to vehicle-treated wells.

2.11. Large Scale Proteomics Analysis

2.11.1. Sample Preparation

Panc-1 cells were seeded onto 10cm culture plates at a density of 2x10^6 cells per plate and left overnight to incubate. The next day cells were treated with LCB2151 20 µM or vehicle. Cells were washed twice with 1X PBS and scraped into new tubes at 6, 9, and 12 hour time points. Each treatment was performed in triplicate for each time point. Two plates were pooled for a single replicate. Cells were lysed and whole cell protein extraction was performed according to the RIPA protocol. Protein concentration was normalized to 1ug/uL and analyzed by HPLC-ESI-MS/MS for large scale protein profiling by the Proteomics Resource Center (Faculty of Medicine, University of Ottawa) who performed experimental steps 2.11.2.-2.11.5.

2.11.2. Chemicals

Urea, dithiothreitol (DTT), ammonium bicarbonate (ABC), and iodoacetamide (IAA) were all purchased from Sigma (St. Louis, MO). HPLC grade water and acetonitrile (ACN) were from J.T baker. Formic acid (FA) and citric acid were obtained from Merck (Darmstadt, Germany). Trypsin was purchased from Promega (Madison, WI). All of the chemicals were of analytical purity grade except ACN and FA, which were of HPLC grade

2.11.3. Filter Aided Sample Preparation (FASP) for Trypsin Digestion

FASP method was modified for exosomal protein digestion. Briefly, samples were loaded onto a 3K filter (Amicon® Ultra-0.5, MilliPore), 8M urea was used to displace the original buffer (Liebler and Ham, 2009). Protein reduction and alkylation were done sequentially in the filter. Urea was then replaced by 50mM ammonium bicarbonate, and a mass ratio of 1:50 between trypsin and protein was used for digestion at 37°C overnight, with continuous shaking. Digested peptides were then desalted on mini tip column packed in house with 10µm ReproSil-Pur C18 beads (200

Å; Dr. Maisch GmbH, Germany) and dried down in SpeedVac (ThermoFisher Scientific, San Jose, CA). Dried samples were reconstituted in 20μL 0.5% (v/v) FA, and 4μL was loaded for MS analysis.

2.11.4. Liquid Chromatography – Mass Spectrometry Analysis

Eksigent 2D+ nanoLC system (Dublin, CA) was hooked up with LTQ-orbitrap Elite mass spectrometer (Thermo Electron, Waltham, MA), equipped with a nano-electrospray interface operated in positive ion mode. The solvent system consists of buffer A of 0.1% FA in water, and buffer B of 0.1%FA in 80% acetonitrile. Dried down protein digests were acidified with 0.5% (v/v) formic acid and loaded on a 75 μm I.D. × 150 mm fused silica analytical column packed in-house with 1.9μm ReproSil-Pur C18 beads (100 Å; Dr. Maisch GmbH, Ammerbuch, Germany) at a flow rate of 500nL/min for 15min. Then the flow rate was changed to 200nL/min to perform the peptide separation. Gradient elution was set as 5–35% buffer B in 2 hours. The spray voltage was set to 2.0 kV and the temperature of heated capillary was 300 °C. The instrument method consisted of one full MS scan from 300 to 1800 *m*/*z* followed by data-dependent MS/MS scan of the 20 most intense ions in ion trap by CID, a dynamic exclusion repeat count of 1 in 30 seconds, and an exclusion duration of 30 seconds. The full mass was scanned in Orbitrap analyzer with R = 60,000 (defined at m/z 400) for MS1. To improve the mass accuracy, all the measurements in the orbitrap mass analyzer were performed with a real-time internal calibration by the lock mass of background ion 445.120025. The charge state rejection function was enabled, and charge states with unknown and single charge state were excluded for subsequent MS/MS analysis. All data were recorded with Xcalibur software (ThermoFisher Scientific, San Jose, CA).

2.11.5. Data Analysis

The peak lists of the raw files were processed and analyzed with software MaxQuant (Version 1.5.3.30) against Uniprot protein database of human (2017 March Release), including commonly observed contaminants (Cox and Mann, 2008). Cysteine carbamidomethylation was selected as a fixed modification; the methionine oxidation, protein N-terminal acetylation ubiquitination, arginine methylation were set for variable modification. Enzyme specificity was set to trypsin, not allowing for cleavage N-terminal to proline. Up to two missing cleavages of trypsin were allowed. The precursor ion mass tolerances were 7 ppm, and fragment ion mass tolerance was 20 ppm. Razor and unique peptides were used for LFQ quantitation. FDR was set 0.01 on protein, peptide and modification-specific site, A minimum length of seven amino acids was used for peptides identification. For protein identification, if the identified peptide sequence of one protein was equal to or contained another protein's peptide set, these two proteins were grouped together by MaxQuant and reported as one protein group.

2.12. Central Carbon Metabolism Analysis

2.12.1. Sample Preparation

Panc-1 cells were seeded onto 150x22 mm plates at a density of 10x10^6 cells per plate and incubated overnight. The next day, cells were treated with 20 µM LCB2151 or vehicle for 6 hours. Cells were washed twice with 1X PBS and spun each time at 500g for 5 minutes. Two plates were pooled for a single replicate and five replicates were collected for each treatment. Cell pellet was flash frozen in liquid nitrogen and stored at -80℃ until Central Carbon Metabolism Analysis (Creative Proteomics, USA). All further steps up to and including 2.12.5. are performed by Creative Proteomics (USA). Cell pellets in each tube were lysed at 30 Hz below 0 °C for 1 min x 2, with the aid of two 3-mm metal balls, on a MM400 Mill Mixer. The metabolites were then extracted in 1 mL of 80% methanol for each sample with ultra-sonication of the tubes in an ice-

water bath for 5 min. The samples were clarified by centrifugation at 15,000 rpm and 4 °C in a 5420 R Eppendorf centrifuge for 15 minutes. The clear supernatants were collected for the following UPLC-MRM/MS analyses and the protein pellets were used for protein assay using a standardized BCA procedure.

2.12.2. UPLC - MRM/MS

All the quantitative analyses were conducted by ultrahigh-performance liquid chromatography–tandem mass spectrometry (UPLC-MS/MS) using multiple-reaction monitoring (MRM). The LC-MS system was an Agilent UHPLC system or a Waters Acquity UPLC system, coupled to a Sciex 4000 QTRAP mass spectrometer. The interface was an atmospheric pressure nebulizing electrospray ionization (ESI) source with detection in either positive- or negative-ion mode. Injection volumes were 10 or 20uL and the column temperatures were 40 or 45 °C, depending on the analytical methods and corresponding measured metabolites.

2.12.3. Quantitation of CCM Carboxylic Acids

Quantitation of CCM carboxyl acids was performed by chemical derivatization-UPLC-MRM/ MS using 3-nitrophenylhydrazine (3-NPH) as a pre-analytical derivatizing reagent. The derivatization followed a protocol as described in the publication by Han *et al.,* 2013 (Han et al., 2013). The measurements were by UPLC-MRM/MS on a C-18 UPLC column (2.1 mm I.D. x 100 mm, 1.7 um) with negative-ion detection. The mobile phase was 0.01% formic acid in water (A) and acetonitrile (B) for binary-solvent gradient elution. The concentrations were calculated from linearly regressed calibration curves of individual acids which were prepared with the use of their standard substances and 9 stable isotope-labeled carboxylic acids as internal calibration (IS) for internal calibration.

2.12.4. Quantification of Glucose and Reduction Sugar Phosphates

Selective quantitation of glucose and 5 sugar phosphates (glucose-6P, mannose-6P, ribose-5P, eryuthrose-4P, and glycerylaldehyde-3P) was performed by pre-column AEC derivatization – UPLC-MRM/MS method according to an approach as described in Analytical Chemistry (Han et al., 2013).

2.12.5. Quantitation of Other 30 Phosphate-Containing CCM Metabolites

Quantitation of other phosphate-containing metabolites including sugar phosphates, phosphor-carboxylic acids, glycerol-phosphates, nucleotides, and enzyme co-factors, etc. was performed using a custom-developed reversed-phased UPLC-MRM/MS method with negative-ion detection (unpublished yet). The concentrations were calculated from the calibration curves of the individual compounds, which were prepared with the use of their standard substances.

2.13. Whole Cell Protein Extraction

After overnight incubation, the cells were treated with drugs or vehicle at the indicated concentration. The medium was removed from the plates after the desired time point and wells were washed with 1X PBS. 250 µL of 1X RIPA buffer (50mM Tris pH 7.5; 150mM NaCl; 1% NP-40; 0.25% desoxycholate; 0.1% SDS; ddH_2O) with freshly added EDTA-free Halt phosphatase and protease inhibitor cocktail (Thermo-Fischer Scientific, Cat 78430) was added to each well and the cells were scraped. Two wells were pooled per replicate in an Eppendorf and passed through a syringe fitted with a 21G needle. Each tube was vortexed for 20 seconds and left on ice for 30 minutes. Samples were vortexed again for 20 seconds and centrifuged at 12,000 g for 15 minutes at 4°C. The supernatant containing the total proteins was transferred to another microcentrifuge tube and stored at -80°C. The DC Protein Assay (Briorad, 5000111) was used to quantify all proteins.

2.14. Immunoprecipitation

Two plates were pooled per condition and whole cell protein was extracted. Lysates (1ug/uL) were incubated with 30ug antibody (anti-DLST, abab72790 or anti-PDH-E2, ab110332) overnight at 4 ^{o}C. Protein-antibody mixture was added to pre-cleared PureProteome Protein S/G Mix Magnetic Beads (Millipore) and shaken for 4 hours at 4 ^{o}C. Beads were washed with lysis buffer and boiled with 2X SDS loading buffer for 3 minutes to elute proteins. Protein lipoylation was analyzed by western blot using 1:1000 dilution anti-lipoic acid (Abcam, ab58724) corrected over total protein.

2.15. Western Blot

Whole cell extracts were placed at 95 ^{o}C in 6X SDS loading buffer and loaded onto TGX Stain-Free FastCast acrylamide gels (Biorad) and resolved by electrophoresis. Proteins were then transferred to nitrocellulose membranes using the Tans-Blot Turbo System (Biorad) for 10 minutes. The membrane was blocked for 1 hour in 5% milk tris-buffered saline with tween (TBST) at room temperature. Primary antibodies (anti-lipoic acid, Abcam, ab58724; anti-nucleolin, Cell Signalling, 14574; anti-pyruvate dehydrogenase E2, Abcam, ab110332; anti-DLST, Abcam, ab72790; anti-COX IV, Abcam, ab33985; anti-PFKP, Abcam, ab204131) were diluted in in 5% milk TBST to the recommended dilution and shaken overnight at 4◦C. Membranes were incubated for 1 hour at room temperature with secondary antibodies (1:25000) conjugated with Horseradish peroxidase in 1% milk TBST. Visualization was done using Clarity ECL substrate (Biorad) as per manufacturer's instructions for 3 minutes incubation.

2.16. Alpha-Ketoglutarate Dehydrogenase Activity

KGDH activity was measured using an assay kit (BioVision, Inc., Cat K678-100). Panc-1 cells were plated at a density of 1x10^6 cells/well in 6-well plates. Cell pellet was lysed in kit

buffer according to manufacturer's instructions and lysate was passed through a 10kDa Amicon® Ultra-0.5 centrifugal filter (Millipore Sigma) to retain KGDH protein and wash away excess NADH, a source of background, as recommended by the manufacturer. Recovered protein was topped up to 100uL with assay buffer and 50uL was loaded into each well of 96-well plate. The absorbance at λ = 450 nm was measured in kinetic mode every 10 minutes up to 60 minutes at 37◦C. Two time points in the linear range of the plot were used to calculate the activity of the samples. The reaction rate of KGDH was expressed in nmol NADH/min/ml or mU/ml. One unit (U) of α-ketoglutarate dehydrogenase is the amount of enzyme that generates 1.0 μmol of NADH per min at pH 7.5 at 37°C per ug protein content.

2.17. Statistical Analysis

Data are means ± standard error of the mean (SEM)., with $p < 0.05$ by Student's *t* test being considered as statistically significant. Dose response curves, SEM, EC_{50} and IC_{50} are generated by GraphPad (Prism). One-way ANOVA was used to calculate statistical significance of Seahorse (Agilent) data on GraphPad (Prism).

3. Results

3.1. Aim 1: To Elucidate the Structure-Activity Relationship of Novel Nucleoside Analogues

3.1.1. Antiproliferative Efficacy of Novel Nucleoside Analogues

Nucleoside analogues synthesized by the Guindon laboratory were tested in human cancer cell lines to determine their anti-neoplastic effects. Four cell lines were selected based on commonly mutated genes found in human liver (HepG2) and pancreatic (BxPC-3, Capan-2, Panc-1) cancers, such as *TP53* and *KRAS* (Table 2) (Hu *et al.*, 2018; Rao *et al*., 2017). Panc-1 was of additional

Table 2. Mutations in human canner cell lines. The four human cancer cell lines HepG-2 (liver), BXPC-3, Capan-2, Panc-1 (pancreatic) and their genotype for commonly mutated genes found in cancer: *TP53* and *KRAS*.

Cell Line	Tissue	*TP53*	*KRAS*
HepG-2	Liver	WT	(*NRAS*) Q61L
BxPC-3	Pancreas	Y220C	WT
Capan-2	Pancreas	WT	G12V
Panc-1	Pancreas	R273H	G12D

interest to us because not only does it harbour mutations in both genes, but it is also used in the mouse xenograft model for pancreatic cancer that is being developed by our collaborators in the Dr. Bell Laboratory (Ottawa Hospital Research Institute). Cell viability was assessed by measuring ATP levels after 96 hours of incubation with molecules at increasing doses (Figure 5). LCB2151 (Figure 5B) and LCB2179 (Figure 5C) were able to kill up to 99% of cells, most remarkably Capan-2 cell line that shows the highest resistance to gemcitabine (Gem) which causes no growth inhibition in this assay (Figure 5A). In this cell line, the concentration at which they reach 50% of their maximum effectiveness, EC_{50}, was 16.84 µM for LCB2179 and 26.32 µM for LCB2151 (Table 3). Having the highest potency and thus the lowest EC_{50} values of the molecules tested in this screening study, LCB2151 and LCB2179 were selected as lead molecules to continue with structure-activity studies.

LCB2151 possesses a quaternary center at C3'and a lipoate derivative attached via an amide bond with the amine of the nucleobase (cytosine) (Table 4). The presence of the lipoate should protect the nucleobase against deamination by CDA (cytidine deaminase) which converts the cytidine nucleobase into its uracil equivalent. The lipophilic character of LCB2151 (from the lipoate) should allow the molecule to penetrate the cell irrespective of the presence of nucleoside transporters.

Lipoic acid and some of its derivatives, CPI-613, are also known to have antioxidant activity for mitochondrial cell metabolism albeit at very high concentration. Guindon's laboratory has synthesized a novel lipoate analogue (LCB2152) containing a Gem-dimethyl in the beta position to prevent β-oxidation. In addition, the thiol moieties are protected with benzyl groups. Substitution of the benzyl groups with a para-CF_3 will also prevent oxidation at this position.

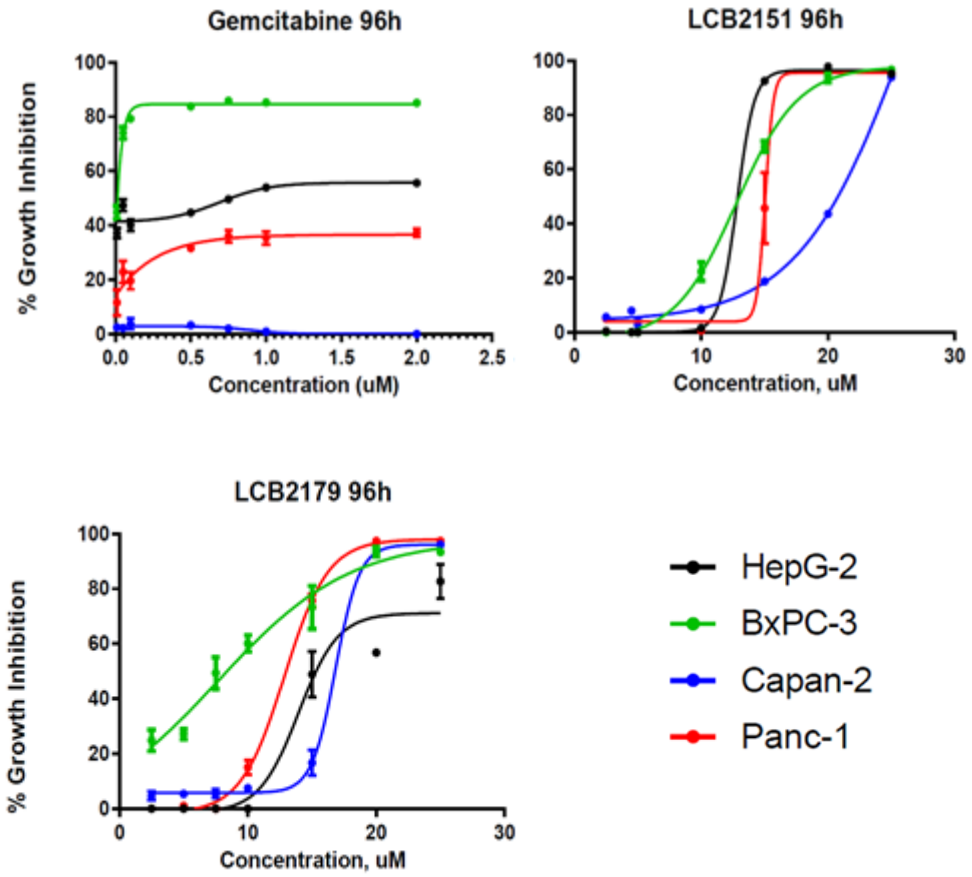

Figure 5. Cytostatic Activity of lead molecules in Human Cancer Cell Lines. Percentage of growth inhibition of (A) gemcitabine, (B) LCB-2151 and (C) LCB-2179 in four human cancer cell lines: HepG2 (hepatocellular carcinoma cell line), BxPC-3, Capan-2 and Panc-1 (pancreatic ductal adenocarcinoma cell lines). Cell viability was measured using the Celltiter-Glo assay (Promega) to determine ATP levels. Gemcitabine has a limited efficacy, especially in Capan-2, while lead molecules LCB2151 and LCB2179 reach up to 99% growth inhibition in most cell lines. N=1

Table 3. Dose response measurements of lead molecules in human cancer cell lines. The concentration at which 50% of the maximum growth inhibition (Max %) is reached (EC_{50}) and the concentration at which 50% growth inhibition is reached (IC_{50}) are presented for each cell line after 96 hours treatment: Capan-2, BxPC-3, Panc-1 (pancreatic adenocarcinoma cell lines), and HepG2 (hepatocellular carcinoma cell line). The IC_{50} and EC_{50} are almost identical for LCB2151 and LCB2179, because they reach up to 99% growth inhibition in most cell lines. Values are measured by GraphPad Prism software.

molecule		pancreas			liver
		Capan-2	Panc-1	BxPC-3	HepG2
LCB2151	**EC_{50}, µM**	26.32	15.06	12.78	12.84
	IC_{50}, µM	22.00	15.17	13.32	12.00
	Max %	97.00	98.11	96.83	96.83
LCB2179	**EC_{50}, µM**	16.84	12.86	7.70	13.93
	IC_{50}, µM	17.09	13.51	8.45	15.00
	Max %	96.08	99.68	98.20	70.92
Gem	**EC_{50}, µM**	0.89	0.64	0.24	0.69
	IC_{50}, µM	x	x	0.09	1.12
	Max %	2.91	36.61	84.63	55.77

Table 4. Summary of lead molecules and controls for cell assays. Molecules classified by structural components. Dose response of all molecules was performed at 6 and 96 hours. Concentration at which molecules reach 50% of maximum inhibition are indicated for each time point (EC_{50}).

Source	Drug	Nucleoside analogue	Lipoate derivative	Natural nucleoside	Natural Lipoate	Monophosphorylated	EC_{50} in Panc-1 6h, uM	Max Inhibition 6h, %	EC_{50} in Panc-1 96h, uM	Max Inhibition 96h, %
LCB from Dr. Guindon Lab	2151	+	+				40.89	87.70	15.1	98.11
	2152		+				x	x	~10	56.82
	1180	+					x	x	x	x
	2216		+	+			22.17	98.02	13.6	96.89
	2179	+	+			+	30.22	13.75	14.76	99.68
Clinically Available	CPI-613		+				23.08	12.01	~ 213	8.6
	(R) Lipoic Acid				+		x	x	x	x
	Gemcitabine	+					x	x	0.0639	43.5

These two structural features could modify the lipophilic character of our novel analogue and its mechanism of action, if cleaved from the nucleobase.

Molecules and controls including clinically available CPI-613, lipoic acid and Gem were tested in Panc-1 cell line for 6 and 96 hours (Figure 6). LCB2151 kills up to 80% of cell by 6 hours (Figure 6A) and both LCB2151 and LCB2179 consistently kill up to 100% of cells by 96 hours (Figure 6B). Although we have no evidence that our novel lipoate analogue, LCB2152, is cleaved from LCB2151 in cell culture providing the free nucleoside (LCB1180), both LCB2152 and LCB1180 were also tested in Panc-1. Interestingly, 80 µM LCB2152 induced a 40% cell death after 96 hours while CPI-613 was inactive at this concentration (Figure 6B). A 200 µM dose of CPI-613 was necessary to reach 40% cell death and 300 µM was needed for 80% inhibition (Figure 6D). Lipoic acid was inactive in this cell line (Figure 6D) along with the free nucleoside LCB1180 (Figure 6B). Gem shows no activity in this cell line at 6 hours and reaches a plateau of 40% killing at 96 hours (Figure 6C). When the sugar analogue of LCB2151 is replaced with a natural nucleoside, as in LCB2216, a similar activity and potency is observed (Figure 6A and 6B).

LCB2179, differs from LCB2151 by having the stereogenic quaternary center at C2' and a monophosphate prodrug at C5'. The presence of a prodrug will avoid the rate-limiting monophosphorylation step by dCK. LCB2179 also possesses the lipoate derivative (LCB2152) attached as an amide to the cytosine nucleobase. LCB2151 is a deoxy nucleoside analogue while LCB2179 is a ribonucleotide analogue, therefore they should have different mechanisms of action.

Our results have helped identify two novel molecules with the ability to kill a panel of Gem-resistant cell lines harboring prevalent mutations in humans with better efficiency than clinically and commercially used drugs.

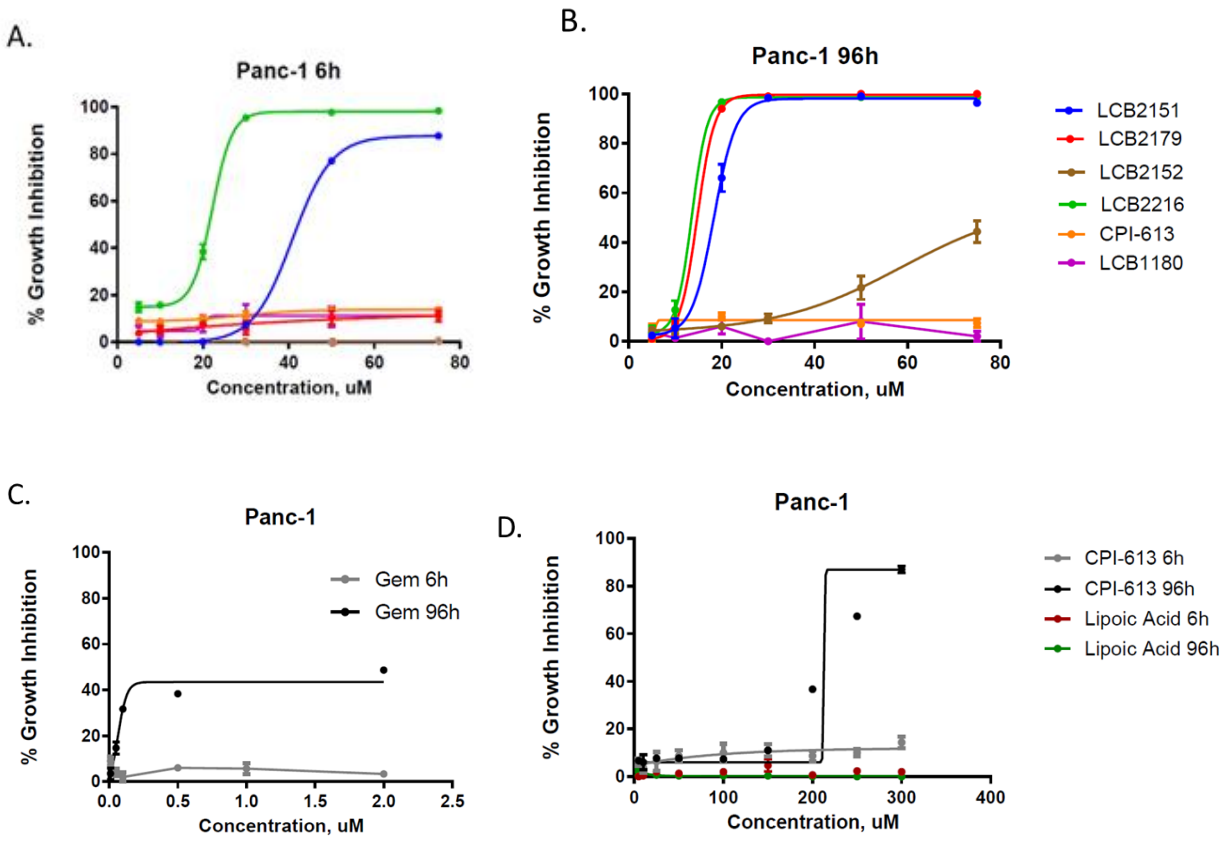

Figure 6. Dose response of lead molecules and controls for cell assays. Panc-1 cell line was treated with increasing concentration of lead molecules LCB2151, LCB2179, structural derivatives of LCB2151 (LCB1180, LCB2152, LCB2216), commercially available compounds ((C) Gemcitabine, (D)CPI-613, (D) Lipoic Acid) or vehicle for (A) 6 and (B) 96 hours to measure and compare bioactivity. LCB2216 shows more activity than LCB2151 or LCB2179 at 6 hours and LCB2152 starts to show moderate activity at 96 hours. Data mean of triplicates, N=1.

3.1.1. LCB2151 can Kill Gemcitabine-Resistant Cell Lines

A major challenge for cancer patients is the high risk of relapse arising from the resistant cells that remain after chemotherapy. These forms of cancer can be even more aggressive than the first encounter. It is therefore crucial that new chemotherapy agents eradicate the highest percentage of cancerous cells possible to lessen the risk of relapse. My previous results show that all cell lines in our panel are resistant to Gem to various degrees (Figure 5A). Previous work done in our lab showed that LCB2151 kills up to 60% of resistant Capan-2 cells remaining immediately after Gem treatment. It was important to test if these results can be replicated in different human cancer cell lines, with new conditions. In all cell lines, HepG2, BxPC-3 and Capan-2, growth inhibition plateaus with doses up to 1.5 µM of Gem after 96 hours of incubation (Figure 7A). Cells were therefore pre-treated with Gem at 1.5 µM for 96 hours. After this, the remaining cells were re-treated with 0.2 µM of Gem or 15 µM of LCB2151. After a 48 hour incubation, growth inhibition was measured. LCB2151 kills 37% of both remaining HepG2 and BxPC-3 cells and 60% of the Capan-2 cells (Figure 7B). Consecutive Gem treatment does not show cytotoxicity above 17% in any cell line tested, supporting that LCB2151 is able to evade the mechanisms of Gem-resistance in a variety of cancer cell lines.

3.1.1. LCB2151 and LCB2179 can Enter the Cell Independently of a Transporter

A key mechanism of nucleoside analogue resistance in pancreatic cancer is the downregulation of the hENT1 transporter (Amrutkar and Gladhaug, 2017). Gem is very hydrophilic and is known to be dependent on this transporter to enter cancer cells and initiate its intracellular activation. To bypass this mechanism of resistance, LCB2151 and LCB2179 were synthesized with a lipoate moiety. The goal of this lipophilic moiety is to allow the analogue to pass through the membrane without the need of a transporter. Using the pan-nucleoside transporter family inhibitor

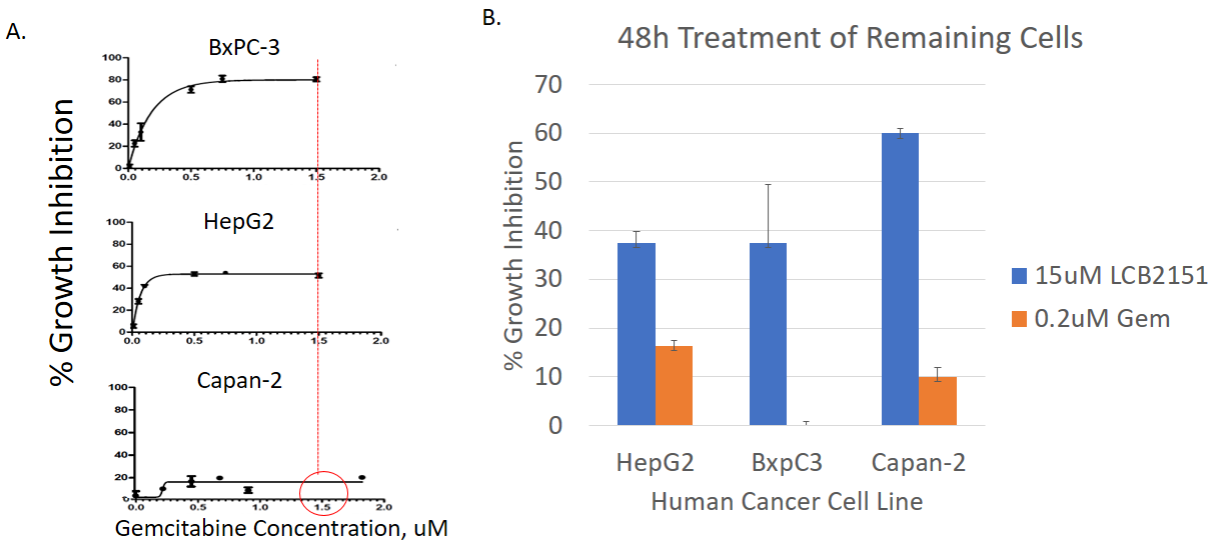

Figure 7. Consecutive treatments in human cancer cells. (A) Percentage of growth inhibition of HEPG2, BXPC3 and CAPAN2 cells treated with increasing dose of gemcitabine for 96h. (B)Percentage of growth inhibition of the remaining cells after a 96h pre-treatment of 1.5 µM gemcitabine (concentration that reaches plateau of killing), treated with 15 µM of LCB2151 or 0.2 µM Gemcitabine for 48hrs. LCB2151 was able to kill gemcitabine-resistant cells after 48h and most remarkably up to 60% of the most resistant cell line capan-2. Data are mean of triplicates. N=1. Capan-2 results courtesy of Claudia Teran, MSc.

Nitrobenzylthioinosine (NBMPR) to mimic drug resistance, we previously showed that LCB2151 activity was independent of hENT1 levels in HepG2 (less resistant) and Capan-2 (most resistant) cell lines, while Gem activity was abrogated by the presence of inhibitor. I chose to replicate these results in the Panc-1 cell line harbouring both the *TP53* and *KRAS* mutations. Cells were treated with Gem, LCB2151, LCB2179 or vehicle for 96 hours, with or without the presence of NBMPR and growth inhibition was measured. While the modest Gem activity was abrogated as expected (Figure 8A), both the activity of LCB2151 (Figure 8B) and LCB2179 (Figure 8C) were unchanged by the presence of NBMPR. My results support the hypothesis that LCB2151 and LCB2179 enter cells independently of hENT1 in Panc-1 cells, bypassing a major chemotherapy-induced mechanism of resistance in cancer cells.

3.1.2. LCB2151 and LCB2179 Activities are Independent of the Rate-Limiting Step by Deoxycytidine Kinase

In addition to deficiency of nucleoside transporters, deficiency of nucleoside kinases such as dCK is related to a decrease in tumor sensitivity of nucleoside analogues (Maréchal *et al*., 2012). Lower expression of dCK was shown to be associated with shorter overall survival in pancreatic cancer patients receiving Gem-based therapy. dCK expression at both the mRNA (*DCK*) and protein level is used as a biomarker to predict tumor cell sensitivity to Gem (Fujita *et al*., 2010; Sebastiani *et al.,* 2006). The novel compound LCB2179 was designed to bypass the rate-limiting step catalyzed by dCK by being monophosphorylated and thus could be activated independently of dCK if metabolised through the traditional pathway. To confirm this hypothesis, a study was done to downregulate the expression of *DCK*. Unlike hENT1 there are no inhibitors specific to dCK that are commercially available, although several research groups have initiated programs to identify small-molecule dCK inhibitors (Nomme *et al*., 2013). Alternatively, the role of dCK in

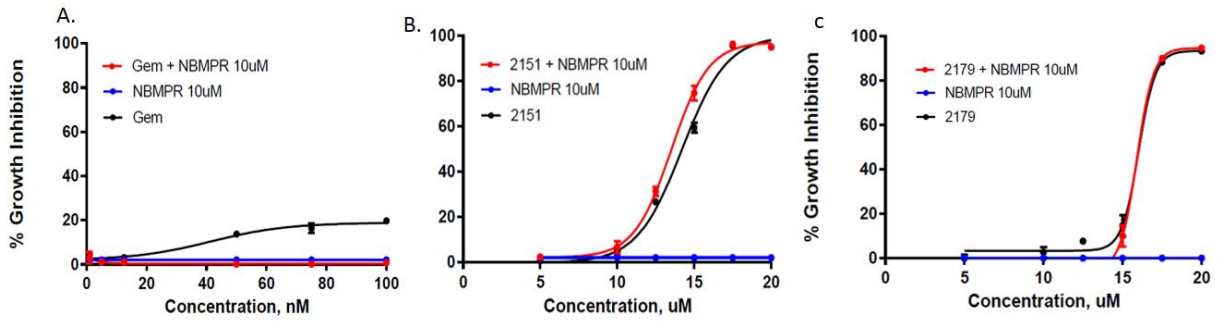

Figure 8. Inhibition of hENT1 in Panc-1 cells. Dependency of molecules on the hENT1 transporter for cell entry was assayed by inhibiting hent1 with the Nitrobenzylthioinosine (NBMPR). (A) Percentage of Growth Inhibition of Panc1 cells treated with increasing concentrations of either Gemcitabine, 10µM of NBMPR, or Gemcitabine and 10 µM of NBMPR for 96hrs. (B) Percentage of Growth Inhibition of Panc-1 cells treated with increasing concentrations of either LCB2151, 10µM of NBMPR, or LCB2151 and 10 µM NBMPR for 96hrs. (C) Percentage of Growth Inhibition of Panc-1 cells treated with increasing concentrations of either LCB2179, 10µM of NBMPR, or LCB2179 and 10 µM NBMPR for 96hrs. NBMPR treatment abolishes gemcitabine activity, while LCB2151 and LCB2179 growth curves are unaffected. ATP measured using Celltitre-Glo (Promega). Data are means of triplicates. N=1

cancer and chemoresistance has been studied by generating *DCK* knockout mice, lentiviral and siRNA-mediated *DCK* knockdown in cancer cell lines (Saiki et al., 2012; Shang et al., 2017a; Toy et al., 2010). I chose to knockdown *DCK* by transfecting Panc-1 cell line with two siRNA sets designed specifically for *DCK* (si*DCK*-1 and si*DCK*-2) or a scrambled sequence (ctrl) in Panc-1 cell line. After 24 hours, *DCK* mRNA expression was reduced by up to 95% (Figure 9A) and dCK protein expression was reduced after 24 & 48 hours (Figure 9B). Interestingly, treatment of Panc-1 cells with dCK knocked down, shows that LCB2151 (unexpectedly) and LCB2179 (expectedly) are unaffected by lowered dCK expression (Figure 9C). The caveat of this experiment was that Panc-1 is highly resistant to Gem, which is dependent on dCK for activation, therefore Gem could not be used as a positive control. Control options are discussed in the Discussion section to verify that the dCK knockdown was successful and this must be performed next.

3.1.3. LCB2151, LCB2179 and Gemcitabine Show Differential Gene Expression of Key Cellular Pathways in KRAS + and KRAS – Cancer Cell Lines

From a medicinal chemistry standpoint, lead molecule LCB2151 is structurally different from LCB2179 and both are different from Gem. While both molecules reach up to 99% cell killing of Gem-resistant cell lines (Figure 5A-C), we see signs that they work through distinct pathways from each other and from Gem. To elucidate the mechanism of action, changes in the mRNA expression of genes in major cellular pathways were analyzed. Genes of interest were selected through an in-depth literature search and organized into markers of resistance, apoptosis, proliferation and cellular stress (Table 5). Pancreatic cancer cell lines Capan-2 (*KRAS*+, most resistant) and BxPC-3 (*KRAS*-, least resistant) were treated with LCB2151, LCB2179, gemcitabine or vehicle for 6 and 18 hours. mRNA was collected, and expression levels were measured using qPCR. The results

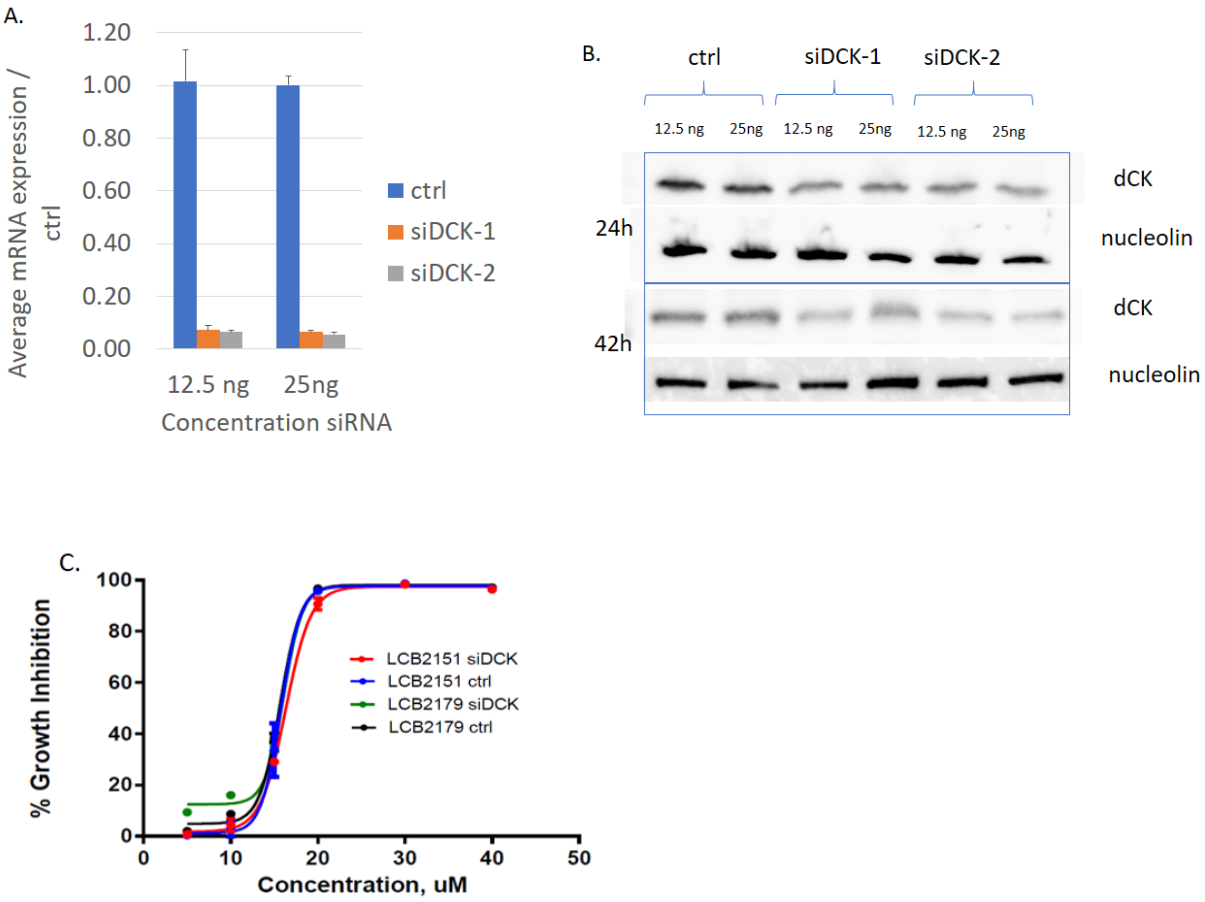

Figure 9. siRNA mediated knockdown of DCK in Panc1 cells. Panc-1 cells were transfected with siRNA designed against DCK to assay the requirements for their intracellular activation. Two sequences were tested at 12.5ng and 25ng doses (A) Both achieved up to 95% knockdown of DCK mRNA expression after 24hrs. Results are a mean of triplicates and normalized over the scrambled sequence (ctrl). (B) Protein levels of DCK are also decreased by both doses at 24 and 48h. Panc1 cells were transfected with siRNA set #1 designed against DCK or the scrambled sequence (ctrl). After 24hrs cells were treated with increasing concentration of (C) LCB2151 or LCB2179 for another 72h. Cell viability was measured using CellTire-Glo (Promega). Data are a mean of triplicates, normalized over vehicle-treated wells. N=1

Table 5. Genes measured in pancreatic cancer cell lines for expression profile. Genes measured for the genetic profile analysis of pancreatic cancer cell lines BxPC-3 and Capan-2, treated at two time points with lead drugs or gemcitabine, are grouped into key markers of resistance, anti/pro-apoptosis, cell proliferation and stress.

Resistance		Pro-apoptosis		Anti-apoptosis		Proliferation		Stress	
Protein	**Gene**	**Protein**	**Gene**	**Protein**	**Gene**	**Protein**	**Gene**	**Protein**	**Gene**
Multi-resistance protein 1 (MRP1)	ABCC1	BH3 interacting-domain death agonist (BID)	BID	BCL2 Family Apoptosis Regulator (MCL1)	MCL1	Nuclear Factor Kappa B Subunit 1	NKFB1	Superoxide Dismutase 1	SOD1
Multi-resistance protein 2 (MRP2)	ABCC2	Bcl-2-interacting killer (BIK)	BIK	X-Linked Inhibitor Of Apoptosis	XIAP	C-X-C Motif Chemokine Ligand 1 (GRO1)	CXCL1	Neutrophil cytosolic factor 2, p67phox	NCF2
Human equilibrative nucleoside transporter 1 (hENT1)	SLC29A1	Bcl-2- associated X protein (BAX)	BAX	BCL2, Apoptosis regulator	BCL2	Cyclin Dependent Kinase Inhibitor 1A (p21)	CDKN1A	Uncoupling Protein 2	UCP2
Cytidine deaminase	CDA	p53 upregulated modulator of apoptosis (PUMA)	BBC3	Bcl-xL, B-cell lymphoma-extra large	BCLXL	Cyclin D2	CCND2	Beclin 1	BECN1
Ribonucleotide reductase subunit M1	RRM1	Diablo IAP-Binding Mitochondrial Protein	DIABLO			Cyclin E1	CCNE1		
Deoxycytidine kinase	DCK	Endonuclease G	ENDOG			Cyclin E2	CCNE2		
		Tumor Protein P53	TP53						

show that lead molecules LCB2151 and LCB2179 have distinct gene expression profiles from one another and from Gem in both cell lines.

3.1.3.1. Resistance Markers

The differential regulation markers by Gem and our lead compounds are striking. Gem in BxPC-3, but not our compounds, upregulates ribonucleotide reductase subunit M1 *(RRM1)* and cytidine deaminase (*CDA*) (Figure 10A). *RRM1* will increase the pool of deoxynucleotides able to compete with Gem while *CDA* will deactivate it. Therefore, these enzymes will decrease the potential activity of Gem. Nucleoside transporter, *SLC29A1*, and *DCK* , the rate-limiting enzyme for nucleoside activation, are also upregulated by Gem. These should increase the potential activity of Gem, a trend that is noted when Capan-2 resistant cells are treated with Gem (Figure 10B). Clearly these markers are not at the origin of Gem resistance. LCB2151 also activates nucleoside transporter *SLC29A1* in Capan-2 while decreasing it in BxPC-3 cell line. These markers alone are not useful in explaining the increase of cell death by lead molecules in resistant cell lines.

3.1.3.2. Pro- and Anti-Apoptosis Markers

In BxPC-3 cells (Figure 10C), Gem significantly increases *DIABLO* and *BBC3* (PUMA) which is not seen in Capan-2 cells (Figure 10D). However, LCB2151 increases *BBC3* in both cell lines while also increasing *BAX* and *BIK* in Capan-2. Clearly, in Capan-2, pro-apoptosis markers are increased in the presence of LCB2151 as opposed to Gem. Importantly, *BCL2*, an anti-apoptosis marker, is reduced in LCB2151 Capan-2 treated cells (Figure 10F) and not in BxPC-3 (Figure 10E). This increase in ratio between *BAX* and *BCL2* and its resulting effects is worth following since it has been suggested to overcome Gem resistance in pancreatic cancer cells (Schniewind et al., 2004). Interestingly, mitochondrial driven apoptosis increases complex II activity, which

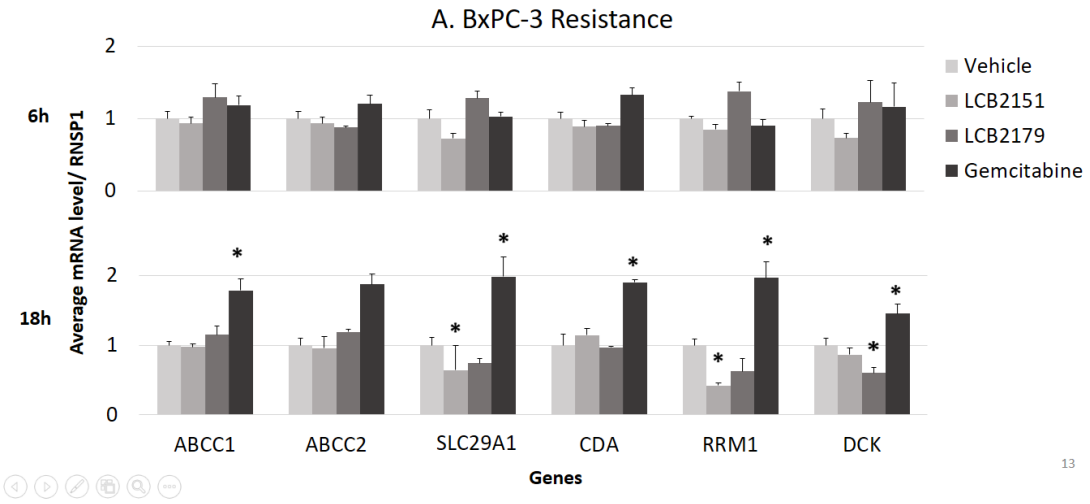
A. BxPC-3 Resistance
6h
18h
Average mRNA level/ RNSP1
Vehicle
LCB2151
LCB2179
Gemcitabine
ABCC1
ABCC2
SLC29A1
CDA
RRM1
DCK
Genes

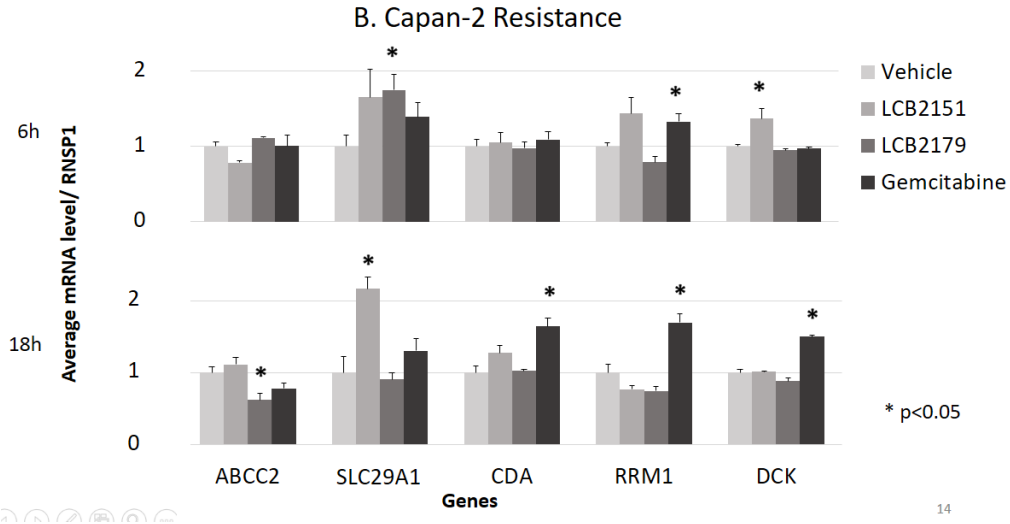
B. Capan-2 Resistance
6h
18h
Average mRNA level/ RNSP1
Vehicle
LCB2151
LCB2179
Gemcitabine
* p<0.05
ABCC2
SLC29A1
CDA
RRM1
DCK
Genes

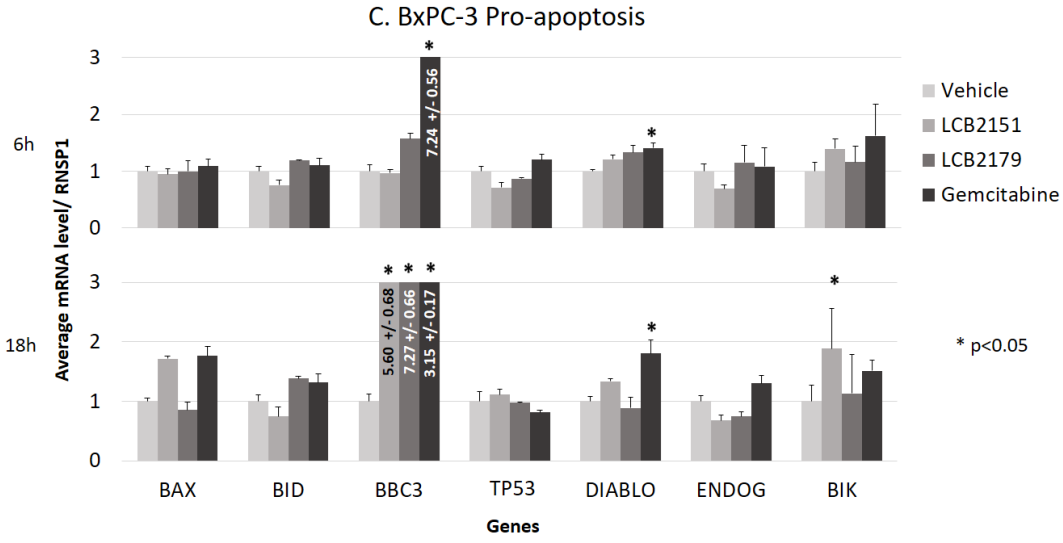
C. BxPC-3 Pro-apoptosis
6h
18h
Average mRNA level/ RNSP1
7.24 +/- 0.56
5.60 +/- 0.68
7.27 +/- 0.66
3.15 +/- 0.17
Vehicle
LCB2151
LCB2179
Gemcitabine
* p<0.05
BAX
BID
BBC3
TP53
DIABLO
ENDOG
BIK
Genes

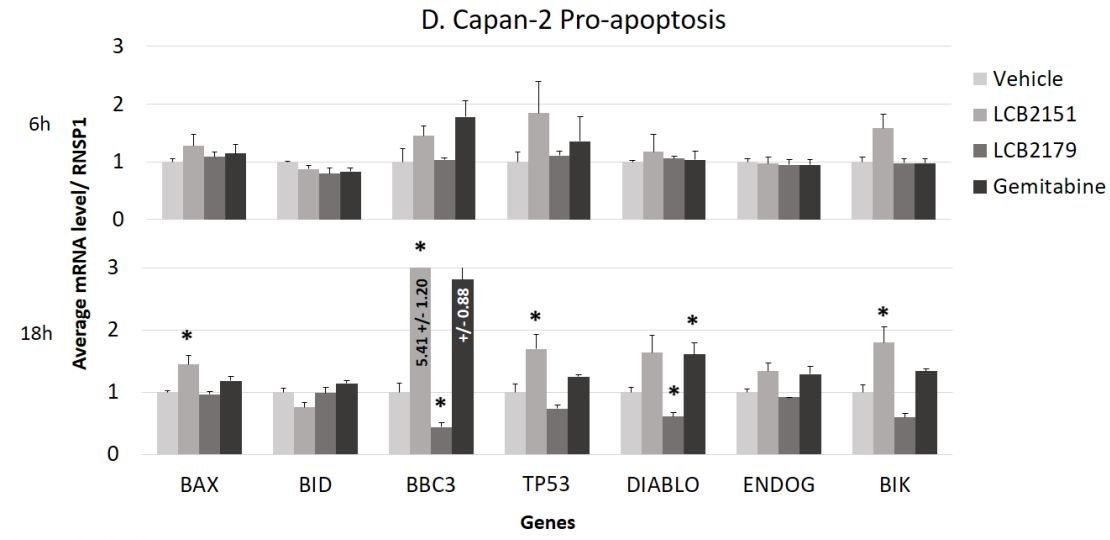
D. Capan-2 Pro-apoptosis
6h
18h
Average mRNA level/ RNSP1
Vehicle
LCB2151
LCB2179
Gemitabine
5.41 +/- 1.20
+/- 0.88
BAX
BID
BBC3
TP53
DIABLO
ENDOG
BIK
Genes

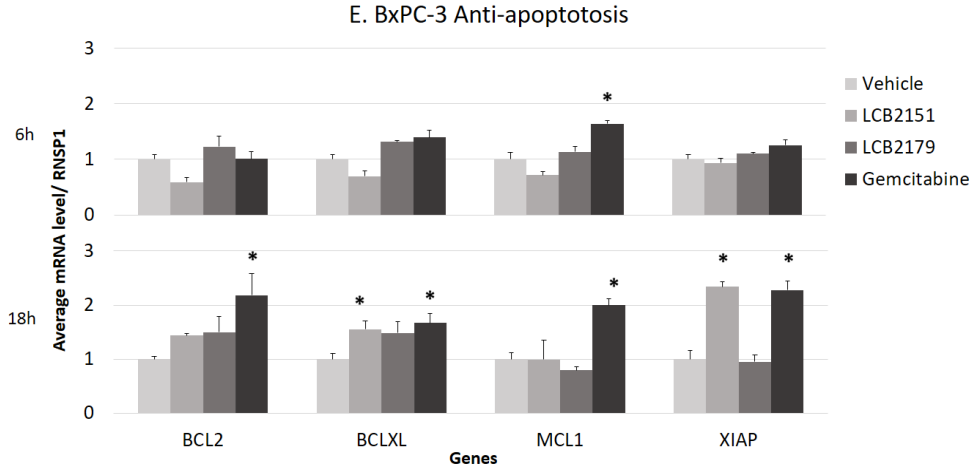
E. BxPC-3 Anti-apoptotosis
6h
18h
Average mRNA level/ RNSP1
Vehicle
LCB2151
LCB2179
Gemcitabine
BCL2
BCLXL
MCL1
XIAP
Genes

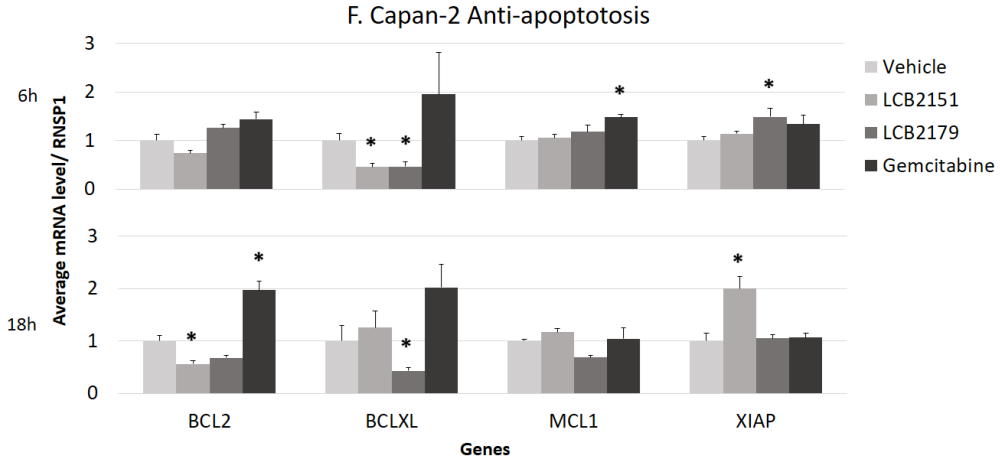
F. Capan-2 Anti-apoptotosis
6h
18h
Average mRNA level/ RNSP1
Vehicle
LCB2151
LCB2179
Gemcitabine
BCL2
BCLXL
MCL1
XIAP
Genes

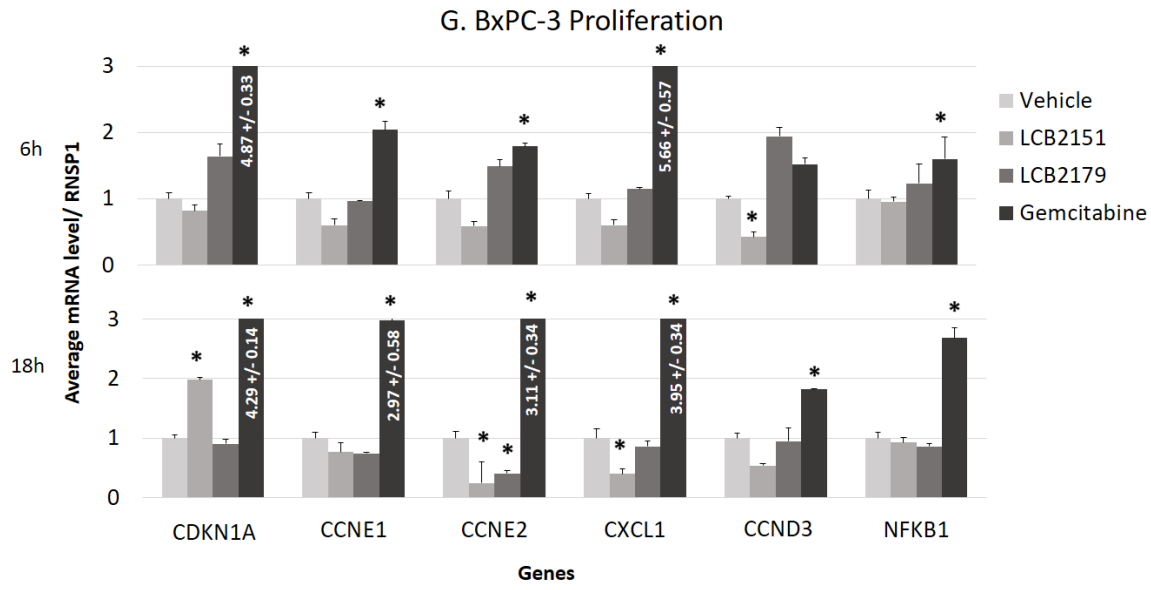
G. BxPC-3 Proliferation
6h
18h
Average mRNA level/ RNSP1
4.87 +/- 0.33
5.66 +/- 0.57
4.29 +/- 0.14
2.97 +/- 0.58
3.11 +/- 0.34
3.95 +/- 0.34
CDKN1A
CCNE1
CCNE2
CXCL1
CCND3
NFKB1
Genes
Vehicle
LCB2151
LCB2179
Gemcitabine

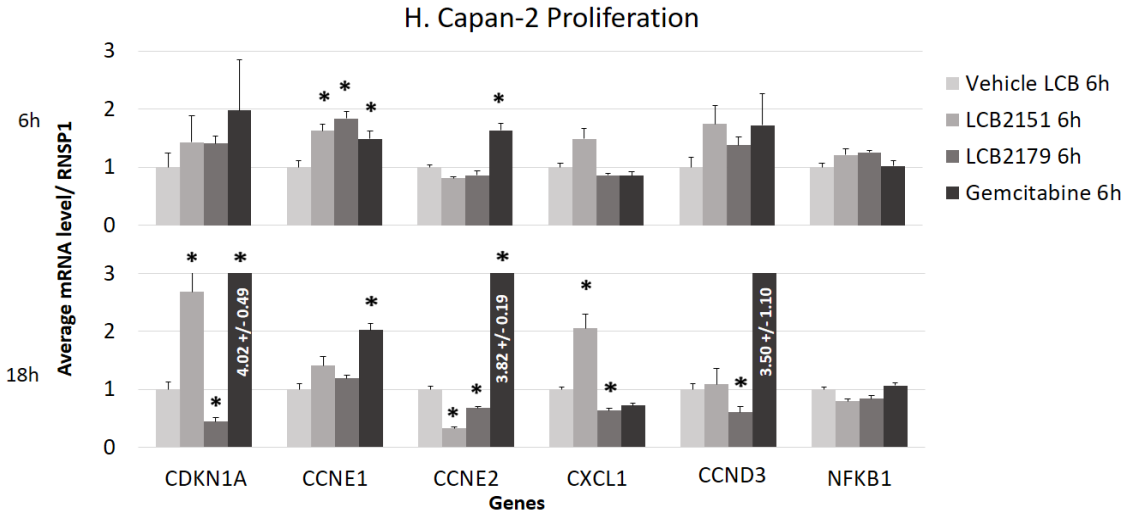
H. Capan-2 Proliferation
6h
18h
Average mRNA level/ RNSP1
4.02 +/- 0.49
3.82 +/- 0.19
3.50 +/- 1.10
CDKN1A
CCNE1
CCNE2
CXCL1
CCND3
NFKB1
Genes
Vehicle LCB 6h
LCB2151 6h
LCB2179 6h
Gemcitabine 6h

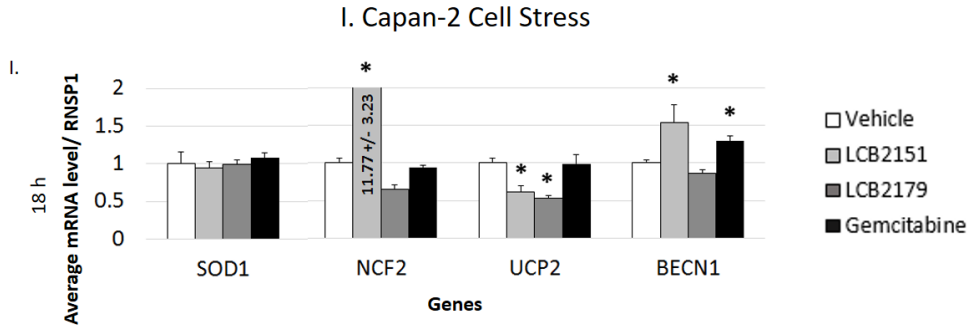
I. Capan-2 Cell Stress
I.
18 h
Average mRNA level/ RNSP1
11.77 +/- 3.23
SOD1
NCF2
UCP2
BECN1
Genes
Vehicle
LCB2151
LCB2179
Gemcitabine

Figure 10. Drug-induced gene expression profiles of pancreatic cancer cell lines. mRNA expression levels of genetic markers of resistance, pro/anti-apoptosis, proliferation and stress measured in BxPC-3 (KRAS+) and Capan-2 (KRAS-) treated with 15 µM LCB2151, 15 µM LCB2179, 1 µM of Gemcitabine or DMSO vehicle for 6 and 18 hours. (A) BxPC-3 resistance gene profile, (B) Capan-2 resistance gene profile, (C) BxPC-2 pro-apoptotic gene profile, (D) Capan-2 pro-apoptotic gene profile, (E) BxPC-3 anti-apoptotic gene profile, (F) Capan-2 anti-apoptotic gene profile, (G) BxPC-3 proliferation gene profile, (H) Capan-2 proliferation gene profile, (I) Capan-2 cellular stress gene profile. Bars represent a mean of four replicates, N=1. Results were normalized to the housekeeping gene RNPS1 mRNA expression, and calibrated to the results with DMSO (fold change of 1). *$p < 0.05$ using t-test.

oxidizes succinate to fumarate (Ehinger et al., 2016). As described later, succinate levels are affected in LCB2151 treated cells.

3.1.3.3. Proliferation Markers

Microarray studies indicate that CPI-613 downregulates the mRNA expression of pro-proliferative Cyclin D3 (*CCND3*), E1 (*CCNE1*), E2 (*CCNE2*) of BxPC-3 pancreatic cancer cells but not of non-transformed NIH-3T3 mouse fibroblast cells (Lee *et al*., 2014). It would be interesting to determine the effects that our lead molecules have on these proliferation markers. The analysis of proliferation markers shows significant differences between the lead molecules and Gem (Figures 10G and 10H). Cell lines treated with Gem upregulated both proliferative genes *CCNE1*, *CCNE2* and *CCND3* and the growth arrest gene of p21, *CDKN1A*. Anti-proliferative *CDKN1A* was increased by LCB2151 in both cell lines at 18 hours while decreased by LCB2179 in only Capan-2 at 18 hours. Overall, LCB2151 and LCB2179, which both contain our lipoate analogue, show a statistically relevant decrease in only *CNNE2* at 18 hours in BxPC3 and Capan-2.

3.1.3.4. Cellular Stress Markers

The effect of our lead molecules on mitochondrial biogenesis was tested next. Since they contain a lipoate moiety designed to interfere with mitochondrial bioenergetics, increased expression of oxidative and other stress markers was expected. Previous investigation into the mechanism of LCB2151 demonstrated an upregulation of Neutrophil Cytosolic Factor 2 (*NCF2)* and a downregulation of cytoplasmic superoxide dismutase (*SOD1)* in HepG2 cell line treated with LCB2151 for 12 hours (C.Teran MSc Thesis). SOD1 is involved in one of the reducing pathways of the cell and NCF2/p67^{phos} (NADPH oxidase) is shown to induce ROS production (Crapo *et al*.,

1992; Roy et al., 2015). These genes were tested in addition to the marker mitochondrial uncoupling protein 2 (*UCP2)* in Capan-2 cell line at 18 hours (Figure 10I). Both lead molecules but not Gem reduced *UCP2* levels , which is overexpressed in pancreatic cancer and promotes cancer progression (Donadelli *et al*., 2015). *NCF2* expression is increased by LCB2151 treatment, while *SOD1* remains unchanged under these conditions. None of the markers tested were significantly changed by Gem, consistent with reports that it does not increase *NCF2* in HepG2 cells (Dalla Pozza *et al*., 2012).

Overall changes in gene expression reveal significant differences, generally associated with more favourable anti-tumour outcomes of the lead molecules as compared to Gem.

3.2. Aim 2: Adaptations to Cellular Pathways in Response to Drug Treatment

Our group has identified two novel compounds, LCB2151 and LCB2179, with anticancer activity that exceed the leading chemotherapy agent Gem *in vitro*. It is increasingly clear that our lead compounds have a different mechanism of action from each other and from that of Gem. Immediate efforts were focused on elucidating the mechanism of action of LCB2151 in the widely used Panc-1 cells using a combination of proteomics, central carbon metabolism as well as mitochondrial bioenergetics (oxidative stress determination, Seahorse XF analysis). Together, these approaches provided key insights into the mechanism of action of these proprietary anticancer agents.

3.2.1. LCB2151 Alters Whole-Cell Protein Expression in Cell Pathways after 6 Hours

Gene profile analysis was a biased method to investigate changes in cellular pathways predicted to be affected by the lead molecules. Proteomics combined with computational bioinformatics was a non-biased strategy adopted to investigate the specific mechanisms by which

LCB2151 efficiently eradicates chemoresistant pancreatic cancer cells. Panc-1 cell line was treated with 20 μM LCB2151 or vehicle for 6 hours and whole cell extracts were submitted for mass spectrometry-based large-scale proteomic analysis. To pass the threshold of significance, Q50 proteins had to be detected in 2 of 3 replicates in each condition. A total of 1327 Q50 proteins were identified, of which 1010 proteins (76.1%) were shared, 296 (22.3%) were detected only in LCB2151-treated samples and 12 (1.6%) were only detected in vehicle-treated samples (Figure 11A). Principal component analysis (PCA) shows that the LCB2151-induced proteome is unique from the vehicle-induced proteome (Figure 11B), suggesting major changes at the protein level in various cellular pathways.

Shared Q50 proteins were analysed by fold change with a 1.5-fold cut off. LCB2151 treatment upregulated 33 proteins (more than 1.5-fold) and 1 protein was downregulated (more than 50%) according to the threshold (Figure 11C). Organization of the shared proteins into cellular pathways reveals 8 cellular pathways that are altered by LCB2151 treatment including redox state, carbon metabolism and respiration, cancer apoptosis, transport, transcription and translation (Table 6).

Functional network analysis of the unshared 296 proteins only detected in LCB2151-treated samples generates a complex functional network (Figure 12). Of these, 212 proteins were further sorted into 107 biological pathways using the String database for analyses, summarised in Table 7. Most proteins were upregulated in metabolic processes such as fatty acid (ex. acyl-CoA synthetase long-chain family member 3), glucose (ex. Hexokinase 1) and nucleotide (ex. Polyribonucleotide nucleotidyltransferase 1) metabolism. Additionally, proteins involved in gene expression, transport, response to stress, cell cycle and oxidative stress were upregulated by LCB2151. Interestingly, DLST protein was detected and matched to 11 biological pathways including metabolism and oxidation-reduction processes.

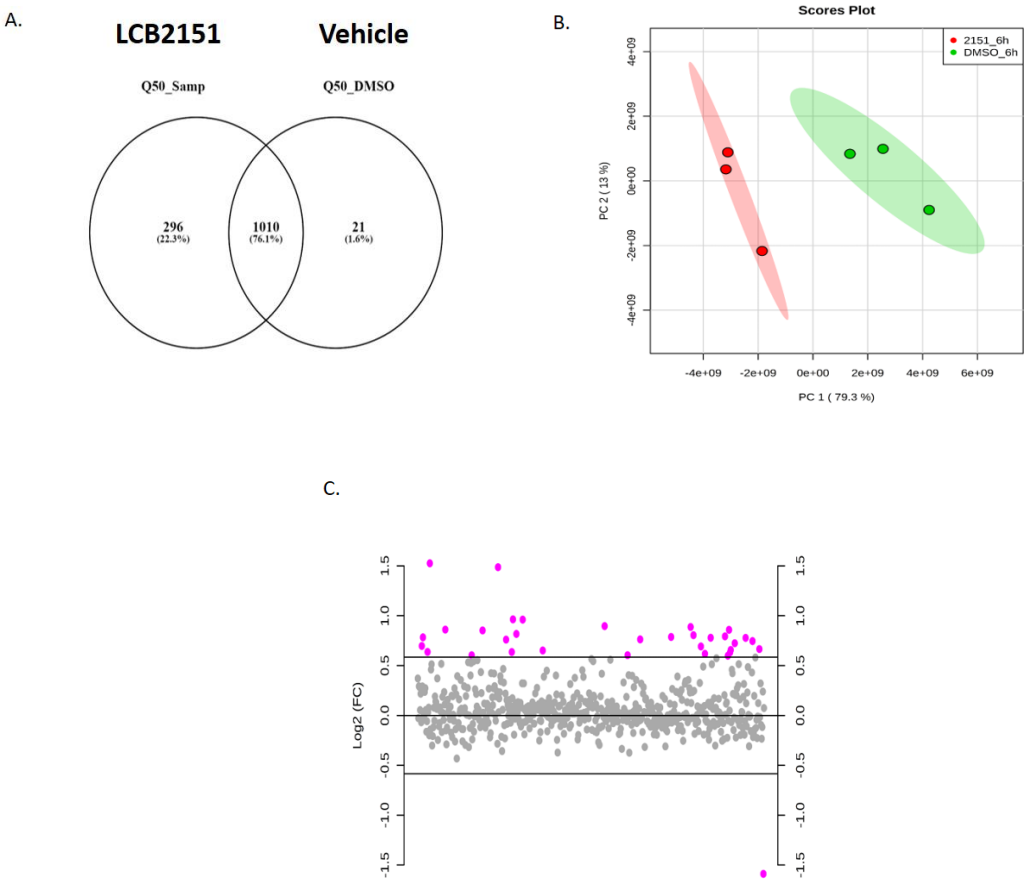

Figure 11. Analysis of total Q50 identified proteins. Panc-1 cells were treated with LCB2151 20 µM or vehicle for 6h. Whole cell protein extracts went through large scale protein analysis. A total of 1327 Q50 proteins (identified in 2 or more samples of triplicates) were identified. (A) Of those, 1010 proteins (76.1%) common to both treatment groups. Furthermore, 296 proteins (22.3%) and 21 proteins (1.6%) were uniquely identified in the LCB2151-treated and vehicle-treated groups, respectfully. Venn diagram generated using Venny 2.1 software. (B) Control proteome is clearly segregated from LCB2151-treated proteomes by PCA using proteomic data from the shared 1010 proteins. PCA analysis performed using Metaboanalyst (v4.0) software. (C) Fold change analysis of shared Q50 proteins. Threshold for analysis was cut-off at a 1.5-fold change. After LCB2151 treatment, 33 proteins were upregulated more than 1.5 fold and 1 protein was downregulated more than 0.5 fold. N=3

Table 6. Major cellular pathways of shared Q50 proteins. Panc-1 cells were treated with LCB2151 20 µM or vehicle for 6 hours. Whole cell protein extracts went through large scale protein analysis. Shared Q50 proteins that passed the 1.5 fold-change cut-off were organized based on major cellular pathways. Analysis was aided using String database and GenATLAS. N=3

Protein	Fold Change
Redox State	
Thioredoxin	1.5707
SH3 domain-binding glutamic acid-rich-like protein 3	1.552
Carbon Metabolism and Respiration	
Glutamine--fructose-6-phosphate aminotransferase [isomerizing] 1	1.6154
Isocitrate dehydrogenase [NADP] cytoplasmic	1.5542
Cytochrome b-c1 complex subunit 2, mitochondrial	1.8058
Cancer Apoptosis	
Coiled-coil-helix-coiled-coil-helix domain-containing protein 2;Putative coiled-coil-helix-coiled-coil-helix domain-containing protein CHCHD2P9, mitochondrial	0.3324
Transport	
Rho-related GTP-binding protein RhoG	1.7472
Dynactin subunit 2	1.7163
Tubulin alpha-1C chain	1.52
Importin-4	1.652
Coatomer subunit delta	1.5203
Brain-specific angiogenesis inhibitor 1-associated protein 2	1.5864
Transcription and Translation	
DNA replication licensing factor MCM7	1.8611
Eukaryotic translation initiation factor 3 subunit H	1.8165
26S proteasome non-ATPase regulatory subunit 5	1.733
Small nuclear ribonucleoprotein F	1.7254
Asparagine--tRNA ligase, cytoplasmic	1.6941
Nucleolar RNA helicase 2	1.6772
Pre-mRNA-processing-splicing factor 8	1.5761
Heterogeneous nuclear ribonucleoprotein D-like	1.621
Splicing factor 3A subunit 3	1.5351
Metastasis	
Nodal modulator 1;Nodal modulator 3;Nodal modulator 2	2.8798
Protein CYR61	2.803
6-phosphogluconolactonase	1.9505
Plasminogen activator inhibitor 1	1.9469
Platelet-activating factor acetylhydrolase IB subunit beta	1.8494
Epidermal growth factor receptor;Receptor protein-tyrosine kinase	1.7625
Eukaryotic translation initiation factor 5B	1.721
Heterogeneous nuclear ribonucleoprotein A3	1.6968
General	
Putative heat shock protein HSP 90-beta 2	1.5146
Tumor protein D54	1.5553
Cancer Favorable Prognosis	
RRP12-like protein	1.8134
Myb-binding protein 1A	1.7147

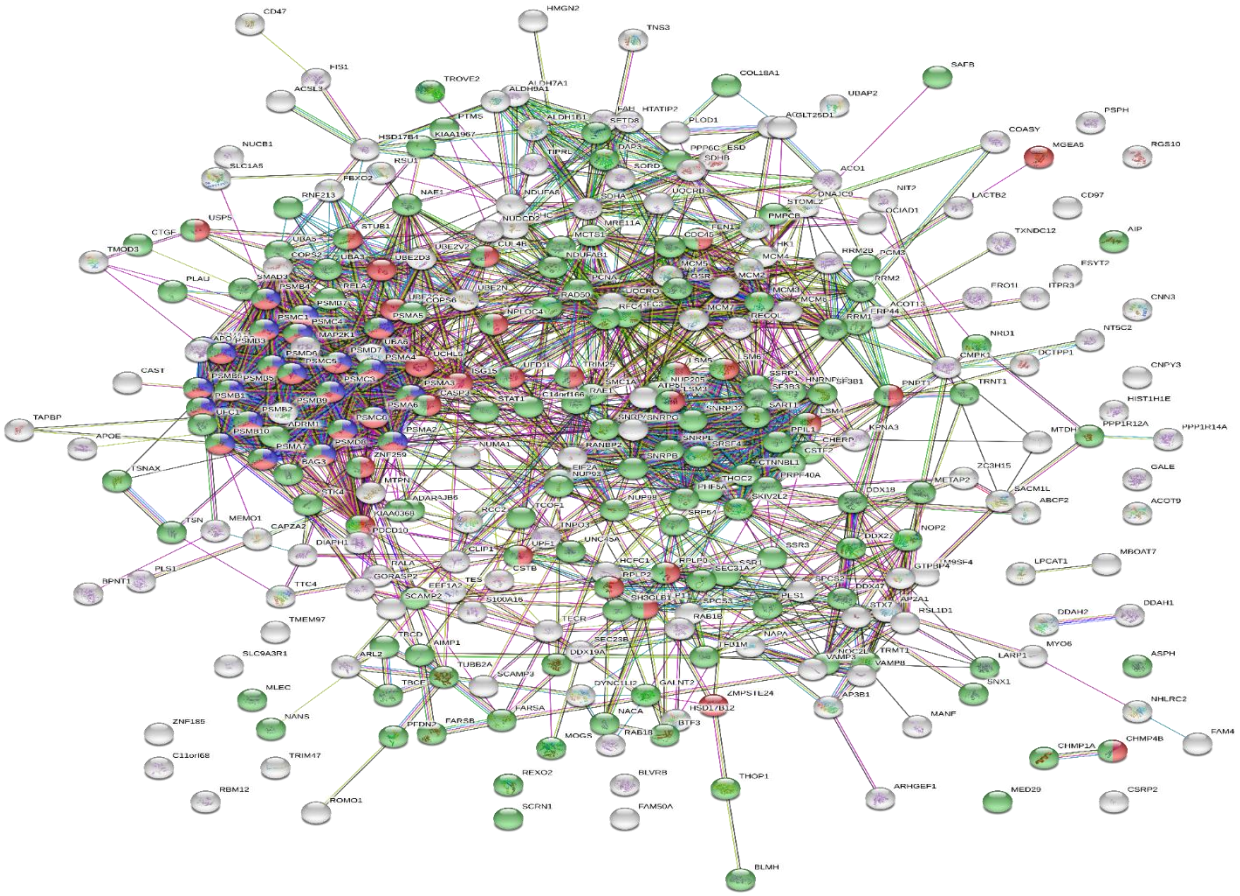

Figure 12. Functional network of proteins only found in LCB2151-treated group. Panc-1 cells were treated with LCB2151 20 µM or vehicle for 6h. Whole cell protein extracts went through large scale protein analysis. 296 proteins were only identified in LCB2151-treated panc-1 samples. A complex functional network of these proteins was generated using String database (v10.5). N=3

Table 7. Major biological pathways of unshared Q50 proteins in LCB2151-treated group. Panc-1 cells were treated with LCB2151 20 µM or vehicle for 6h. Whole cell protein extracts went through large scale protein analysis. Of the 296 unshared Q50 proteins in LCB-2151 treated samples, 212 were organized based on biological pathways. Most proteins upregulated by LCB2151 are involved with metabolism. (*****) denotes pathways where DLST is involved. Analysis was aided using String database. N=3

Pathway Description	Observed Gene Count	FDR	Example of Protein	Protein Function
*metabolic process	117	0.00422	Aldehyde dehydrogenase 1 family, member B1	detoxification of alcohol-derived acetaldehyde and role in lipid oxidation
			Polyribonucleotide nucleotidyltransferase 1	RNA-binding protein implicated in nucleotide metabolism
			acyl-CoA synthetase long-chain family member 3	synthesis of cellular lipids and degradation via beta-oxidation
			Solute carrier family 25 (mitochondrial carrier; phosphate carrier), member 24	role in protecting cells against oxidative stress- induced cell death
			Hexokinase 1	glucose transport, localizes to the outer membrane of mitochondria
gene expression	59	0.0248	Adenosine deaminase, RNA-specific	deamination of adenosine to inosine in double-stranded RNA (dsRNA)
transport	58	0.000912	HIV-1 Tat interactive protein 2,	Oxidoreductase required for tumor suppression
response to stress	57	0.00181	Stomatin (EPB72)-like 2	regulates the biogenesis and the activity of mitochondria
cell cycle	32	0.000518	Malignant T cell amplified sequence 1	Anti-oncogene that plays a role in cell cycle regulation
*oxidation-reduction process	22	0.0301	Peptidylprolyl isomerase F	In cooperation with TP53 is involved in activating oxidative stress-induced cell death

This data set is a valuable tool and can be analyzed multiple ways, continuously revealing new information. Using publicly available software we have been able to show that LCB2151 has a significant effect on the proteome of cancer cells, driven by changes in expression of proteins involved in mostly metabolic pathways. We are in the process of acquiring Ingenuity® Pathway Analysis (IPA®, Qiagen) analysis and search tool that will provide further in-depth analysis, integration, and interpretation of data derived from 'omics' experiments such as proteomics. With the increased power of tool we hope to uncover effected pathways and identify candidate targets of our drugs, without repeating the experiment.

3.2.2. LCB2151 Treatment Targets Two Key Enzymatic Steps in Central Carbon Metabolism

Considering that LCB2151 is designed to interfere with cancer cell metabolism and that its treatment upregulated protein expression related to metabolic processes, investigation was focused on changes in carbon metabolism and mitochondrial biogenesis induced by LCB2151. A high-throughput analysis of the glycolysis and TCA pathways was done using Panc-1 cells treated/untreated with 20 μM LCB2151 for 6 hours. This involved identifying and quantifying 50 metabolites (quintuplet samples) by HPLC-MS/MS (Creative Proteomics). The results indicate that LCB2151 treatment led to significant changes in approximately half of the metabolites, increasing 14 and decreasing 9 significantly (Table 8). A map of central carbon metabolism combining proteomic and metabolomic analyses identifies two enzymatic reactions targeted by LCB2151 (Figure 13). The first is apparent inhibition of the reaction catalyzed by cytoplasmic phosphorofructokinase-1 (PFK-1), the rate-limiting step of glycolysis (Figure 14A). The substrates glucose-6-phosphate and fructose-6-phosphate are increased by 3.17 and 2.21-fold, respectively, while the product fructose 1,6-bisphosphate is decreased by 0.29-fold, a surprising result. The

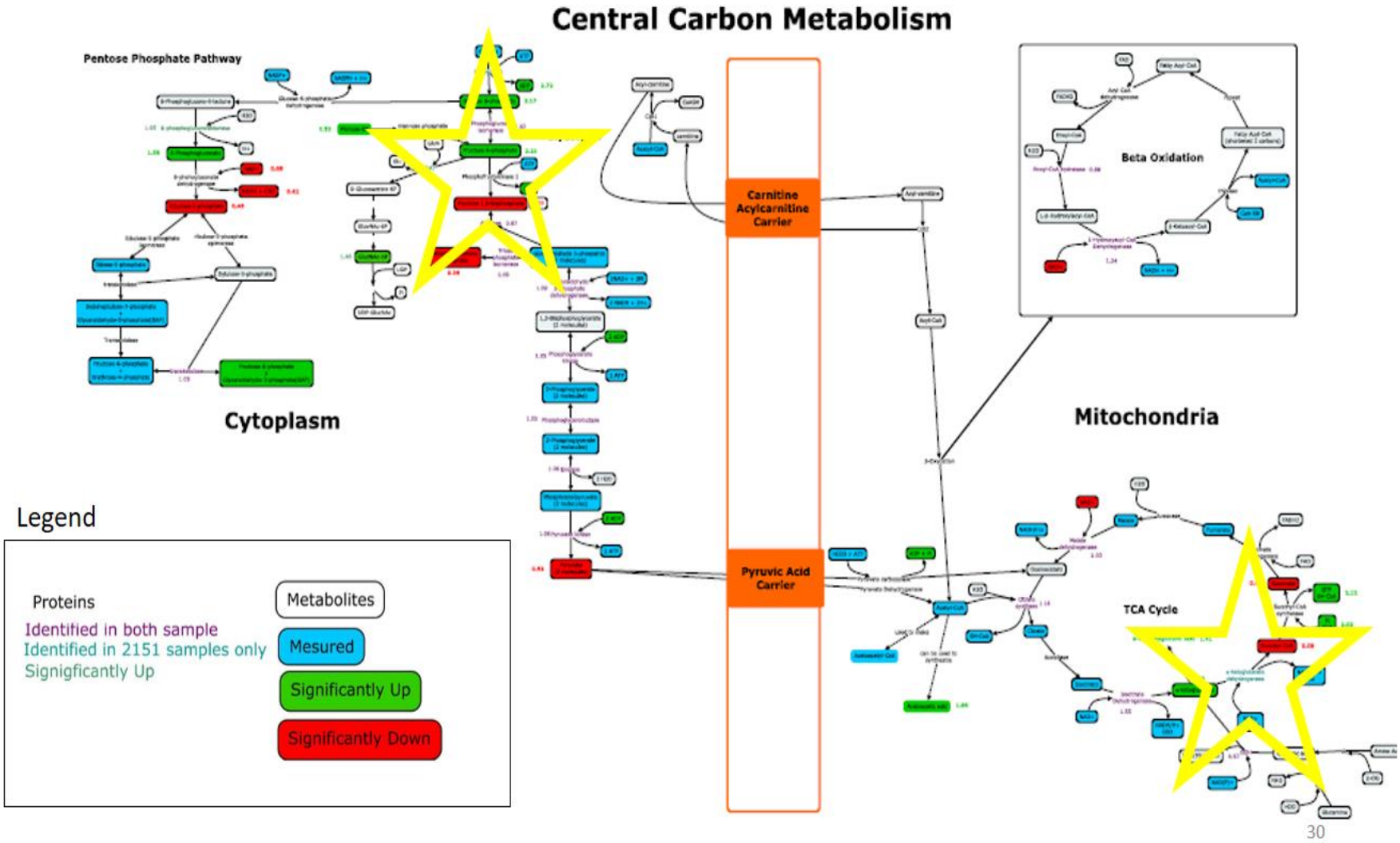

Figure 13. Overview of central carbon metabolism combining metabolomic and proteomic data. Panc-1 cells were treated by LCB-2151 20uM or vehicle for 6 hours. 50 metabolites in 5 central carbon metabolism pathways were measured by HPLC-MS/MS (Creative Proteomics). Protein expression was also measured at 6 hours by MS analysis (University of Ottawa). Proteomic and metabolomic data combined in the above poster (an overview) reveals inhibition of two metabolic reactions (yellow stars). Protein expressions are indicated by font colour and metabolite fold changes are indicated by bubble colour, with the fold change amount beside them. Metabolite analysis was an average of 5 replicates for each treatment and proteomic analysis was performed in triplicate. N=5

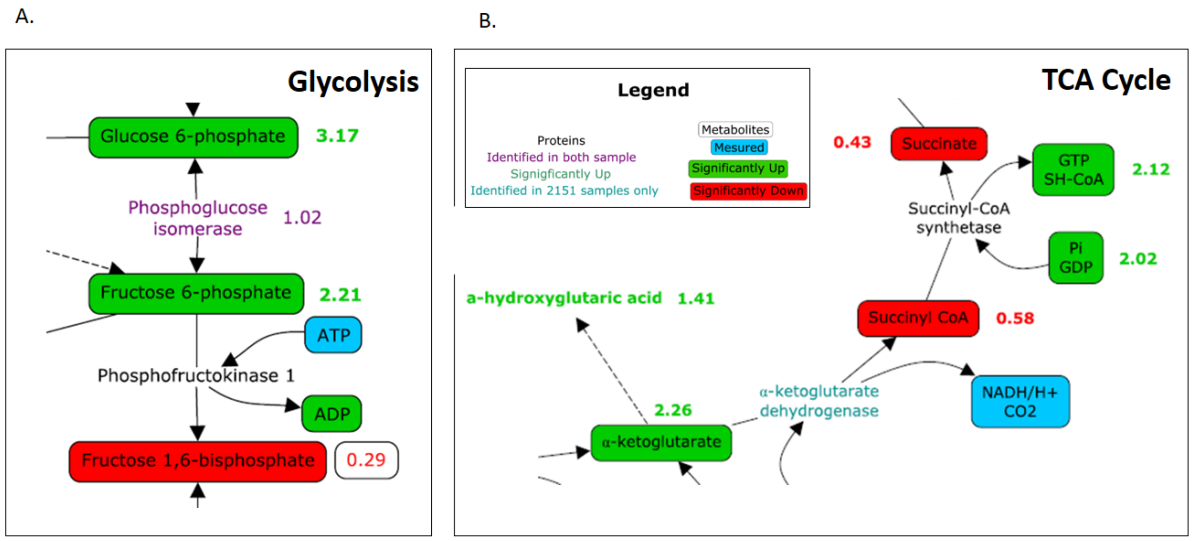

Figure 14. LCB2151 targets two metabolic reactions in central carbon metabolism. Panc-1 cells were treated with LCB2151 or vehicle for 6 hours before undergoing proteomic and metabolomic analyses (A) Cytoplasmic phosphofructokinase-1 targeted by LCB-2151. Metabolomic analysis reveals an increase of PFK-1 substrates Glucose-6-phosphate and fructose-6-phosphate and a decrease of the product fructose-1,6-bisphosphate. (B) Mitochondrial α-Ketoglutarate dehydrogenase targeted by LCB-2151. Proteomic analysis only detected α-KGDH subunit E2 (DLST) expression in LCB-2151 treated samples. Metabolomic analysis reveals an increase of α -KGDH substrate α -ketoglutarate and a decrease of products succinyl Co-A and downstream succinate. Combined results suggest inhibition of the TCA cycle in the mitochondria at the level of α -KGDH. Fold changes are measured with respect to vehicle-treated samples. Red, decrease; green, increase. N=5

Table 8. Central Carbon Metabolism Analysis. Panc-1 cells were treated by LCB-2151 20 µM or vehicle for 6 hours. 50 metabolites in 5 central carbon metabolism pathways were measured by HPLC-MS/MS (Creative Proteomics). Metabolite analysis was an average of 5 replicates for each treatment. Fold-change was calculated between vehicle and LCB2151-treated samples. Green, upregulated & red, downregulated. $p<0.05$ considered significant. N=5

Metabolite	fold change	p-value
Phosphocreatine	3.68	0.000
Glucose-6P	3.17	0.004
ADP	2.72	0.000
Mannose-6P	2.33	0.012
α-Ketoglutaric acid	2.26	0.001
Fructose-6P	2.21	0.000
GTP	2.12	0.034
GDP	2.02	0.000
Acetoacetic acid	1.65	0.005
Ribulose-1,5bisP	1.58	0.010
6P-Gluconate	1.56	0.002
Glucosamine-6P	1.47	0.019
Acetylglucosamine-1P	1.46	0.006
α-Hydroxyglutaric acid	1.41	0.028
NAD+	0.68	0.001
Succinyl-CoA	0.58	0.041
Pyruvic acid	0.51	0.003
Ribulose-5P	0.46	0.020
Succinic acid	0.43	0.000
NADH	0.42	0.005
DHAP	0.35	0.006
Glycerol-3P	0.30	0.000
total_Glucose-bisP/Fructose-bisP	0.29	0.010

second is apparent inhibition of the reaction catalyzed by mitochondrial KGDH of the TCA cycle (Figure 14B). The substrate α-ketoglutarate is increased by 2.26-fold, while the products succinyl-CoA and downstream succinate are decreased by 0.58 and 0.43-fold respectively. Inhibition of KGDH was an expected outcome since LCB2151 is designed with a lipophilic CPI-613 derivative. As mentioned before, CPI-613 was reported to interfere with the metabolism of cancer cells, albeit at high concentration, through inhibition of PDC and KGDH, and increased intracellular ROS (Stuart et al., 2014; Zachar et al., 2011). Meanwhile, pyruvate dehydrogenase complex (PDH) does not appear to be affected by LCB2151. This is consistent with *in vitro* studies (Reaction Biology Corporation, Pennsylvania) that revealed no significant effect of LCB2151 on PDK1-4 enzymatic activity (data not shown), which regulate PDH. Inhibition of PFK-1 by LCB2151 is an unexpected result that merits further investigation, since neither Gem (nucleoside analogue) nor CPI-613 (lipoate) were reported to interfere with this pathway.

3.2.1. LCB2151 Significantly Impairs Mitochondrial Respiration of Panc-1 Cell Line

Our lab investigated oxidative and glycolytic metabolic characteristics of Panc-1 cell lines treated with LCB2151, LCB2179, Gem or vehicle for 6 hours (Figure 15). Mitochondrial function was assessed in real-time by measuring oxygen consumption rate (OCR) after performing the Mito Stress Test using the Seahorse XF Analyzer (Agilent) technology in high glucose medium. LCB2151 significantly lowers maximal respiration (Figure 15B), ATP production (Figure 15E) and spare respiratory capacity (Figure 15F). Meanwhile, basal respiration (Figure 15A), proton leak (Figure 15D) and non-mitochondrial oxygen consumption (Figure 15C) remain unaffected in cells treated with LCB2151. Under these conditions, neither LCB2179 nor Gem seem to cause any significant mitochondrial impairment.

3.2.2. LCB2151 Decreases Glycolytic Capacity of Panc-1 Cell Line

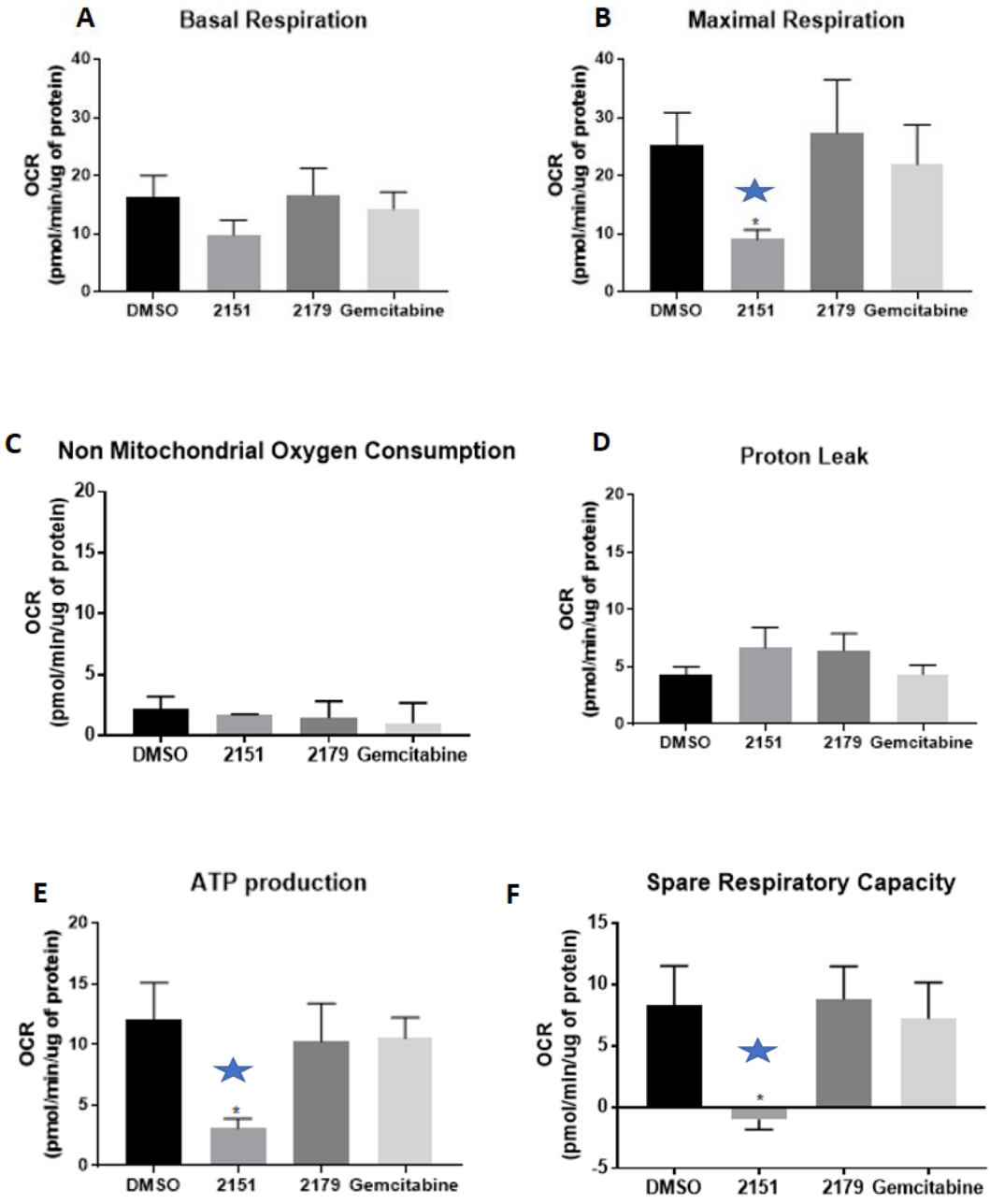

Figure 15. Seahorse XF24 analyzer bioenergetic determinations for in PANC1 cells treated with 2151 for 6 hours. Oxygen consumption rate (OCR) normalized to protein content are presented for basal respiration (A), maximal respiration (B), non-mitochondrial oxygen consumption (C) proton leak (D), ATP production (E) and spare respiratory capacity (F). LCB2151 significantly lowers ATP production, spare capacity and coupling efficiency of treated cells. N=3, data are presented as mean ± SEM. * $p<0.05$, Student's t test comparing DMSO vs 2151. Statistical analysis done using GraphPad Prism 7 one-way ANOVA. Concentrations: 2151:15μM; 2179: 15μM and Gemcitabine: 0.75μM.

It is suggested by the previously described metabolomics data, that LCB2151 interferes PFK-1 in the cytoplasm. Thus, an impairment of the cells ability to increase glycolysis to meet metabolic and bioenergetic demands should be observed. The glycolysis stress test was performed in Panc-1 cells starved of glucose and pyruvate that were treated for 6 hours to measure in real-time the capacity of the glycolytic pathway by driving cells toward glycolysis when glucose is re-introduced to the media. Extracellular acidification rate (ECAR) measurements show that LCB2151 treatment reduces the glycolytic reserve of the cells (Figure 16C), defined as the difference between glycolysis under basal condition and maximal glycolytic capacity (Mookerjee et al., 2016). This reserve is unused in the basal state but could be recruited in response to increases in ATP demand. Therefore, by reducing glycolytic reserve LCB2151 would render cells more sensitive to ATP depletion. Basal glycolysis (Figure 16A) and maximal glycolytic capacity (Figure 16B) were not significantly affected by LCB2151.

3.2.3. LCB2151 Decreases the GSH/GSSG Ratio in Panc-1 Cell Line

Analysis of mRNA levels showed that LCB2151 treatment increases levels of *NCF2*, an essential component of NADPH oxidative function, and reduces the levels of *SOD1* in HepG2 cell line, as well as *UCP2* in Capan-2 cell line after 12 and 18 hours, respectively. Together with potential inhibition of KGDH in the mitochondria (Figure 11B), it can be suggested that LCB2151 treatment induces oxidative stress. Glutathione (GSH) is an abundant antioxidant found in all human cells, involved in protection of cells from oxidative stress (Griffith, 1999; Pompella et al., 2003; Sies, 1999). A change in GSH levels is important in the assessment of toxicological responses and is an indicator of oxidative stress, potentially leading to apoptosis or cell death. Certain chemicals react

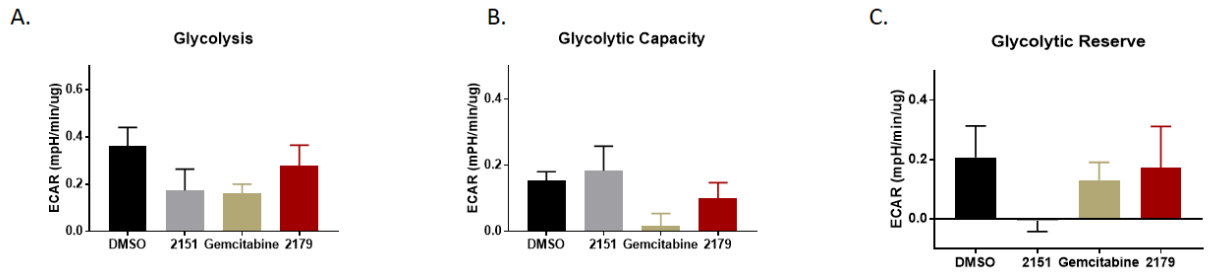

Figure 16. Glycolysis Stress test determinations for in PANC1 cells treated with 2151 for 6 hours. (ECAR) is measured in cells are incubated in the glycolysis stress test medium without glucose or pyruvate and after sequential injections of saturating 1-glucose (10mM), 2-oligomycin (1 µM) and 3-2 deoxyglucose (50mM). (A) The glucose-induced response reported as the rate of glycolysis under basal conditions. (B) Subsequent increase in ECAR revealing the cellular maximum glycolytic capacity after inhibiting ATP synthase. (B) ECAR after inhibition of glycolysis. The difference between glycolytic capacity and glycolysis rate defines glycolytic reserve. LCB2151 appears to decrease glycolytic reserve of cells. N=3, data are presented as mean ± SEM. Statistical analysis done using GraphPad Prism 7 one-way ANOVA shows no significant changes in glycolysis by any treatment, compared to vehicle DMSO. Concentrations: 2151:15µM; 2179: 15µM and Gemcitabine: 0.75µM.

with GSH to increase the oxidized glutathione (GSSG) levels, decreasing the ratio of reduced to oxidized glutathione (GSH/GSSG). The redox state induced by LCB2151 was assessed by directly measuring reduced glutathione as well as the oxidized form in cells to calculate the glutathione/glutathione disulfide ratio (GSH/GSSG) using a luminescence-based GSH/GSSG-Glo™ assay (Promega). Panc-1 cells were treated with Gem, LCB2151 and LCB2179 for 2 and 6 hours (Figure 17). As shown in Figure 17A, no changes were observed at 2 hours. However, LCB2151 resulted in a significant decrease of the GSH/GSSG ratio after 6 hours (Figure 17B), indicative of an oxidizing cellular environment.

3.2.4. LCB2151 Induces More H_2O_2 Production than Gemcitabine or CPI-613

The role of ROS in pancreatic ductal adenocarcinoma (PDAC) depends on its concentration in cells. ROS facilitates cancer progression and promotes the malignant phenotype, while excessive ROS changes mitochondrial morphology, potentially leading to cell death (Martinez-Useros *et al*., 2017). Gem causes strong induction of ROS accumulation in various pancreatic cancer cell lines (Mihailidou *et al*., 2017). However, a study associated lower levels of ROS with resistance to Gem and other chemotherapies in PDAC cells (Donadelli *et al*., 2011). In addition, CPI-613 targets KGDH by a strong mitochondrial ROS burst, resulting in KGDH inactivation due to glutathionylation of its sulfhydryl groups (Stuart et al., 2014). To support the hypothesis that LCB2151 interferes with mitochondrial metabolism associated with generation of oxidative stress, the amount of generated ROS was tested. Panc-1 cell line was treated for 6 hours with LCB2151 along with its controls, LCB2179, Gem, CPI-613 or vehicle. ROS levels were detected through measurement of hydrogen peroxide (H_2O_2) directly in cultured Panc-1 cell line using the ROS-Glo™ H_2O_2 bioluminescent assay (Promega). This study shows that LCB2216 (natural nucleoside + lipoate) is the most potent ROS inducer (Figure 18). LCB2151 produces more ROS than Gem

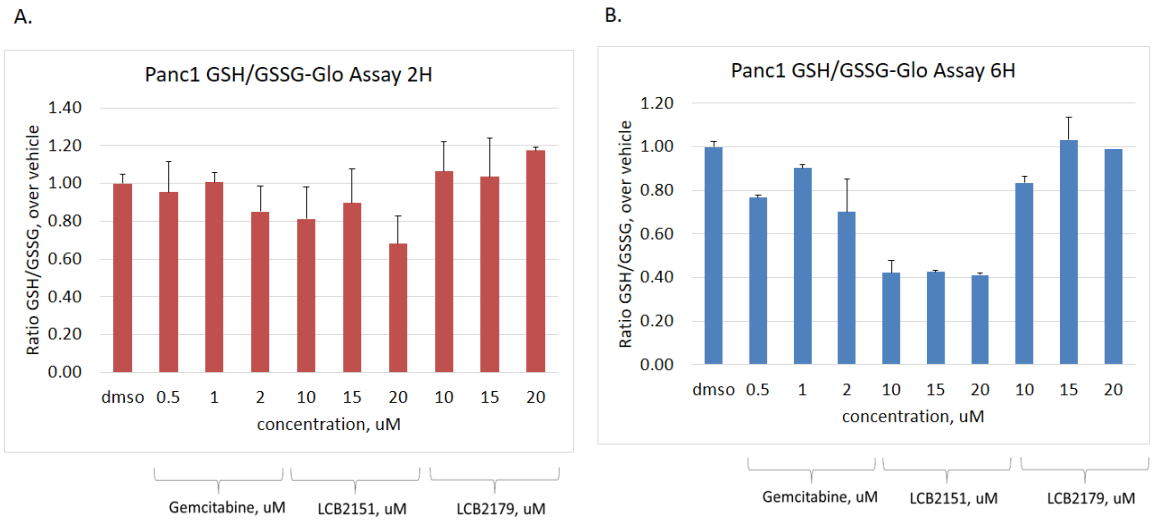

Figure 17. Reduced GSH/GSSG ratio in LCB2151-treated cells after 6h. Panc1 cells were treated with vehicle or increasing dose of gemcitabine, LCB2151 and LCB2179 for (A) 2h and (B) 6h . GSH/GSSG ratios was determined as an indicator of oxidative stress using the luminescence-based system GSH/GSSG-Glo™ Assay (Promega). LCB2151 induces a decrease in the GSH/GSSG ratio after 6h treatment, indicative of an increase in oxidative stress. Data are a mean of duplicates corrected over vehicle treatment.

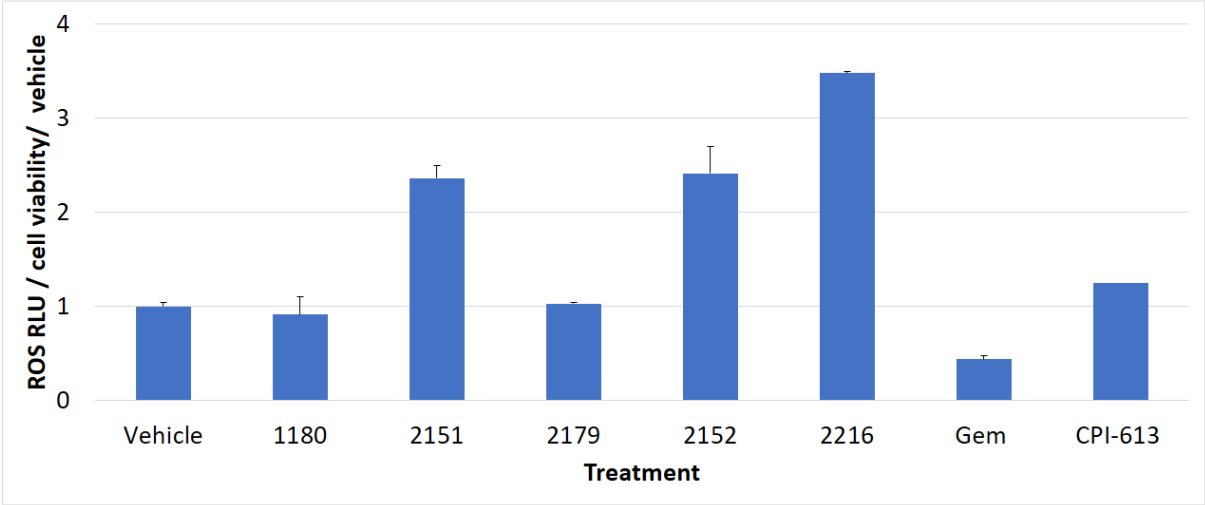

Figure 18. **H_2O_2 production in Panc-1**. Cells were treated with 15 µM of LCB1180, LCB2151, LCB2179, LCB2152, LCB2216 and 1 µM Gem, 200 µM CPI-613 or vehicle for 6h. ROS level was detected by ROS-Glo™ H_2O_2 Assay (Promega) following the non-lytic protocol. ROS level was detected through the measurement of H_2O_2 in the cells, because most of ROS converted to H_2O_2 and easy to be detected due to the long half-life, according to the instructions of the kit (ROS-Glo™ H_2O_2 Assay, Promega)(Alfadda and Sallam, 2012). LCB2216 induced more ROS than any other treatments. The data represented as mean values ± standard deviation of triplicates in single experiment. Relative luminescence units (RLU) were first corrected over cell viability (Celltitre-Glo, Promega) and then over vehicle treatment (fold change of 1).

and CPI-613, and the same amount as LCB2152 (lipoate alone). Gem reduces ROS, while LCB2179 and LCB1180 (nucleoside alone) do not induce any change in ROS levels. The sum of results presented thus far show that LCB2151 acts through a unique mechanism that disrupts mitochondrial metabolism pathways in resistant pancreatic cancer cells.

3.3. Aim 3: To Validate the Molecular Targets of LCB2151 in Pancreatic Cancer Cells.

3.3.1. Proteomics and Metabolomics Validation: Effect of LCB2151 on DLST Protein Expression

With possible inhibition of the metabolic reaction catalyzed by KGDH (Figure 14B) and detection of DLST subunit protein expression via proteomics after a 6 hours treatment with LCB2151 (Table 7), it was important to check protein levels of DLST by western blot to validate the large-scale results. I treated Panc-1 cells with LCB2151 20 μM or vehicle for 6 hours, the same conditions as the metabolomics and proteomics experiments, and additionally for 9 & 12 hours. DLST protein levels are not significantly changed after up to 12 hours of LCB2151 treatment (Figure 19A & 19B). Contrarily, DLST is also detected in vehicle treatments, and this experiment does not validate proteomics results, detecting DLST only in LCB2151-treated samples after 6 hours (Table 7). Another antibody recognizing a different epitope of DLST should be tested.

3.3.1. LCB2151 and Derivatives Change Enzymatic Activity of KGDH Complex

Changes in DLST protein levels do not directly indicate that KGDH activity may be altered. To confirm if LCB2151 inhibits the overall KGDH complex activity, whole-cell lysates of treated Panc-1 cells were analyzed for KGDH enzymatic activity using an assay kit (Biovision). Stuart *et al* report that CPI-613 treatment of H460 cells produced a significant, reproducible reduction in KGDH activity in the resulting lysates and it is currently marketed as a KGDH inhibitor

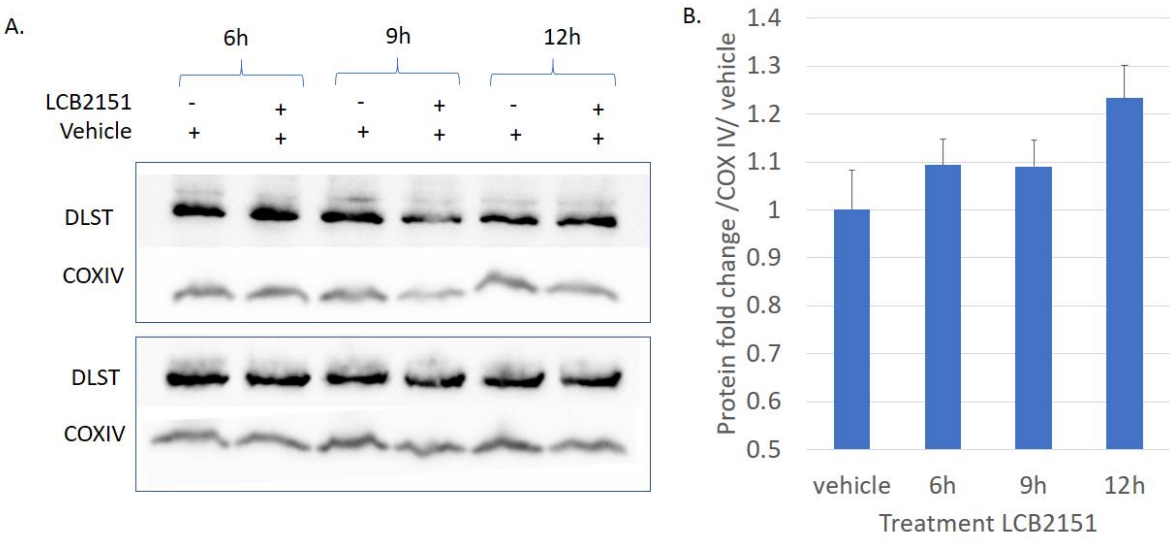

Figure 19. Validation of proteomics and metabolomics for DLST protein expression. Panc-1 cells were treated with LCB2151 20 µM or vehicle for 6h, 9h and 12h. (A) Western blot of whole cell protein extracts comparing DLST protein expression to mitochondrial marker COXIV protein expression. (B) Quantification of DLST protein expression corrected over COXIV and then over vehicle (fold change of 1) for each time point. DLST protein expression slightly increases over time after LCB2151 treatment. N=2

(Egawa *et al*., 2018; Stuart *et al*., 2014). Our lipoate analogue is a derivative of CPI-613, therefore testing LCB2151, LCB2152 (lipoate alone) and LCB2216 (natural nucleoside + lipoate) is of interest.

After a 6 hour treatment LCB2216 reduced KGDH activity by 40% compared to vehicle (Figure 20). The effect of LCB2151 and LCB2152 treatments on KGDH activity is highly variable and will need to be repeated. Removal of excess NADH with a 10 kDA filter column to reduce background may have also washed away the drugs (smaller than 10kDa), and we are therefore seeing the residual post-translational effects of the treatment on KGDH rather than the direct effects of our drugs. This will need to be addressed in future experiments where extracted KGDH protein is treated with drug *in vitro* immediately before reading the enzymatic activity.

3.3.2. LCB2151 Decreases Lipoylation of α-Ketoglutarate Dehydrogenase Complex

LCB-2151 could on its own, or as the free lipoate LCB2152, interfere with the homeostasis of KGDH lipoylation which is necessary for its activity (Stuart *et al*., 2014). For instance, it could interfere with the ligase responsible for adding the lipoate onto the enzyme, thus inhibiting the enzyme and leading to a decrease in lipoylation. Also, LCB2152 could be incorporated thus replacing the "natural" lipoate.

To test if LCB2151 interferes with KGDH lipoylation, an antibody that recognizes native lipoate was used. Panc-1 cells were treated with vehicle or increasing concentrations of LCB2151 and Gem for 6 hours. DLST was immunoprecipitated from whole cell extracts and western blot analysis revealed bound lipoic acid levels (Figure22A). Quantification of LA over total DLST shows that lipoylation of DLST decreases up to 50% with increasing doses of LCB2151 (Figure 21B). Defects in PDH and KGDH lipoylation was shown to inhibit their activity and repress

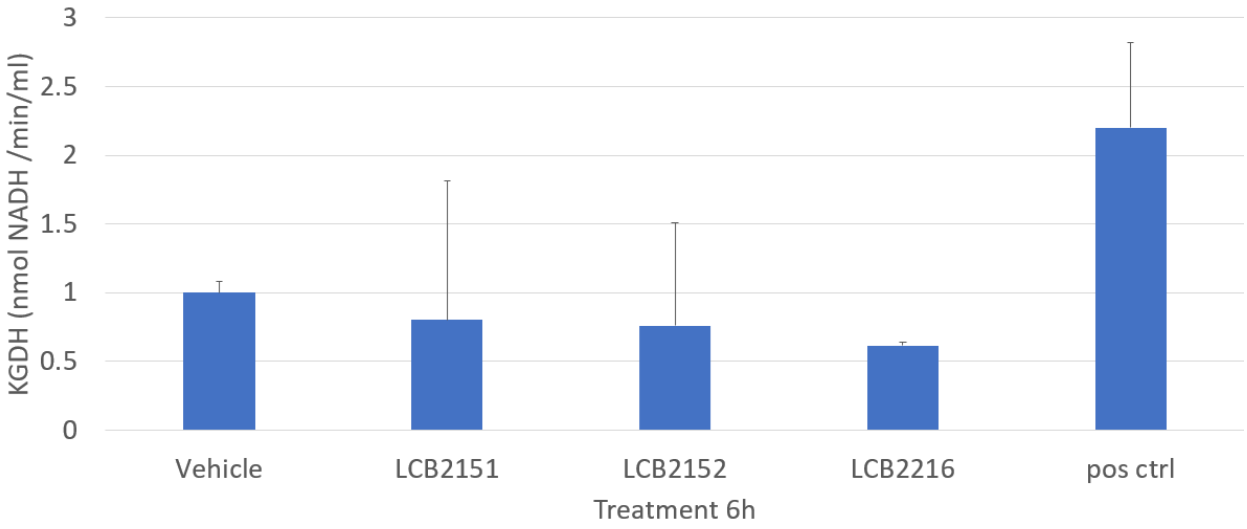

Figure 20. Changes in KGDH enzymatic activity. Panc-1 cells were treated with 15 µM LCB2151 and derivatives containing the lipoate moiety (LCB2152, LCB2216) for 6 hours. KGDH enzymatic activity was measured by colorimetric assay (BioVision) from whole cell extracts. LCB2151 and derivatives all lower enzymatic activity after 6h, LCB2216 the most, which contains the natural nucleoside attached to the lipoate of LCB2151. Positive control (pos ctrl) supplied by assay kit. Performed in triplicate and each replicate was read in duplicate in a single experiment. Readings were normalized over protein concentration. N=1

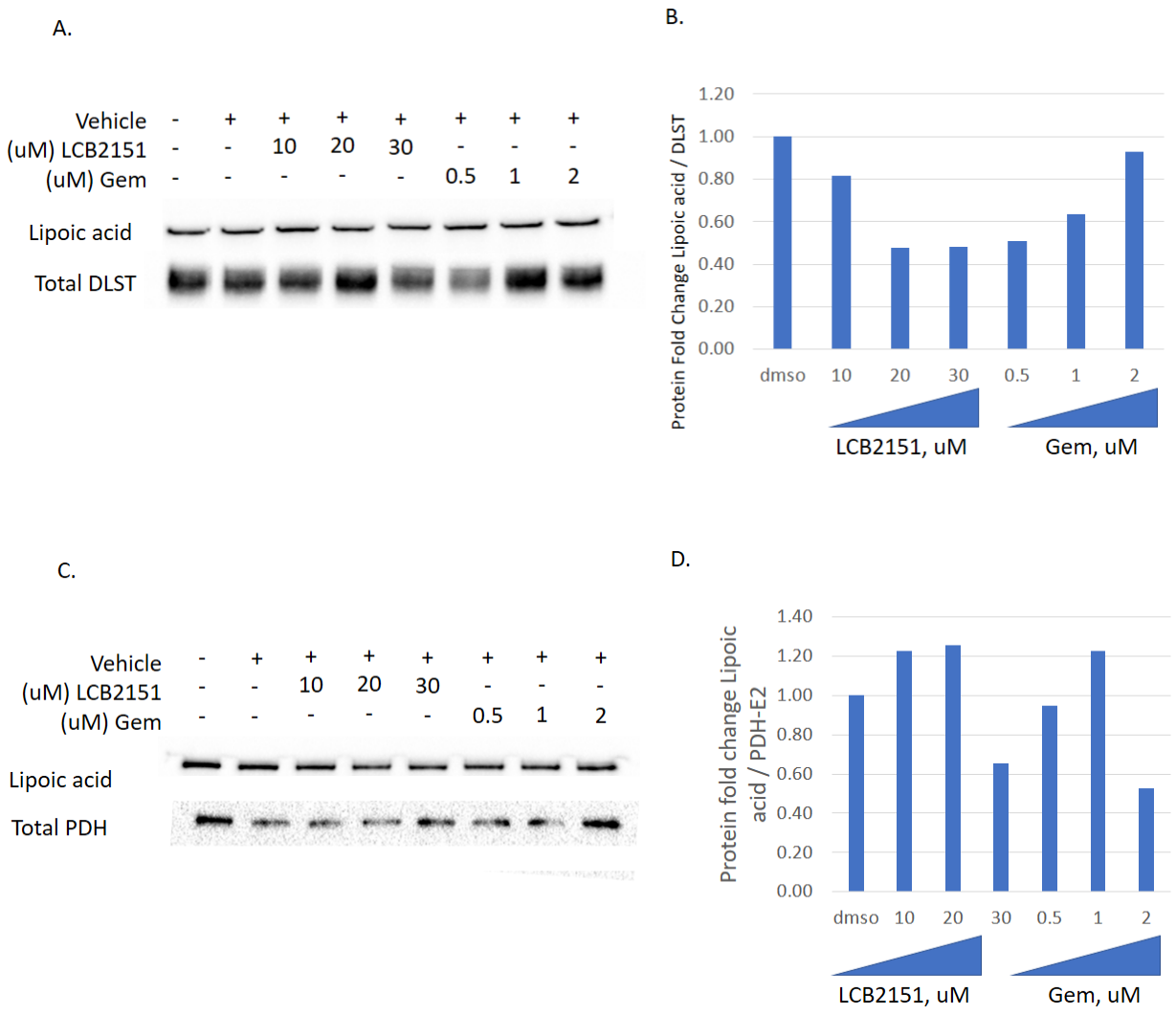

Figure 21. Lipoylation levels of α-ketoglutarate dehydrogenase and pyruvate dehydrogenase. Panc-1 cell line was treated with increasing doses of LCB2151 (10, 20 & 30 µM) or Gemcitabine, Gem (0.5, 1 & 2 µM) for 6 hours. (A) α -KGDH subunit E2 (DLST) and (C) PDH subunit E2 (PDH-E2) was immunoprecipitated from whole cell protein extracts. Levels of lipoylation was measured by blotting for protein-bound lipoic acid. Quantification of lipoic acid over (B) DLST expression shows a decrease in lipoylation by LCB2151 compared to vehicle, suggesting interference of α -KGDH activity by LCB-2151. Quantification of lipoic acid over (D) PDH-E2 expression shows no change in lipoylation. N=1

mitochondrial function (Burr et al., 2016; Paredes et al., 2018). The decrease in KGDH lipoylation we see could contribute to KGDH inhibition, consistent with decreased OCR measured previously (Figure 15). Surprisingly, Gem initially decreases lipoylation (Figure 21B), then levels recover to normal with increasing dose. This could be due to a replicative stress response that is alleviated once resistance mechanisms are activated.

The same assay was performed for the second LA-dependent enzyme PDH by immunoprecipitating the E2 subunit and revealing lipoic acid (Figure 21C). Quantification of lipoic acid over total PDH-E2 subunit showed no trends in lipoylation levels after LCB2151 treatment, consistent with the metabolomics data showing no significant inhibition of the reaction catalyzed by PDH (Figure 21D). Unexpectedly, there is a drop in lipoylation at high doses of LCB2151 and Gem, bringing attention to the different role of lipoylation for KGDH and PDH regulation that could be explored. The selectivity of our antibody to LCB2152 or LCB2151 will have to be measured to confirm that only lipoylation of the native lipoate is measured.

3.3.3. Proteomics and Metabolomics Validation: LCB2151 Decreases Protein Expression of Phosphofructokinase-1

Experiments have been initiated to investigate the second LCB2151 target, PFK-1, that controls the rate-limiting step of glycolysis in the cytoplasm. Metabolomics analysis suggested inhibition of the reaction catalyzed by PFK-1 at 6 hours of LCB2151 treatment. While PFK-1 detection did not pass the threshold of significance in the proteomics analysis, the peptides detected in some samples were predominantly of the platelet type (PFKP). Human PFK-1 is a tetramer enzyme that has three isoforms: muscle (M), liver (L) and platelets (P) (Vora *et al*., 1985). It has been demonstrated that PFKP is the predominant isoform in human glioblastoma

cells and human breast cancer tissues which positively correlated with the total activity of PFK-1 in both cases (Lee et al., 2017b; WANG et al., 2013). Knowing that PFKP is the predominant isoform in human cancers supported selection of the anti-PFKP antibody to reveal protein levels of PFK-1 in Panc-1 cell line. Cells were treated with vehicle or LCB2151 for 6 and 12 hours. Western blot quantification shows a 40% decrease in PFKP expression by 12 hours (Figure 22A & 23B). Significance will have to be determined by repeating the assay. This reduction in expression correlates to the inhibition of PFK-1 suggested by metabolomics analysis (Figure 14A). Enzymatic inhibition in response to LCB2151 treatment remains to be confirmed by performing a PFK-1 enzymatic activity assay with LCB2151 and derivatives.

3.3.4. A Photoaffinity Probe to Test Direct Target Binding of LCB2151

Identification of direct binding targets of a lead molecule is often the limitation to decipher its mechanism of action. Our results suggest that LCB2151 inhibits PFK-1 and KGDH in carbon metabolism, however it is unknown whether this is due to direct binding or secondary effects. Photoaffinity labelling (PAL) provides a non-bias approach to drug target identification that can be performed in live cells and has been applied to a variety of anti-cancer compounds (Colca *et al*., 2013). A photoaffinity probe (PAP) of LCB2151, LCB2212 has been designed by the Guindon group. This probe has been designed to covalently bind to its targets upon UV-radiation (Figure 23A). Obviously, it is important that modifications to LCB2212 to not change the mechanism of action from the parent molecule LCB2151. Cancer cell lines HepG2, Panc-1 and BxPC-3 were treated with LCB2151 or LCB2212. Dose response curves show that the activity of LCB2212 is comparable to the parent molecule after 96 hours (Figures 24B-24D). Subsequent attachment of a biotin affinity tag using Cu(II)-catalysed azide-alkyne cycloaddition will allow purification of target proteins from cell lysates and final identification by tandem mass spectrometry.

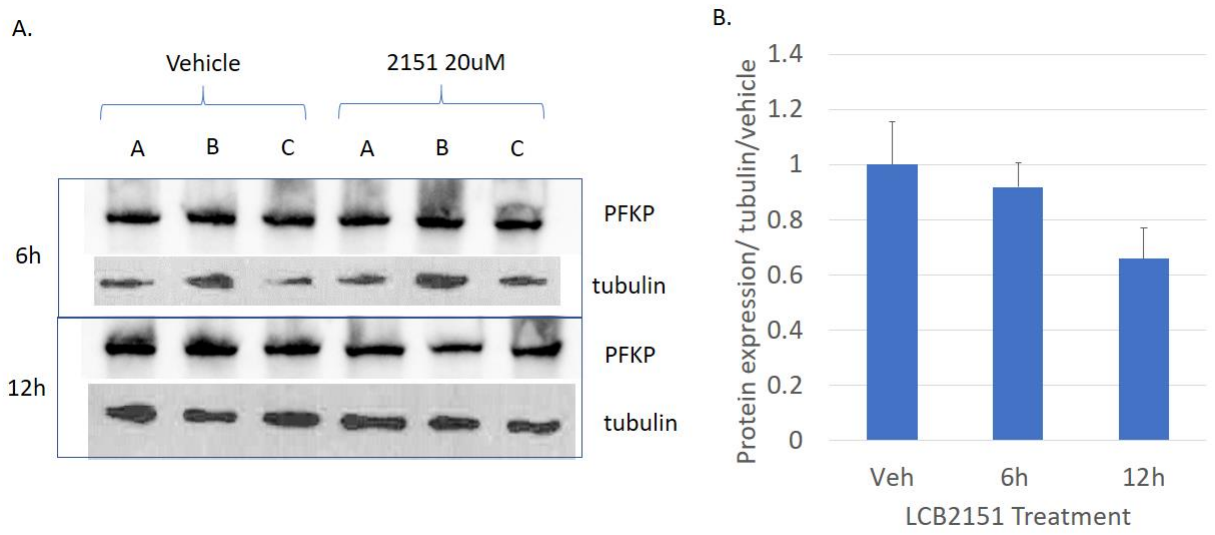

Figure 22. Validation of proteomics and metabolomics for PFK-1 protein expression. Panc-1 cells were treated with LCB2151 20 µM or vehicle for 6 and 12 hours. (A) Western blot of whole cell protein extracts comparing PFK platelet subtype (PFKP) protein expression to mitochondrial marker COXIV protein expression. (B) Quantification of PFKP protein expression corrected over COXIV and then over vehicle (fold change of 1) for each time point. PFKP protein expression decreases over time after LCB2151 treatment. N=2.

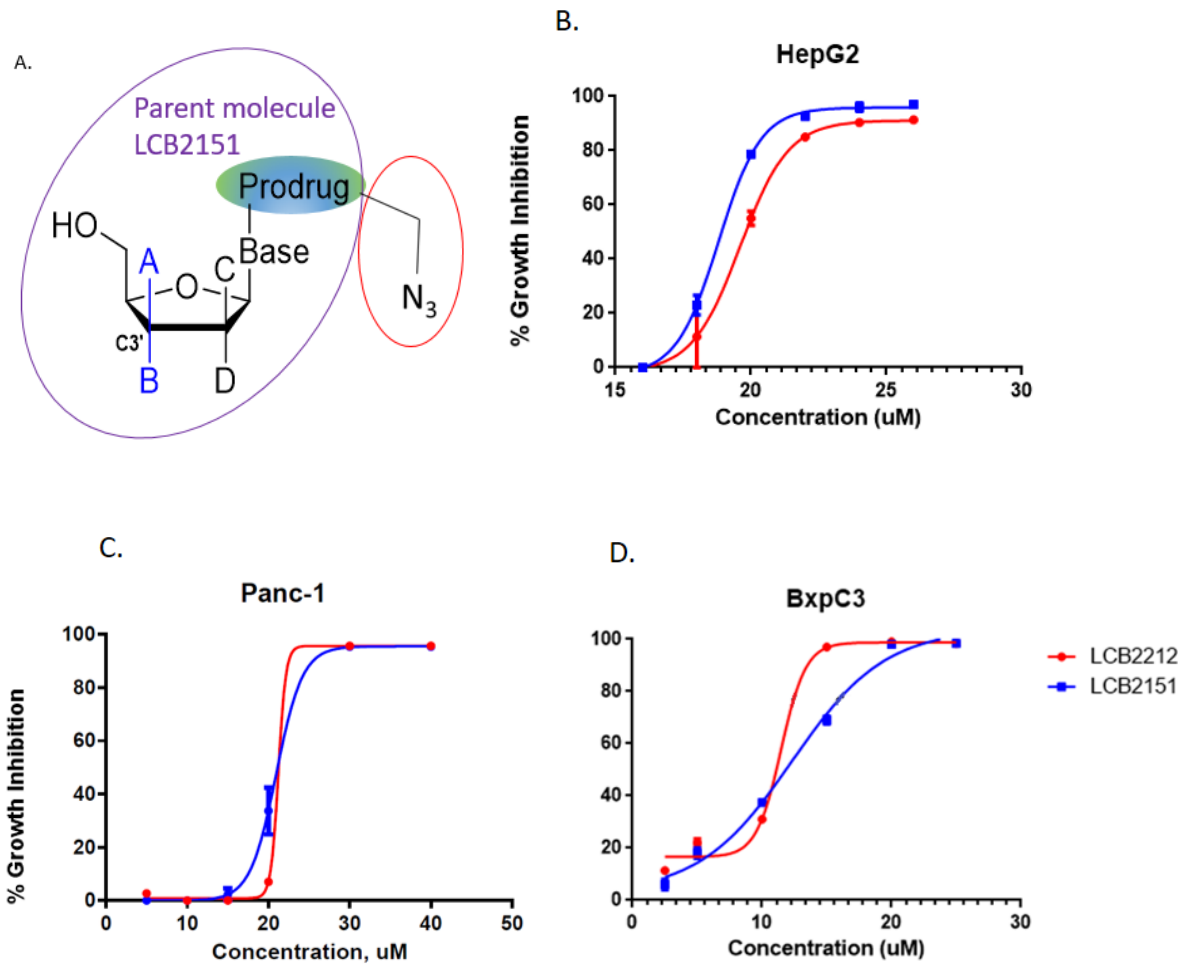

Figure 23. Photoaffinity probe of LCB-2151 tested in human cancer cell lines. (A) LCB-2212 has photoreactive adduct (red circle), incorporated in the lipoate (prodrug) of parent molecule LCB2151 (purple circle). This probe was synthesized by G. Tambutet (Guindon Lab, IRCM). Dose response of probe LCB-2212 (red) shows a similar bioactivity to LCB2151 (blue) in three human cancer cell lines (B) HepG2, (C) Panc-1 and (D) BxpC-3 treated at increasing doses of drug for 96h. N=1

(Breinbauer and Köhn, 2003; Shi *et al*., 2012). Continuation of the PAL experiment with LCB2212 will confirm direct binding targets of LCB2151 in carbon metabolism and possibly identify new targets in other cellular pathways.

4. Discussion

4.1. Current State of the Treatment for Gastrointestinal Cancers

Gastrointestinal (GI) cancers remain a major health issue worldwide. Hepatocellular carcinoma (HCC) is the most common primary liver cancer, accounting for 90% of cases, and is considered a highly resistant cancer to therapy. Pancreatic ductal adenocarcinoma (PDAC) is the most prevalent form of pancreatic cancer and is currently the fourth leading cause of cancer-associated mortality (Ghaneh et al., 2007; Rahib et al., 2014). The nucleoside analogue (NA) Gemcitabine (Gem) is the recommended first-line chemotherapeutic agent for PDAC patients with limited efficacy due to increasing instances of intrinsic and extrinsic resistances, whose mechanisms are extensively studied (Akada et al., 2005; Ju et al., 2015; Koay et al., 2014). Even if screening and detection improve, there is a need for ameliorated chemotherapy agents to improve patient outcomes (Siegel et al., 2017).

4.2. Strategies to Overcome Drug Resistance

Despite advances in Gem-based treatment, there has been no significant improvement in the overall survival (OS) and chemotherapy refractory pancreatic cancer has continued to increase (Gresham et al., 2014; Siegel et al., 2015, 2017). To overcome NA resistance, we have embarked on the conceptualization and synthesis of a novel family of NAs in collaboration with the Guindon medicinal chemistry research group. These proprietary molecules are NAs bearing all-carbon quaternary centers with lipoate-derived adducts. They are inducing a controlled conformational

bias and some are additionally phosphorylated prodrugs that would overcome the dCK rate-limiting step in their activation. Additionally, a lipophilic moiety is attached to the nucleobase to protect the nucleoside against CDA inactivation and allow cell penetration independently of transporters. Once inside the cell, the NA could interfere with cell proliferation and the lipophilic attachment could interfere with mitochondrial metabolism. Alteration of cellular metabolism is a hallmark of cancer, a phenomenon first described by Warburg as increased glucose consumption and lactic acid secretion by rapidly-dividing cancer cells (Warburg et al., 1927). Entry of carbon into the TCA cycle becomes tightly regulated by pyruvate dehydrogenase (PDH) and alpha-ketoglutarate dehydrogenase (KGDH) complexes that rely on a-lipoic acid (LA) as a cofactor. Our lipoate is an LA analogue based on the commercially availably and clinically tested derivative CPI-613, designed to simultaneously target the activity of these key metabolic enzymes in cancer (Stuart et al., 2014; Zachar et al., 2011).

4.3. Characterization of the Structure-Function Relationship of Lead Molecules

PDAC is well characterized genomically, and the most common driver mutations are oncogenic mutations in *KRAS*, mutated in approximately 95% of advanced and/or metastatic pancreatic carcinomas, and loss of tumour suppressors *TP53*, *CDKN2A* and *SMAD4* (Waddell et al., 2015; Yachida et al., 2010; Zeitouni et al., 2016). Our panel of human cancer cell lines vary in the most common *KRAS* and *TP53* mutations and are all Gem-resistant to various degrees. Not only do we identify one, but two molecules that can kill up to 100% of the most resistant cell lines, namely pancreatic Capan-2 and Panc-1, with EC_{50} values between 12-20 µM. This dose is significantly lower than that required for CPI-613, which is in late phase clinical trials and only targets metabolism (Lycan et al., 2016; Pardee et al., 2014b). This was the first sign that our

molecules act though a different mechanism than Gem and CPI-613, which made their exact mechanism of action very interesting to investigate further.

While both lead compounds are composed of a NA attached to a lipophilic moiety, it is worth noting that the NA is not chemically identical on these two molecules, and LCB2179 is additionally monophosphorylated. These small changes could have major impacts on their mechanism of action, therefore to begin structure-activity analysis we focused on our most consistently performing molecule LCB2151 in Panc-1 cell line. Cell-killing profiles reveal that the lipoate component plays a key role in the anti-cancer activity of the drug (Figure 6). The lipoate alone shows modest activity (LCB2152), yet when attached to the natural nucleoside cytidine (LCB2216) we see the highest potency. The NA is a bulkier structure than cytidine, possibly leading to steric hinderance, taking more time to achieve the same effect. On the other hand, the nucleobase of LC2151 alone (LCB1180) is inactive, suggesting that the molecule is not cleaved to exert its effects. These findings are consistent with previous results that do not detect LCB1180 by mass spectrometry in whole cell lysates from cells treated with LCB2151. The nucleobase could also be important for localization and trafficking of the molecule inside the cell, and specifically within the mitochondria (Carling et al., 2011; Gandhi and Samuels, 2011; Kakuda, 2000; Lam et al., 2005). LCB2152 could not be measured in this experiment because lipids were not extracted with metabolites, although lipid extraction for mass-spec detection is available and would be valuable to perform next.

4.4. Overcoming Gemcitabine-Induced Drug Resistance Mechanisms

Based on our results it is evident that LCB2151 and LCB2179 indeed follow a unique mechanism, and that they both follow a different mechanism than Gem or CPI-613. The ability of LCB2151 to kill the cells that survive Gem treatment is the first piece of evidence. After HepG2,

BxPC-3 and Capan-2 cell lines received a 96 hour high-dose treatment of Gem, subsequent LCB2151 treatment was able to kill more remaining cells than re-treatment with Gem. The fact that Gem was still able to kill some remaining cells is due to the short length of a single pre-treatment, which most likely did not eradicate all the Gem-sensitive cells before continuation. To be certain that only resistant cells remain, a Gem-resistant cell line should be generated by passaging cells with increasing concentrations of Gem over several weeks, as demonstrated in the MiaPaCa-2 pancreatic cancer cell line, before sequential treatment with LCB2151 (Samulitis et al., 2014). Nevertheless, this assay suggests that LCB2151 can bypass cellular mechanisms of resistance already activated by Gem. Clinically, this novel agent could be used to treat refractory tumours in patients previously treated with a Gem-based regimen to improve overall survival rates.

Low expression of hENT1 is a main factor that contributes to Gem resistance in cell lines and in patients (Spratlin et al., 2004). Therefore, it is important to find novel therapeutic strategies to overcome Gem resistance induced by low hENT1 expression. Gem is naturally hydrophilic and would not permeate the cellular lipid bilayer by passive diffusion, whereas our molecules are designed with a lipoate moiety to allow for passive diffusion across the membrane. In this study, we used *S*-(4-nitrobenzyl)-6-thioinosine (NBMPR) to simulate low hENT1 expression. Previous work in our lab showed that LCB2151 maintains activity in the presence of NBMPR in HepG2 liver cancer cell line. My work replicates this effect in the more resistant cell line Panc-1, with not only LCB2151 but LCB2179 as well. A similar strategy was used to recently prove that Gem-loaded human serum albumin nanoparticle can be taken into BxPC-3 cells through endocytosis and bypass the transport of hENT1, while Gem activity is abrogated (Guo et al., 2018). Lastly, our gene profile analysis shows that hENT1 mRNA expression is increased by Gem in BxPC-3, but only by LCB2151 in the most resistant Capan-2 at 18 hours. Gem may be failing in resistant

tumours because it cannot be transported into the cell, while LCB2151 may be a useful primary treatment, increasing the import of a secondary agent into the resistant tumour cells.

Deficiency of dCK is another factor that contributes to NA resistance and its expression in both protein and mRNA levels serve as a biomarker to predict tumor cell sensitivity to Gem (Ciccolini et al., 2010; Fujita et al., 2010; Jordheim and Dumontet, 2007; Maréchal et al., 2012). We recapitulated this chemoresistance by siRNA-mediated knockdown of dCK in Panc-1 cell line to show that both LCB2179 and unexpectedly LCB2151 act independently of dCK levels, unlike Gem theoretically (Figure 9). These results emphasize that LCB2151 could be acting primarily through the lipoate-dependent mechanism and does not follow the classical NA mechanism that requires dCK for activation. We cannot draw the same conclusions for LCB2179, which is monophosphorylated, yet it is the only molecule to lower dCK mRNA expression (Figure 10A), suggesting this feature still plays a role in the classical NA mechanism. A limitation is that residual dCK protein remains in the cell, which could be enough for LCB activation but not for Gem. Although, a study on cervical cancer Hela cells that were treated with shRNA-DCK reported a comparable protein knockdown sufficient to observe significant effects on proliferation and apoptosis (Shang et al., 2017b).

The group investigating pro-tide technology report the ability of the novel agent 6f to bypass the requirement for dCK-mediated activation in pancreatic cells, however they mimic low dCK expression using the kinase inhibitor 2T2D instead of a knocking it down (Slusarczyk et al., 2014). There is no evidence that this inhibitor is specific to dCK and has not been used in any other published studies, making it an unreliable comparison for our study. Despite these uncertainties, the ProTide NUC-1031 (6f) is currently advancing through phase I/II clinical studies, with promising early efficacy signals and a favorable safety profile (Ghazaly et al., 2013). Under our

conditions, the cells were already highly resistant to Gem, suggesting their dCK expression was low to begin with. Therefore, these results could be confirmed by repeating this knockdown in a less resistant cell line such as BxPC-3 or in non-cancerous pancreatic cell line with normal dCK expression , in which siRNA-mediated knockdown of *DCK* yielded Gem resistance (Saiki et al., 2012). Taken together and with the proper controls, LCB2151 and LCB2179 could overcome Gem resistance induced by low hENT1 and dCK expression in pancreatic cancer, leading to their potential for clinical application.

4.5. LCB2151 and LCB2179 Generate Unique Genetic Profiles of Cancer Cell Markers

To analyze the effects of our lead molecules on gene expression a candidate gene approach was used to measure changes in the same genes in Capan-2 (most resistant) and BxPC-3 (least resistant) cell lines. Capan-2 carries the *KRAS* mutation (KRAS-) and WT *TP53* (TP53 +). On the other hand, BxPC-3 has WT *KRAS* (KRAS +) but a mutated *TP53* (TP53 -). Activating mutations in *KRAS* gene are found in nearly all PDAC cases and is essential for PDAC growth and deactivating mutations in *TP53* gene were found in 77% of PDAC cases (Sausen et al., 2015; Waters and Der, 2018). Comparison of the changes brought about by LCB2151 and LCB2179 and Gem in these cell lines allowed us to examine the role of p53 and Ras in the lead molecules' mechanism of action.

Consistent with the cell killing profile, Gem upregulated markers of drug resistance such as *RRM1* and *CDA,* while our lead molecules did not (Figure 10A & 10B). Clinical studies have shown that high levels of RR subunits M1 or M2 are associated with a poor prognosis in both pancreatic and lung cancers (Ashida et al., 2009; Chantrill et al., 2015; Wang et al., 2014). Previous studies have also indicated that increased CDA levels may also contribute to Gemcitabine resistance in PDAC (Weizman et al., 2014). An increase of these genetic markers would increase

the pool of deoxynucleosides to compete with in DNA synthesis and increases Gem deactivation, leading to the cellular resistance profile we observe in our panel of cell lines. Lead molecules promisingly avoid activation of these cellular resistance mechanisms at the mRNA level.

Previous work in our lab showed no significant changes in *TP53* levels induced by LCB2151 treatments in HepG2 cells at the mRNA or protein level and a lack of p53 activation. This contrasted with Gem that induced robust p53 expression and is known to be p53 dependent. Further results confirmed apoptosis as the mechanism of cell death, which led us to propose that LCB2151 induces p53-independent apoptosis, similar to CPI-613 (Pardee et al., 2014b). My results differ where LCB2151 induces *TP53* expression in the resistant Capan-2 cell line, suggesting that p53 plays a more significant role in the mechanism of LCB2151 in resistant tumours harbouring *KRAS* mutations. This result is expected given the significant upregulation of *BBC3* by LCB2151 (Figure 10 C and 10D), which causes rapid p53-dependent apoptosis and growth inhibition (Nakano and Vousden, 2001). Contrarily, LCB2179 lowers *BBC3* in the resistant cells, matching a lack of p53 induction and highlights the difference in mechanism of our lead molecules (Figure 10D). *In vitro* and *in vivo* studies demonstrated that Gem requires *PUMA* transcription to instigate an apoptotic programme yet primary colon or pancreatic cancer patient sample analysis revealed the activation of p53 in tumour tissues in the absence of the PUMA protein (unlike Bax protein) (Hill et al., 2013). This provides an explanation for Gem-resistance and raises the possibility that targeting the Bax-dependent pathway could offer an improved therapy. LCB2151 upregulates *BAX* in the resistant cell line Capan-2, unlike Gem (Figure 10D). This supports the possibility that LCB2151 is targeting a Bax-dependent pathway and provides an explanation for why it can kill Gem resistant cells. Lastly, lead molecules lower anti-apoptotic genes *BCL2* and *BCLXL*, whereas Gem raises them (Figure 10F). These changes in the pro-: anti-

apoptotic marker ratio would direct cells towards apoptosis more efficiently than Gem and could attribute the observed potency of lead molecules to this difference.

Dysregulation in genes involved in cell proliferation can also attribute to chemoresistance of tumour cells (Garrido-Laguna and Hidalgo, 2015; Kleeff et al., 2006). In our study, Gem treatment upregulated most proliferative genes (cyclins E1, E2, D3 & *CXCL1*), while LCB2151 did not or even decreased some of these markers such as Cyclin E2 (*CCNE2*) and *CXCL1*. Although both drugs induce growth arrest p21 (*CDKN1A*) gene expression, perhaps the overexpression of proliferative genes by Gem is enough to drive unwanted proliferation, unlike LCB2151. Microarray studies report that CPI-613 down-regulated the expression of Cyclin D3, E1 and E2 in BxPC-3 but not in non-transformed mouse fibroblasts (Lee et al., 2014). LCB2151 more closely recapitulates the genetic profile of CPI-613 than Gem (Figures 10G & 10H), supporting the notion that the lipoate plays a key role in the mechanism of action of LCB2151 rather than it being metabolised via the classical NA pathway, which leads to resistance in Gem-resistant cell lines. It would be expected therefore, that if non-cancerous fibroblasts were treated with LCB2151, the decrease in proliferation markers would also not be seen. This is yet to be tested but would reveal the selectivity of our molecule. Meanwhile, gene analysis of LCB2179 shows that it also decreases *CCNE2*, but with no effect on p21 gene expression (Figures 10G & 10H). This again demonstrates that none of the three molecules share an identical mechanism of action, although LCB2151 and LCB2179 are more cytotoxic than Gem in cancer cells. Overall changes in gene expression reveal differences, generally associated with more favourable anti-tumour outcomes of lead LCB molecules over Gem.

Analysis of the gene markers for cell stress was an early indication that lead molecules disrupt the redox balance in cancer cells through suppression of UCP2 expression and

enhanced expression of NCF2/p67 to promote an oxidized environment. Uncoupling protein 2 (UCP2) sustains the Warburg effect and is overexpressed in pancreatic cancer cells (Brandi et al., 2016). Mitochondrial uncoupling mediated by UCP2 was also found to inhibit cell death, rendering pancreatic cancer cells as well as HCC patients resistant to Gem (Yu et al., 2015, 2016). These findings imply that UCP2 is a great therapeutic target for future anti-cancer drugs. It is also possible that inhibition of UCP2 could act synergistically with other agents for pancreatic and liver cancer therapy. LCB2151 also decreases *NCF2* gene expression (Figure 10I), coding for $p67^{phox}$, the cytosolic component of NAPDH oxidase complex whose activation generates reactive oxygen species (ROS) (Bedard and Krause, 2007; Kim and Cho, 2014). These results are consistent with previous results from our lab showing that *NCF2* is upregulated in HepG2 cell line by LCB2151 and not by Gem (MSc Thesis, C. Teran). Contrarily, several studies report that Gem treatment also significantly increased mRNA expression of NADPH oxidases in pancreatic cancer cell lines, albeit using a 100X higher dose of Gem and in less resistant KRAS+ cell lines (Zhang et al., 2016). Nevertheless, it is suggested that blockade of such a signaling pathway in combination with Gem treatment may enhance the efficacy of chemotherapy by suppressing pancreatic cancer stem cells (Zhang et al., 2016). LCB2151, containing a derivative of Gem attached to a lipoate analogue supports this hypothesis with its enhanced cell killing profile.

The role of ROS in PDAC depends on the concentration in the cells. A moderate ROS level facilitates cancer progression, while over-production of ROS can damage cancer cells dramatically and leads to cell death via apoptosis (changes in mitochondrial morphology and potential) (Afanas'ev, 2010; Zhang et al., 2015a). In contrast, lower levels of ROS were associated with resistance to Gem and other chemotherapies in PDAC cells (Donadelli et al., 2011). In agreement with these observations, Gem reduced H_2O_2 production in treated Panc-1 cell lines (Figure 18).

We also noticed higher induced H_2O_2 levels in the LCB2151-treated samples compared with Gem or CPI-613, reported to induce a burst of ROS associated with redox modification of KGDH and correlating with KGDH inactivation (Stuart et al., 2014). Next, we need to determine the source of H_2O_2 generated by LCB2151 and its impact on our potential target KGDH.

Moreover, levels of H_2O_2 generated by LCB2151 matched the levels by the lipoate LCB2152, whereas the lipoate attached to the natural nucleoside, LCB2216, surpasses all other drugs in this measurement, emphasising that the lipoate plays a key role in the mechanism of LCB2151 (Figure 18). Interestingly, LCB2179 did not increase H_2O_2 production, matching the effects of the NA LCB1180. Knowing NADPH oxidase is a major source of intracellular ROS in pancreatic cancer cells, these results agree with the gene expression of stress markers where LCB2151 significantly increased *NCF2* by 11-fold but LCB2179 did not (Figure 10I) (Vaquero et al., 2004). Once again, this data demonstrates that LCB2151 and LCB2179 act through unique mechanisms of action. A similar study found that the antifungal agent Ciclopirox olamine (CPX) caused a pronounced decrease in cell proliferation and increased tumour regression in pancreatic cancer models over Gem alone, which was accompanied by a higher induction of ROS (Mihailidou et al., 2017). Thus, LCB2151 might be increasing oxidative stress by generating ROS to levels where they are toxic to cancer cells, which may be an effective way to treat Gem-resistant tumours.

4.6. LCB2151 Induces Global Changes to Metabolism and Cell Stress Pathways in Cancer

Having explored the structure-function relationship of lead molecules and seeing significant changes at the mRNA expression level prompted a non-bias investigation into LCB2151-induced changes at the protein level. Comprehensive large-scale proteomic analysis can provide a system-wide view of signaling networks and assist in understanding drug mechanisms of action and interactions in pancreatic cancer research. By designing a NA with a lipoate

derivative, we would expect the lipoate to interfere with mitochondrial metabolism pathways and the NA to cause replicative stress. Not surprisingly, the majority of proteins effected by LCB2151 (296 unshared and upregulated Q50 proteins) mainly related to metabolic pathways (Table 7). Of these proteins, DLST was only detected in LCB2151-treated samples at 6 hours. This could be an early compensatory mechanism by the cell to overcome enzyme complex inhibition by LCB2151. Proteomic results are also consistent with the transcript analysis that indicated gene expression changes related to apoptosis (ex. mitochondrial chchd2p9) and redox state homeostasis (ex. thioredoxin) (Table 6). A proteomic analysis of Gem-resistant Panc-1 cells versus Gem-sensitive pancreatic cells identify an overexpression of proteins involved in biosynthesis and detoxification in Panc-1 cells, while pathways responsible for biomolecule degradation are downregulated (Chen et al., 2011). This might provide an explanation for the rapid proliferation of Gem-resistant cells, which require more building blocks than Gem-sensitive cells. A more recent proteomic analysis of Gem in Panc-1 cells identified that pathways relating to DNA damage response, DNA repair, anti-apoptosis, pro-migration/invasion were implicated as underlying mechanisms for Gem resistance (Zhu et al., 2018). Considering that LCB2151 does not induce the same pathways as Gem and instead induces additional functional pathways in metabolism supports the hypothesis that LCB2151 is evading drug resistance mechanisms by acting through a different mechanism of action than Gem, resulting in better efficacy. In depth analysis of the protein pathways will surely reveal more details into the mechanism(s) of action of LCB2151.

Carbon metabolism controls synthesis of nucleotides, aminoacids, S-adenosylmethionine (SAM), glutathione, and other cellular processes important for rapidly proliferating malignant cells (Locasale, 2013). Moreover, it can contribute to the energy balance, providing molecules of ATP and NADH (Tedeschi et al., 2013; Vazquez et al., 2011). Gem-resistant pancreatic cancer cells are

characterized by an increased glycolytic phenotype and dependence on glucose, which is fed through the non-oxidative arm of the pentose phosphate pathway (PPP) (Nath et al., 2013). Thereby, targeting central carbon metabolism could overcome Gem resistance in pancreatic cancer. The combination of proteomics results showing alterations in metabolic pathways, of structure-function analysis showing the important role of the lipoate, and together with the strategic design of our lipoylated molecule to target mitochondrial metabolism made it crucial to focus on the effects of LCB2151 on central carbon metabolism. The experimental design was matched to the proteomics analysis in order to get a snapshot of the mechanism of action of LCB2151 at the level of mRNA, the protein, and now metabolites at 6 hours. Results suggest inhibition of two important metabolic reactions in central carbon metabolism when mapped out (Figure 13): (i) phosphofructokinase-1 (PFK-1, rate-limiting glycolysis step in the cytoplasm) and (ii) KGDH (TCA cycle in the mitochondria) (Figures 14A and 14B). Interfering with not only glycolysis, but also mitochondrial respiration would have severe impacts on cancer cells, who tightly regulate these two processes for rapid growth and proliferation. It would be remarkable if the single agent LCB2151 proves to attack two important metabolic pathways simultaneously in cancer cells. With KGDH as an expected target of LCB2151 and the reported attack on KGDH by CPI-613, KGDH became our primary molecular target to validate (Stuart et al., 2014).

4.7. Proposed Mechanisms for the Interference of Mitochondrial Respiration by LCB2151

The α-KGDH is at the crossroad of numerous metabolic routes and is also interconnected with the respiratory chain of the tumor cell. It catalyses the oxidative decarboxylation of α-ketoglutarate to succinyl-CoA exploiting the reduction of NAD^+ to NADH (DeBerardinis et al., 2007; Fendt et al., 2013; Mullen et al., 2011; Wise et al., 2011). One of its components, the E2 subunit DLST requires lipoic acid as cofactor. High levels of ROS lead to enzyme inactivation and

reduced cell proliferation. We propose that LCB2151 inhibits KGDH through three possible mechanisms: (i) inhibitory levels of ROS production, (ii) direct binding of the lipoate derivative to dihydrolipoamide succinyltransferase (DLST) or (iii) inhibition of lipoyl transferases. We have begun to investigate whether the apparent inhibition we see is a result of one, two or all three possibilities.

The most important known regulator of α-KGDH is NADH/NAD^+ ratio that controls ROS levels, placing the enzyme on the front line to adapt to variations in ETC efficiency (Vatrinet et al., 2017b). Since α-KGDH is a TCA enzyme found in the mitochondria, it was important to first test the effects of LCB2151 on mitochondrial function. Our analyses in Panc-1 revealed that LCB2151 significantly impacted mitochondrial respiration as demonstrated in Figures 15B, 15E and 15F. These findings are consistent with our mRNA and proteomic analysis as well as a study that shows inhibition of maximal respiration and ATP depletion as a consequence of CPI-613 exposure, from which the lipoate moiety of LCB2151 is derived (Pardee et al., 2014b). Insight into the mechanism of mitochondrial dysfunction induced by LCB2151 suggests that cells are more sensitive to oxidative stress. KGDH has been shown to be a sensitive target of oxidative damage where an increase in ROS levels inhibit α-KGDH function due to glutathionylation of lipoic acid, a required cofactor covalently linked to the E2 subunit. (Applegate et al., 2008). Glutathionylation of the lipoyl moiety prevents oxidative damage to the E1 component and may contribute to oxidative damage by E3-mediated ROS production (Mailloux et al., 2016). We showed that the lipoate (LCB2152) is capable of increasing H_2O_2 and even more potently when attached to the natural nucleoside (LCB2216) (Figure 18). Accordingly, LCB2151 decreases GSH/GSSG ratio in panc-1 cells (Figure 17) , which could also be indicative of oxidative stress (Schafer and Buettner, 2001). Lastly, studies show that reduction in intracellular GSH content

causes an inhibited Panc-1 invasiveness (Fujita et al., 2017). Taken altogether, the observed cytotoxicity of LCB2151 in cancer cells could be partially due to impaired redox control of α-KGDH .

A second option is that LCB2151 binds directly to KGDH via the E2 subunit, competitively preventing the natural LA cofactor from binding, and thus inhibiting overall complex activity. Attachment of exogenous lipoic acid to the lipoyl-dependent enzymes is catalysed by a lipoate ligase in a two-step ATP-dependent reaction. The first step involves the activation of lipoic acid to form lipoyl-AMP. The conserved lysine residue on the apodomain then reacts at the activated carbonyl of lipoyl-AMP to form the lipoamide bond and release AMP (Morris et al., 1994). Taking advantage of an antibody that recognises lipoylated proteins, I measured lipoylation of DLST in cells treated with LCB2151. Preliminary results show a dose dependent decrease in lipoylation of DLST (Figures 22A and 22B), which is necessary to confirm in mitochondrial extracts using an optimized protocol (see supplemental information). Work on polymerase-δ interacting protein 2 (Poldip2) in breast cancer shows that preventing KGDH complex lipoylation inhibits enzymatic activity and represses mitochondrial function. On the other hand, increasing mitochondrial lipoylation increases respiration (Paredes et al., 2018). In agreement, we see reduced KGDH enzymatic activity (Figure 20) in synchrony with reduced lipoylation levels and mitochondrial dysfunction induced by LCB2151. Noteworthy is that LCB2216 showed a reduction in enzymatic activity, emphasising the important role of the lipoate in the mechanism of LCB2151.

The last proposed mechanism for KGDH inhibition is interference of LCB2151 with lipoyltransferases. Lipoyltrasferase 1 (LIPT1) is a mitochondrial protein that participates in the mammalian salvage pathway of lipoylation. That is to say, it catalyzes the transfer of the lipoyl group from lipoyl-AMP to the specific lysine residue of lipoyl domains of lipoate-dependent

enzymes in oxidative catabolism, namely the DLST subunit of the α-KGDH complex (Paredes et al., 2018). Two cases of *LIPT1* mutations in humans showed low lipoylation of the PDH and αKGDH complexes resulting in severely decreased PDH and α-KGDH enzyme activities (Soreze et al., 2013, 2013; Tort et al., 2014) . These plausible mechanisms will all be addressed by performing a non-bias photoaffinity labelling (PAL) to identify direct binding targets of LCB2151 using the photoreactive probe LCB2212 that shows the same activity as its parent molecule in pancreatic cancer cell lines (Figure 23). The identification of putative protein hits is a crucial step toward a better understanding of the protein interaction profile of LCB2151, which could ultimately lead to the development of a novel class of anticancer therapeutics.

4.8. Proposed Mechanism for the Interference of Glycolysis by LCB2151

Studies in pancreatic cancer cell lines describe synergistic anticancer effects with glycolytic inhibitors and standard-of-care drugs, such as Gem (Cheng et al., 2014). Their findings reinforce a therapeutic strategy that combines glycolytic inhibitors and standard-of-care drugs, such as Gem. The second potential target of LCB2151 in glycolysis, PFK-1, is currently being investigated. It is the main regulator of glycolysis and catalyzes the formation of fructose-1,6-bisphosphate (F16BP) from fructose-6-phosphate (F6P) in the cytoplasm of prokaryotic and eukaryotic cells. The regulation of PFK-1 is complex, being influenced by more than 20 effectors (Schöneberg et al., 2013; Sols, 1981; Tejwani, 1978). The physiologically most relevant activators of PFK-1 are AMP and fructose-2,6-bisphosphate (F26BP) and inhibitors are ATP and citrate (Reinhart and Lardy, 1980; Schöneberg et al., 2013; Usenik and Legiša, 2010; Zancan et al., 2007, 2008). Interestingly, F26BP concentration was significantly decreased by LCB2151 in Panc-1 cells after 6 hours, corresponding to an increase in immediate upstream metabolites F6P and glucose-6-phosphate (G6P) (Table 8).

It is reported that caspases impair glycolysis, resulting in decreased levels of ATP during apoptosis of cancer cells. The caspase-dependent inhibition of glycolysis was found to occurs between PFK and pyruvate kinase (PK), because neither G6P nor F6P were modified upon the induction of apoptosis (Pradelli et al., 2014). Since we did see a significant change in the concentration of these metabolites, inhibition of PFK-1 could be an early effect of LCB2151 and not a secondary effect due to induction of apoptosis. Moreover, inhibition of PFK-1 in several cancer cell lines redirected glucose flux through the pentose phosphate pathway resulting in a growth advantage of the cancer cells (Yi et al., 2012). Promisingly, we did not see activation of this pathway in our metabolomics analysis at 6 hours (Figure 13), encouraging us to focus next on the role of PFK-1 in the LCB2151 mechanism. In our validation efforts, we observed that protein expression of PFKP is decreased by LCB2151 treatment (Figure 22), known to positively correlate with total enzymatic activity in cancer cells (Lee et al., 2017b). Decreased PFK-1 activity, yet to be measured, would be expected to inhibit glycolysis. Despite all indications, we did not observe a strong impairment of glycolysis by LCB2151 (Figure 16). Possible cellular recovery mechanisms of glycolysis need to be investigated and thus we cannot yet conclude that LCB2151 inhibits glycolysis at the level of PFK-1.

As with KGDH, multiple direct and indirect mechanisms of PFK-1 inhibition are possible. To begin, the enzyme may recognize the NA of LCB2151 as fructose. Fortunately, the crystal structure of human PFK-1 in the physiologically active state is reported that characterizes the structure and molecular basis of the enzyme mechanism and allosteric regulation (Kloos et al., 2015). This knowledge may serve as a useful guide to model how LCB2151 could be interacting with PFK-1. On the other hand, the lipoate moiety of LCB2151 could also be playing a role in this inhibition. Glycolysis and fatty acid β-oxidation are coordinately regulated by specific metabolites

of each bioenergetic network (Hue and Taegtmeyer, 2009). Moreover, glycolytic flux was shown to be regulated by modulation of PFK-1 activity by interaction with fatty acids (Jenkins et al., 2011). Noteworthy, the lipoate moiety of LCB2151 is chemically protected from β-oxidation and could thus interfere with this process. In light of recent preliminary results in our Lab that show LCB2151 is affecting β-oxidation, PFK-1 could be influenced indirectly by interfering with fatty acid metabolism.

The last possibility needed to be addressed is the indirect inhibition of PFK-1 via regulation of 6-phosphofructo-2-kinase/fructose-2,6-biphosphatase 3 (PFK-2, PFKFB3). PFKFB3 activates glycolysis by synthesizing F26BP, an allosteric activator of PFK-1(Van Schaftingen et al., 1982). PFKFB3 plays a crucial role in many types of tumor cells, particularly through the oncogenic Ras signaling pathway (Kole et al., 1991; Telang et al., 2006). Most studies have demonstrated that cancer cell growth, proliferation, migration and metastasis are promoted when PFKFB3 expression is increased (Minchenko et al., 2014). Thus, there has been an increased interest in the identification and development of PFKFB3 inhibitors. 3PO and its derivative PFK158 have been shown to reduce glucose metabolism and exhibit potent antitumor activity in several human cancer xenograft models (Chen et al., 2016; Li et al., 2017; Zhu et al., 2016). Interestingly, binding competition between 3PO and F6P for the binding area of PFKFB3 is possible and could also be a possibility for LCB2151 and F6P (Clem et al., 2008). The role of LCB2151 in glycolysis by acting through a similar mechanism as 3PO would be promising since it demonstrates a good safety profile in addition to efficacy *in vivo* (Clem et al., 2008).

Another noteworthy conclusion is with respect PDH, which appears to be unaffected by LCB2151. A steady-state metabolomics analysis in BxPC-3 cells demonstrated that treatment with CPI-613 reduced citrate levels, consistent with the inhibition of PDH activity by this compound

(Stuart et al., 2014; Zachar et al., 2011). In comparison, we did not observe any changes in citrate nor metabolites directly related to the PDH reaction at the metabolic level by LCB2151 (Table 8) that could explain PDH inhibition. Additionally, lipoylation of PDH was not changed significantly by LCB2151 treatment (Figure 21C and 21D). These results are consistent with *in vitro* studies carried out in parallel that reveal no significant effect of LCB2151 on PDK1-4 enzymatic activity (data not shown), which regulate PDH. It is possible that PDH activity is affected by LCB2151 at a different time point than KGDH or PFK-1, which was focused around 6 hours treatment. Since the lipoate of LCB2151 is designed to target lipoate-dependent enzymes such as PDH, it is worth testing treatments at earlier or later time points to rule this out.

4.9. Experimental Limitations and Future Work

This study on LCB2151 in carbon metabolism and cellular stress pathways has so far given great insight into its mechanism of anticancer action. However, there are other cellular pathways that LCB2151 is designed to target that have yet to be investigated in depth. These pathways include DNA/RNA synthesis, known to be the target of Gem mechanism, as well as fatty acid metabolism. The lipoate moiety of our NAs is designed to be resistant to beta-oxidation, thus avoiding degradation and prolonging the activity of our drug. As mentioned, preliminary results using seahorse technology (Agilent) suggests that LCB2151 is severely interrupting the process of lipid metabolism. We could have potentially developed anticancer agents that target multiple cellular pathways at once, making it crucial to investigate all metabolic pathways of the cell. Execution of the PAL assay will ultimately reveal the direct molecular targets of LCB2151. We now have access to powerful molecular tools such as proteomics, metabolomics and genomics assays that can be utilized to support these targets.

A limiting factor in our study is the number of molecules and variety of cancer and non-cancer cell lines we can test at once by hand. Testing in a cell line array such as the NCI-60 Human Tumour Cell Lines Screen would generate biological response patterns, which can be utilized to select compounds that most likely interact with a specific molecular target (Su et al., 2011). To better determine the safety profile and selectivity of our drugs in addition to efficacy, the transition into an *in vivo* mouse model of pancreatic cancer is underway. A promising pilot study in a BxPC-3 xenograft mouse model in nonobese diabetic/severe combined immunodeficiency (NOD-SCID) mice showed a 30% tumour growth arrest and that 20% of these regressed or disappeared in LCB2151-treated mice (n=3, data not shown). All the Gem-treated mice died after 3rd intraperitoneal injection due to organ failure, while all the LCB2151-treated mice survived. The next step is to test our novel compounds in human pancreatic cancer xenograft models established by our collaborators at the Bell Lab (Ilkow et al., 2015; Murphy et al., 2012). These mice bear MiaPaCa-2 or Panc-1 tumours that should allow us to see and compare the translation of our *in vitro* results using the Panc-1 cell line model. *In vivo* studies will also help with the optimization of the chemical structure of LCB2151 for maximum specificity, efficacy and safety.

4.10. Conclusion

GI cancers, namely liver and pancreatic tumors, share a poor prognosis due to late detection and high incidence of drug resistance. Of great concern is pancreatic cancer by marked rapid resistance to the cornerstone therapy, Gem, demanding for the development of more effective drug treatments. An increasing understanding of the mechanisms underlying drug resistance is a prerequisite for the development of novel agents that could bypass these mechanisms for the treatment of patients with relapsing or refractory disease. In collaboration with the Guindon Lab, we are developing novel anticancer drugs designed to interfere with mitochondrial energetics and

DNA replication, while able to bypass cellular mechanisms of resistance in cancer. To date, we have identified two lead molecules LCB2151 and LCB2179 that show high efficacy in Gem-resistance pancreatic cancer cell lines, likely through unique mechanisms of action. The single agent prodrug LCB2151 simultaneously interferes with metabolism in cancer cells, while avoiding key resistance mechanisms. Similar approaches as those achieved for LCB-2151 are planned to determine the mechanism of action of LCB-2179. Elucidating the anticancer mechanism of action of these proprietary molecules will pave the way for *in vivo* and clinical studies leading to superior cancer therapies than is currently available to patients.

5. Supplemental Information

5.1. Methods: Mitochondrial Isolation

Samples were collected at various time points. Media was removed, cells were washed and scraped in 1X PSB. Mitochondria were extracted as previously described (Frezza et al., 2007). Cell suspension was centrifuged at 600*g* at 4 °C for 10 minutes and pellet was resuspended in ice-cold IB_c (0.01M Tris-MOPS,1mM EGTA/Tris, 10mM sucrose, pH 7.4). Samples were homogenized by passing through a 23G needle and vortexed. Homogenate was centrifuged at 600g for 10 min at 4 °C. Supernatant was centrifuged it at 7,000*g* for 10 min at 4 °C. Pellet was washed in ice-cold IB_c and homogenate was centrifuged at 7,000*g* for 10 min at 4 °C. The supernatant contained the nuclear and cytoplasmic fractions. Final pellet containing mitochondria was redistributed in appropriate buffer for the assay.

5.1.1. Optimization of Mitochondrial Extraction for Analysis of Mitochondrial Proteins

As the two potential targets of LCB2151 reside in different compartments of the cell, KGDH in the mitochondria and PFK-1 in the cytoplasm, the efficiency of a mitochondrial isolation protocol outlined by Frezza *et al.* was tested to better validate the large-scale proteomics and metabolomics results, and to help elucidate the mechanism of action of LCB2151 (Frezza *et al*., 2007). Mitochondrial isolation was performed on untreated Panc-1 cell line and the cytoplasmic/nuclear fraction was reserved for analysis of protein content (Figure 19). The mitochondrial fraction was identified by the mitochondrial marker COXIV and further by lipoate-dependent enzymes DLST and PDH-E2 that localize in the mitochondrial matrix (Kim *et al*., 2018). Probing of nucleoli and alpha-actin confirmed isolation of the nuclear and cytoplasmic fractions, respectfully. This is a

valuable technique to apply to future assays such as immunoprecipitation, western blot and enzymatic assays for the investigation into the mechanism of action of LCB2151.

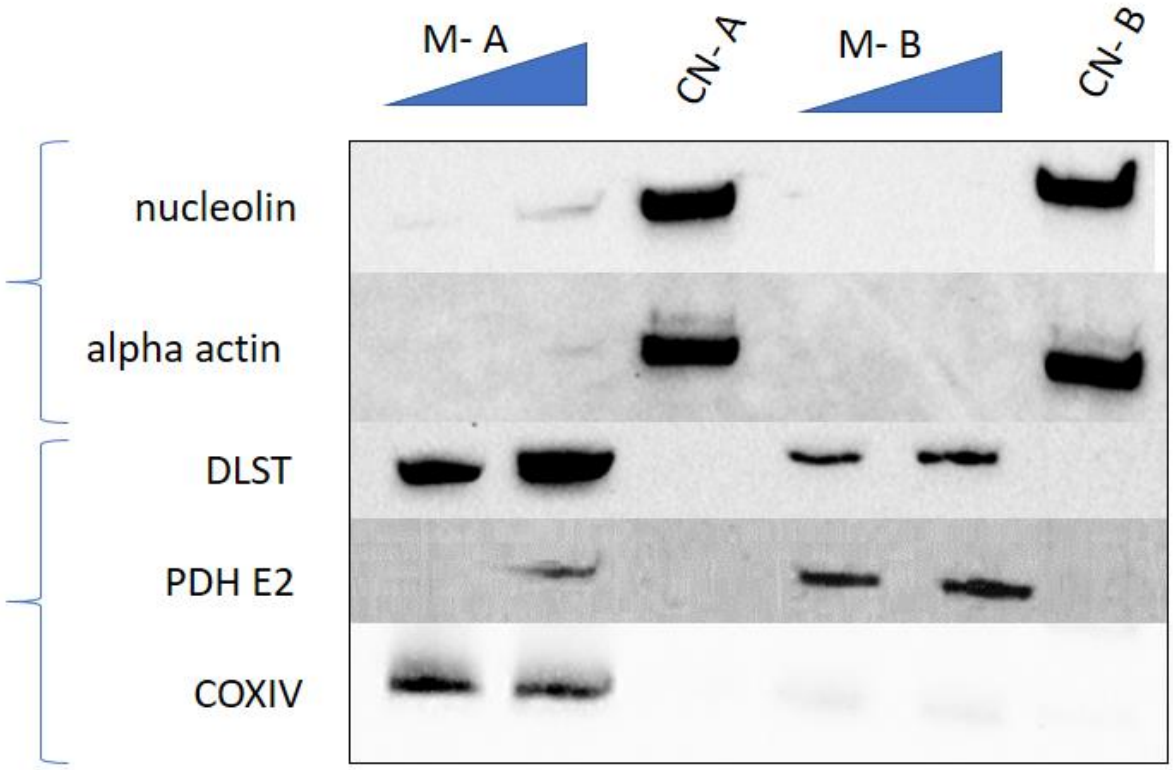

Figure S1. Mitochondrial isolation optimization. Mitochondria were isolated from untreated panc-1 cells according to the protocol by Frezza *et al.* 2007. Two concentrations of mitochondrial extract were loaded into gel, 20ug and 30ug of protein, and 20ug of cytoplasmic and nuclear extracts were loaded for each sample. Sample A mitochondria were resuspended in isolation buffer only and Sample B mitochondria underwent an additional protein extraction step. Cytoplasmic marker alpha-actin and nuclear marker nucleolin (top blots) identify the isolation of cytoplasmic and nuclear extracts while mitochondrial markers DLST, PDH-E2 and COXIV (bottom blots) identify isolation of mitochondrial extracts. M, mitochondrial fraction; CN, cytoplasmic and nuclear fraction; A, Sample A; B, Sample B.

6. References

Abbruzzese, J.L., Grunewald, R., Weeks, E.A., Gravel, D., Adams, T., Nowak, B., Mineishi, S., Tarassoff, P., Satterlee, W., and Raber, M.N. (1991). A phase I clinical, plasma, and cellular pharmacology study of gemcitabine. J. Clin. Oncol. Off. J. Am. Soc. Clin. Oncol. *9*, 491–498.

Achiwa, H., Oguri, T., Sato, S., Maeda, H., Niimi, T., and Ueda, R. (2004). Determinants of sensitivity and resistance to gemcitabine: The roles of human equilibrative nucleoside transporter 1 and deoxycytidine kinase in non-small cell lung cancer. Cancer Sci. *95*, 753–757.

Adamska, A., Elaskalani, O., Emmanouilidi, A., Kim, M., Abdol Razak, N.B., Metharom, P., and Falasca, M. (2017). Molecular and cellular mechanisms of chemoresistance in pancreatic cancer. Adv. Biol. Regul.

Adamska, A., Elaskalani, O., Emmanouilidi, A., Kim, M., Abdol Razak, N.B., Metharom, P., and Falasca, M. (2018). Molecular and cellular mechanisms of chemoresistance in pancreatic cancer. Adv. Biol. Regul. *68*, 77–87.

Afanas'ev, I. (2010). Reactive Oxygen Species Signaling in Cancer: Comparison with Aging. Aging Dis. *2*, 219–230.

Ahn, C.S., and Metallo, C.M. (2015). Mitochondria as biosynthetic factories for cancer proliferation. Cancer Metab. *3*, 1.

Akada, M., Crnogorac-Jurcevic, T., Lattimore, S., Mahon, P., Lopes, R., Sunamura, M., Matsuno, S., and Lemoine, N.R. (2005). Intrinsic Chemoresistance to Gemcitabine Is Associated with Decreased Expression of BNIP3 in Pancreatic Cancer. Clin. Cancer Res. *11*, 3094–3101.

Akiba, S., Matsugo, S., Packer, L., and Konishi, T. (1998). Assay of protein-bound lipoic acid in tissues by a new enzymatic method. Anal. Biochem. *258*, 299–304.

Alexander, P., Kucera, G., and Pardee, T.S. (2016). Improving nucleoside analogs via lipid conjugation: Is fatter any better? Crit. Rev. Oncol. Hematol. *100*, 46–56.

Alfadda, A.A., and Sallam, R.M. (2012). Reactive oxygen species in health and disease. J. Biomed. Biotechnol. *2012*, 936486.

Al-Hawary, M.M., Francis, I.R., Chari, S.T., Fishman, E.K., Hough, D.M., Lu, D.S., Macari, M., Megibow, A.J., Miller, F.H., Mortele, K.J., et al. (2014). Pancreatic Ductal Adenocarcinoma Radiology Reporting Template: Consensus Statement of the Society of Abdominal Radiology and the American Pancreatic Association. Radiology *270*, 248–260.

Ali, S.M., Khan, A.R., Ahmad, M.U., Chen, P., Sheikh, S., and Ahmad, I. (2005). Synthesis and biological evaluation of gemcitabine-lipid conjugate (NEO6002). Bioorg. Med. Chem. Lett. *15*, 2571–2574.

Alistar, A., Morris, B.B., Desnoyer, R., Klepin, H.D., Hosseinzadeh, K., Clark, C., Cameron, A., Leyendecker, J., D'Agostino, R., Topaloglu, U., et al. (2017). Safety and tolerability of the first-in-class agent CPI-613 in combination with modified FOLFIRINOX in patients with metastatic pancreatic cancer: a single-centre, open-label, dose-escalation, phase 1 trial. Lancet Oncol. *18*, 770–778.

Allain, V., Bourgaux, C., and Couvreur, P. (2012). Self-assembled nucleolipids: from supramolecular structure to soft nucleic acid and drug delivery devices. Nucleic Acids Res. *40*, 1891–1903.

Altman, B.J., Stine, Z.E., and Dang, C.V. (2016). From Krebs to clinic: glutamine metabolism to cancer therapy. Nat. Rev. Cancer *advance online publication*.

Amelio, I., Cutruzzolá, F., Antonov, A., Agostini, M., and Melino, G. (2014). Serine and glycine metabolism in cancer. Trends Biochem. Sci. *39*, 191–198.

Amrutkar, M., and Gladhaug, I.P. (2017). Pancreatic Cancer Chemoresistance to Gemcitabine. Cancers *9*.

Applegate, M.A.B., Humphries, K.M., and Szweda, L.I. (2008). Reversible inhibition of alpha-ketoglutarate dehydrogenase by hydrogen peroxide: glutathionylation and protection of lipoic acid. Biochemistry *47*, 473–478.

Ashida, R., Nakata, B., Shigekawa, M., Mizuno, N., Sawaki, A., Hirakawa, K., Arakawa, T., and Yamao, K. (2009). Gemcitabine sensitivity-related mRNA expression in endoscopic ultrasound-guided fine-needle aspiration biopsy of unresectable pancreatic cancer. J. Exp. Clin. Cancer Res. *28*, 83.

Aye, Y., Li, M., Long, M.J.C., and Weiss, R.S. (2015). Ribonucleotide reductase and cancer: biological mechanisms and targeted therapies. Oncogene *34*, 2011–2021.

Bardeesy, N., Aguirre, A.J., Chu, G.C., Cheng, K., Lopez, L.V., Hezel, A.F., Feng, B., Brennan, C., Weissleder, R., Mahmood, U., et al. (2006). Both p16Ink4a and the p19Arf-p53 pathway constrain progression of pancreatic adenocarcinoma in the mouse. Proc. Natl. Acad. Sci. U. S. A. *103*, 5947–5952.

Bedard, K., and Krause, K.-H. (2007). The NOX family of ROS-generating NADPH oxidases: physiology and pathophysiology. Physiol. Rev. *87*, 245–313.

Bensinger, S.J., and Christofk, H.R. (2012). New aspects of the Warburg effect in cancer cell biology. Semin. Cell Dev. Biol. *23*, 352–361.

Bergman, A.M., Pinedo, H.M., Jongsma, A.P.M., Brouwer, M., Ruiz van Haperen, V.W.T., Veerman, G., Leyva, A., Eriksson, S., and Peters, G.J. (1999). Decreased resistance to gemcitabine (2′,2′-difluorodeoxycitidine) of cytosine arabinoside-resistant myeloblastic murine and rat leukemia cell lines: role of altered activity and substrate specificity of deoxycytidine kinase. Biochem. Pharmacol. *57*, 397–406.

Bergman, A.M., Eijk, P.P., Ruiz van Haperen, V.W.T., Smid, K., Veerman, G., Hubeek, I., van den Ijssel, P., Ylstra, B., and Peters, G.J. (2005). In vivo induction of resistance to gemcitabine results in increased expression of ribonucleotide reductase subunit M1 as the major determinant. Cancer Res. *65*, 9510–9516.

Bergman, A.M., Adema, A.D., Balzarini, J., Bruheim, S., Fichtner, I., Noordhuis, P., Fodstad, O., Myhren, F., Sandvold, M.L., Hendriks, H.R., et al. (2011). Antiproliferative activity, mechanism of action and oral antitumor activity of CP-4126, a fatty acid derivative of gemcitabine, in in vitro and in vivo tumor models. Invest. New Drugs *29*, 456–466.

Biankin, A.V., Waddell, N., Kassahn, K.S., Gingras, M.-C., Muthuswamy, L.B., Johns, A.L., Miller, D.K., Wilson, P.J., Patch, A.-M., Wu, J., et al. (2012). Pancreatic cancer genomes reveal aberrations in axon guidance pathway genes. Nature *491*, 399–405.

Bilimoria, K.Y., Bentrem, D.J., Ko, C.Y., Ritchey, J., Stewart, A.K., Winchester, D.P., and Talamonti, M.S. (2007). Validation of the 6th edition AJCC pancreatic cancer staging system. Cancer *110*, 738–744.

Boroughs, L.K., and DeBerardinis, R.J. (2015). Metabolic pathways promoting cancer cell survival and growth. Nat. Cell Biol. *17*, 351–359.

Borst, P., Evers, R., Kool, M., and Wijnholds, J. (2000). A Family of Drug Transporters: the Multidrug Resistance-Associated Proteins. J. Natl. Cancer Inst. *92*, 1295–1302.

Brandi, J., Cecconi, D., Cordani, M., Torrens-Mas, M., Pacchiana, R., Dalla Pozza, E., Butera, G., Manfredi, M., Marengo, E., Oliver, J., et al. (2016). The antioxidant uncoupling protein 2 stimulates hnRNPA2/B1, GLUT1 and PKM2 expression and sensitizes pancreas cancer cells to glycolysis inhibition. Free Radic. Biol. Med. *101*, 305–316.

Breinbauer, R., and Köhn, M. (2003). Azide-alkyne coupling: a powerful reaction for bioconjugate chemistry. Chembiochem Eur. J. Chem. Biol. *4*, 1147–1149.

Burr, S.P., Costa, A.S.H., Grice, G.L., Timms, R.T., Lobb, I.T., Freisinger, P., Dodd, R.B., Dougan, G., Lehner, P.J., Frezza, C., et al. (2016). Mitochondrial Protein Lipoylation and the 2-Oxoglutarate Dehydrogenase Complex Controls HIF1α Stability in Aerobic Conditions. Cell Metab. *24*, 740–752.

Burris, H.A., Moore, M.J., Andersen, J., Green, M.R., Rothenberg, M.L., Modiano, M.R., Cripps, M.C., Portenoy, R.K., Storniolo, A.M., Tarassoff, P., et al. (1997). Improvements in survival and clinical benefit with gemcitabine as first-line therapy for patients with advanced pancreas cancer: a randomized trial. J. Clin. Oncol. *15*, 2403–2413.

Cairns, R.A., Harris, I.S., and Mak, T.W. (2011). Regulation of cancer cell metabolism. Nat. Rev. Cancer *11*, 85–95.

Carling, P.J., Cree, L.M., and Chinnery, P.F. (2011). The implications of mitochondrial DNA copy number regulation during embryogenesis. Mitochondrion *11*, 686–692.

Chaiswing, L., Zhong, W., and Oberley, T.D. (2014). Increasing discordant antioxidant protein levels and enzymatic activities contribute to increasing redox imbalance observed during human prostate cancer progression. Free Radic. Biol. Med. *67*, 342–352.

Chantrill, L.A., Nagrial, A.M., Watson, C., Johns, A.L., Martyn-Smith, M., Simpson, S., Mead, S., Jones, M.D., Samra, J.S., Gill, A.J., et al. (2015). Precision Medicine for Advanced Pancreas Cancer: The Individualized Molecular Pancreatic Cancer Therapy (IMPaCT) Trial. Clin. Cancer Res. *21*, 2029–2037.

Chen, L., Zhao, J., Tang, Q., Li, H., Zhang, C., Yu, R., Zhao, Y., Huo, Y., and Wu, C. (2016). PFKFB3 Control of Cancer Growth by Responding to Circadian Clock Outputs. Sci. Rep. *6*.

Chen, P., Chien, P.-Y., Khan, A.R., Sheikh, S., Ali, S.M., Ahmad, M.U., and Ahmad, I. (2006). In-vitro and in-vivo anti-cancer activity of a novel gemcitabine-cardiolipin conjugate. Anticancer. Drugs *17*, 53–61.

Chen, Y.-W., Liu, J.-Y., Lin, S.-T., Li, J.-M., Huang, S.-H., Chen, J.-Y., Wu, J.-Y., Kuo, C.-C., Wu, C.-L., Lu, Y.-C., et al. (2011). Proteomic analysis of gemcitabine-induced drug resistance in pancreatic cancer cells. Mol. Biosyst. *7*, 3065–3074.

Cheng, G., Zielonka, J., McAllister, D., Tsai, S., Dwinell, M.B., and Kalyanaraman, B. (2014). Profiling and targeting of cellular bioenergetics: inhibition of pancreatic cancer cell proliferation. Br. J. Cancer *111*, 85–93.

Chin, V., Nagrial, A., Sjoquist, K., O'Connor, C.A., Chantrill, L., Biankin, A.V., Scholten, R.J., and Yip, D. (2018). Chemotherapy and radiotherapy for advanced pancreatic cancer. Cochrane Database Syst. Rev.

Christofk, H.R., Vander Heiden, M.G., Harris, M.H., Ramanathan, A., Gerszten, R.E., Wei, R., Fleming, M.D., Schreiber, S.L., and Cantley, L.C. (2008). The M2 splice isoform of pyruvate kinase is important for cancer metabolism and tumour growth. Nature *452*, 230–233.

Ciccolini, J., Dahan, L., André, N., Evrard, A., Duluc, M., Blesius, A., Yang, C., Giacometti, S., Brunet, C., Raynal, C., et al. (2010). Cytidine deaminase residual activity in serum is a predictive marker of early severe toxicities in adults after gemcitabine-based chemotherapies. J. Clin. Oncol. Off. J. Am. Soc. Clin. Oncol. *28*, 160–165.

Clem, B., Telang, S., Clem, A., Yalcin, A., Meier, J., Simmons, A., Rasku, M.A., Arumugam, S., Dean, W.L., Eaton, J., et al. (2008). Small-molecule inhibition of 6-phosphofructo-2-kinase activity suppresses glycolytic flux and tumor growth. Mol. Cancer Ther. *7*, 110–120.

Clem, B.F., O'Neal, J., Tapolsky, G., Clem, A.L., Imbert-Fernandez, Y., Kerr, D.A., Klarer, A.C., Redman, R., Miller, D.M., Trent, J.O., et al. (2013). Targeting 6-phosphofructo-2-kinase (PFKFB3) as a therapeutic strategy against cancer. Mol. Cancer Ther. *12*, 1461–1470.

Colca, J.R., McDonald, W.G., Cavey, G.S., Cole, S.L., Holewa, D.D., Brightwell-Conrad, A.S., Wolfe, C.L., Wheeler, J.S., Coulter, K.R., Kilkuskie, P.M., et al. (2013). Identification of a

Mitochondrial Target of Thiazolidinedione Insulin Sensitizers (mTOT)—Relationship to Newly Identified Mitochondrial Pyruvate Carrier Proteins. PLOS ONE *8*, e61551.

Coller, H.A. (2014). Is cancer a metabolic disease? Am. J. Pathol. *184*, 4–17.

Collisson, E.A., Sadanandam, A., Olson, P., Gibb, W.J., Truitt, M., Gu, S., Cooc, J., Weinkle, J., Kim, G.E., Jakkula, L., et al. (2011). Subtypes of Pancreatic Ductal Adenocarcinoma and Their Differing Responses to Therapy. Nat. Med. *17*, 500–503.

Conroy, T., Desseigne, F., Ychou, M., Bouché, O., Guimbaud, R., Bécouarn, Y., Adenis, A., Raoul, J.-L., Gourgou-Bourgade, S., de la Fouchardière, C., et al. (2011). FOLFIRINOX versus Gemcitabine for Metastatic Pancreatic Cancer.

Costa Leite, T., Da Silva, D., Guimarães Coelho, R., Zancan, P., and Sola-Penna, M. (2007). Lactate favours the dissociation of skeletal muscle 6-phosphofructo-1-kinase tetramers down-regulating the enzyme and muscle glycolysis. Biochem. J. *408*, 123–130.

Costantino, C.L., Witkiewicz, A.K., Y, Y.K., Cozzitorto, J.A., Kennedy, E.P., Dasgupta, A., Keen, J.C., Yeo, C.J., Gorospe, M., and Brody, J.R. (2009). HuR's role in gemcitabine efficacy in pancreatic cancer: HuR upregulates the expression of the gemcitabine metabolizing enzyme, deoxycytidine kinase. Cancer Res. *69*, 4567–4572.

Couvreur, P., Reddy, L.H., Mangenot, S., Poupaert, J.H., Desmaële, D., Lepêtre-Mouelhi, S., Pili, B., Bourgaux, C., Amenitsch, H., and Ollivon, M. (2008). Discovery of new hexagonal supramolecular nanostructures formed by squalenoylation of an anticancer nucleoside analogue. Small Weinh. Bergstr. Ger. *4*, 247–253.

Cox, E., and Bonner, J. (2001). Ecology. The advantages of togetherness. Science *292*, 448–449.

Cox, J., and Mann, M. (2008). MaxQuant enables high peptide identification rates, individualized p.p.b.-range mass accuracies and proteome-wide protein quantification. Nat. Biotechnol. *26*, 1367–1372.

Crapo, J.D., Oury, T., Rabouille, C., Slot, J.W., and Chang, L.Y. (1992). Copper,zinc superoxide dismutase is primarily a cytosolic protein in human cells. Proc. Natl. Acad. Sci. U. S. A. *89*, 10405–10409.

Dalla Pozza, E., Fiorini, C., Dando, I., Menegazzi, M., Sgarbossa, A., Costanzo, C., Palmieri, M., and Donadelli, M. (2012). Role of mitochondrial uncoupling protein 2 in cancer cell resistance to gemcitabine. Biochim. Biophys. Acta *1823*, 1856–1863.

Davidson, J.D., Ma, L., Flagella, M., Geeganage, S., Gelbert, L.M., and Slapak, C.A. (2004). An increase in the expression of ribonucleotide reductase large subunit 1 is associated with gemcitabine resistance in non-small cell lung cancer cell lines. Cancer Res. *64*, 3761–3766.

Davidson, S.M., Papagiannakopoulos, T., Olenchock, B.A., Heyman, J.E., Keibler, M.A., Luengo, A., Bauer, M.R., Jha, A.K., O'Brien, J.P., Pierce, K.A., et al. (2016). Environment Impacts the Metabolic Dependencies of Ras-Driven Non-Small Cell Lung Cancer. Cell Metab. *23*, 517–528.

DeBerardinis, R.J., and Cheng, T. (2010). Q's next: the diverse functions of glutamine in metabolism, cell biology and cancer. Oncogene *29*, 313–324.

DeBerardinis, R.J., Mancuso, A., Daikhin, E., Nissim, I., Yudkoff, M., Wehrli, S., and Thompson, C.B. (2007). Beyond aerobic glycolysis: Transformed cells can engage in glutamine metabolism that exceeds the requirement for protein and nucleotide synthesis. Proc. Natl. Acad. Sci. U. S. A. *104*, 19345–19350.

Deberardinis, R.J., Sayed, N., Ditsworth, D., and Thompson, C.B. (2008). Brick by brick: metabolism and tumor cell growth. Curr. Opin. Genet. Dev. *18*, 54–61.

DeBerardinis, R.J., Lum, J.J., Hatzivassiliou, G., and Thompson, C.B. (2008). The biology of cancer: metabolic reprogramming fuels cell growth and proliferation. Cell Metab. *7*, 11–20.

Deeley, R.G., and Cole, S.P.C. (1997). Function, evolution and structure of multidrug resistance protein (MRP). Semin. Cancer Biol. *8*, 193–204.

Deep, G., and Agarwal, R. (2013). Targeting tumor microenvironment with silibinin: promise and potential for a translational cancer chemopreventive strategy. Curr. Cancer Drug Targets *13*, 486–499.

Deplanque, G., Demarchi, M., Hebbar, M., Flynn, P., Melichar, B., Atkins, J., Nowara, E., Moyé, L., Piquemal, D., Ritter, D., et al. (2015). A randomized, placebo-controlled phase III trial of masitinib plus gemcitabine in the treatment of advanced pancreatic cancer. Ann. Oncol. Off. J. Eur. Soc. Med. Oncol. *26*, 1194–1200.

Deprez, J., Vertommen, D., Alessi, D.R., Hue, L., and Rider, M.H. (1997). Phosphorylation and activation of heart 6-phosphofructo-2-kinase by protein kinase B and other protein kinases of the insulin signaling cascades. J. Biol. Chem. *272*, 17269–17275.

Dhayat, S.A., Mardin, W.A., Seggewiß, J., Ströse, A.J., Matuszcak, C., Hummel, R., Senninger, N., Mees, S.T., and Haier, J. (2015). MicroRNA Profiling Implies New Markers of Gemcitabine Chemoresistance in Mutant p53 Pancreatic Ductal Adenocarcinoma. PLoS ONE *10*.

Di, B., Pan, B., Ge, L., Ma, J., Wu, Y., and Guo, T. (2018). Targeted agents for patients with advanced/metastatic pancreatic cancer. Medicine (Baltimore) *97*.

Dimou, A., Syrigos, K.N., and Saif, M.W. (2012). Overcoming the stromal barrier: technologies to optimize drug delivery in pancreatic cancer. Ther. Adv. Med. Oncol. *4*, 271–279.

Donadelli, M., Dando, I., Zaniboni, T., Costanzo, C., Dalla Pozza, E., Scupoli, M.T., Scarpa, A., Zappavigna, S., Marra, M., Abbruzzese, A., et al. (2011). Gemcitabine/cannabinoid combination triggers autophagy in pancreatic cancer cells through a ROS-mediated mechanism. Cell Death Dis. *2*, e152.

Donadelli, M., Dando, I., Dalla Pozza, E., and Palmieri, M. (2015). Mitochondrial uncoupling protein 2 and pancreatic cancer: A new potential target therapy. World J. Gastroenterol. WJG *21*, 3232–3238.

Dörsam, B., Göder, A., Seiwert, N., Kaina, B., and Fahrer, J. (2014). Lipoic acid induces p53-independent cell death in colorectal cancer cells and potentiates the cytotoxicity of 5-fluorouracil. Arch. Toxicol. *89*, 1829–1846.

Dostie, S., Prévost, M., Mochirian, P., Tanveer, K., Andrella, N., Rostami, A., Tambutet, G., and Guindon, Y. (2016). Diastereoselective Synthesis of C2′-Fluorinated Nucleoside Analogues Using an Acyclic Approach. J. Org. Chem. *81*, 10769–10790.

Dozio, E., Ruscica, M., Passafaro, L., Dogliotti, G., Steffani, L., Marthyn, P., Pagani, A., Demartini, G., Esposti, D., Fraschini, F., et al. (2010). The natural antioxidant alpha-lipoic acid induces p27(Kip1)-dependent cell cycle arrest and apoptosis in MCF-7 human breast cancer cells. Eur. J. Pharmacol. *641*, 29–34.

Durand, M., and Mach, N. (2013). [Alpha lipoic acid and its antioxidant against cancer and diseases of central sensitization]. Nutr. Hosp. *28*, 1031–1038.

Dwivedi, N., Flora, G., Kushwaha, P., and Flora, S.J.S. (2014). Alpha-lipoic acid protects oxidative stress, changes in cholinergic system and tissue histopathology during co-exposure to arsenic-dichlorvos in rats. Environ. Toxicol. Pharmacol. *37*, 7–23.

Eda, H., Ura, M., F-Ouchi, K., Tanaka, Y., Miwa, M., and Ishitsuka, H. (1998). The antiproliferative activity of DMDC is modulated by inhibition of cytidine deaminase. Cancer Res. *58*, 1165–1169.

Egawa, Y., Saigo, C., Kito, Y., Moriki, T., and Takeuchi, T. (2018). Therapeutic potential of CPI-613 for targeting tumorous mitochondrial energy metabolism and inhibiting autophagy in clear cell sarcoma. PLoS ONE *13*.

Ehinger, J.K., Piel, S., Ford, R., Karlsson, M., Sjövall, F., Frostner, E.Å., Morota, S., Taylor, R.W., Turnbull, D.M., Cornell, C., et al. (2016). Cell-permeable succinate prodrugs bypass mitochondrial complex I deficiency. Nat. Commun. *7*, 12317.

Elia, I., Schmieder, R., Christen, S., and Fendt, S.-M. (2016). Organ-Specific Cancer Metabolism and Its Potential for Therapy. Handb. Exp. Pharmacol. *233*, 321–353.

Fan, J., Kamphorst, J.J., Mathew, R., Chung, M.K., White, E., Shlomi, T., and Rabinowitz, J.D. (2013). Glutamine-driven oxidative phosphorylation is a major ATP source in transformed mammalian cells in both normoxia and hypoxia. Mol. Syst. Biol. *9*, 712.

Fan, J., Ye, J., Kamphorst, J.J., Shlomi, T., Thompson, C.B., and Rabinowitz, J.D. (2014). Quantitative flux analysis reveals folate-dependent NADPH production. Nature *510*, 298–302.

Fendt, S.-M., Bell, E.L., Keibler, M.A., Olenchock, B.A., Mayers, J.R., Wasylenko, T.M., Vokes, N.I., Guarente, L., Vander Heiden, M.G., and Stephanopoulos, G. (2013). Reductive glutamine metabolism is a function of the α-ketoglutarate to citrate ratio in cells. Nat. Commun. *4*, 2236.

Freed-Pastor, W.A., and Prives, C. (2012). Mutant p53: one name, many proteins. Genes Dev. *26*, 1268–1286.

Frezza, C., Cipolat, S., and Scorrano, L. (2007). Organelle isolation: functional mitochondria from mouse liver, muscle and cultured filroblasts. Nat. Protoc. *2*, 287–295.

Fujita, H., Ohuchida, K., Mizumoto, K., Itaba, S., Ito, T., Nakata, K., Yu, J., Kayashima, T., Souzaki, R., Tajiri, T., et al. (2010). Gene Expression Levels as Predictive Markers of Outcome in Pancreatic Cancer after Gemcitabine-Based Adjuvant Chemotherapy. Neoplasia N. Y. N *12*, 807–817.

Fujita, M., Imadome, K., and Imai, T. (2017). Metabolic characterization of invaded cells of the pancreatic cancer cell line, PANC-1. Cancer Sci. *108*, 961–971.

Funamizu, N., Okamoto, A., Kamata, Y., Misawa, T., Uwagawa, T., Gocho, T., Yanaga, K., and Manome, Y. (2010). Is the resistance of gemcitabine for pancreatic cancer settled only by overexpression of deoxycytidine kinase? Oncol. Rep. *23*, 471–475.

Galluzzi, L., Kepp, O., Vander Heiden, M.G., and Kroemer, G. (2013). Metabolic targets for cancer therapy. Nat. Rev. Drug Discov. *12*, 829–846.

Galmarini, C.M., Mackey, J.R., and Dumontet, C. (2002). Nucleoside analogues and nucleobases in cancer treatment. Lancet Oncol. *3*, 415–424.

Gandhi, V.V., and Samuels, D.C. (2011). A review comparing deoxyribonucleoside triphosphate (dNTP) concentrations in the mitochondrial and cytoplasmic compartments of normal and transformed cells. Nucleosides Nucleotides Nucleic Acids *30*, 317–339.

Garrido-Laguna, I., and Hidalgo, M. (2015). Pancreatic cancer: from state-of-the-art treatments to promising novel therapies. Nat. Rev. Clin. Oncol. *12*, 319–334.

Genini, D., Adachi, S., Chao, Q., Rose, D.W., Carrera, C.J., Cottam, H.B., Carson, D.A., and Leoni, L.M. (2000). Deoxyadenosine analogs induce programmed cell death in chronic lymphocytic leukemia cells by damaging the DNA and by directly affecting the mitochondria. Blood *96*, 3537–3543.

Ghaneh, P., Costello, E., and Neoptolemos, J.P. (2007). Biology and management of pancreatic cancer. Gut *56*, 1134–1152.

Ghazaly, E.A., Joel, S., Gribben, J.G., Mohammad, T., Emiloju, O., Stavraka, C., Hopkins, T., Gabra, H., Wasan, H., Habib, N.A., et al. (2013). ProGem1: Phase I first-in-human study of the novel nucleotide NUC-1031 in adult patients with advanced solid tumors. J. Clin. Oncol. *31*, 2576–2576.

Goodwin, M.L., Jin, H., Straessler, K., Smith-Fry, K., Zhu, J.-F., Monument, M.J., Grossmann, A., Randall, R.L., Capecchi, M.R., and Jones, K.B. (2014). Modeling alveolar soft part sarcomagenesis in the mouse: a role for lactate in the tumor microenvironment. Cancer Cell *26*, 851–862.

Gottesman, M.M., Fojo, T., and Bates, S.E. (2002). Multidrug resistance in cancer: role of ATP-dependent transporters. Nat. Rev. Cancer *2*, 48–58.

Gourgou-Bourgade, S., Bascoul-Mollevi, C., Desseigne, F., Ychou, M., Bouché, O., Guimbaud, R., Bécouarn, Y., Adenis, A., Raoul, J.-L., Boige, V., et al. (2013). Impact of FOLFIRINOX compared with gemcitabine on quality of life in patients with metastatic pancreatic cancer: results from the PRODIGE 4/ACCORD 11 randomized trial. J. Clin. Oncol. Off. J. Am. Soc. Clin. Oncol. *31*, 23–29.

Gresham, G.K., Wells, G.A., Gill, S., Cameron, C., and Jonker, D.J. (2014). Chemotherapy regimens for advanced pancreatic cancer: a systematic review and network meta-analysis. BMC Cancer *14*, 471.

Griffith, O.W. (1999). Biologic and pharmacologic regulation of mammalian glutathione synthesis. Free Radic. Biol. Med. *27*, 922–935.

Griffiths, M., Beaumont, N., Yao, S.Y., Sundaram, M., Boumah, C.E., Davies, A., Kwong, F.Y., Coe, I., Cass, C.E., Young, J.D., et al. (1997a). Cloning of a human nucleoside transporter implicated in the cellular uptake of adenosine and chemotherapeutic drugs. Nat. Med. *3*, 89–93.

Griffiths, M., Yao, S.Y., Abidi, F., Phillips, S.E., Cass, C.E., Young, J.D., and Baldwin, S.A. (1997b). Molecular cloning and characterization of a nitrobenzylthioinosine-insensitive (ei) equilibrative nucleoside transporter from human placenta. Biochem. J. *328*, 739–743.

Gruzman, A., Hidmi, A., Katzhendler, J., Haj-Yehie, A., and Sasson, S. (2004). Synthesis and characterization of new and potent alpha-lipoic acid derivatives. Bioorg. Med. Chem. *12*, 1183–1190.

Guais, A., Baronzio, G., Sanders, E., Campion, F., Mainini, C., Fiorentini, G., Montagnani, F., Behzadi, M., Schwartz, L., and Abolhassani, M. (2012). Adding a combination of hydroxycitrate and lipoic acid (METABLOC^{TM}) to chemotherapy improves effectiveness against tumor development: experimental results and case report. Invest. New Drugs *30*, 200–211.

Guo, Z., Wang, F., Di, Y., Yao, L., Yu, X., Fu, D., Li, J., and Jin, C. (2018). Antitumor effect of gemcitabine-loaded albumin nanoparticle on gemcitabine-resistant pancreatic cancer induced by low hENT1 expression. Int. J. Nanomedicine *13*, 4869–4880.

Han, C., Yang, L., Choi, H.H., Baddour, J., Achreja, A., Liu, Y., Li, Y., Li, J., Wan, G., Huang, C., et al. (2016). Amplification of USP13 drives ovarian cancer metabolism. Nat. Commun. *7*, 13525.

Han, J., Tschernutter, V., Yang, J., Eckle, T., and Borchers, C.H. (2013). Analysis of Selected Sugars and Sugar Phosphates in Mouse Heart Tissue by Reductive Amination and Liquid Chromatography-Electrospray Ionization Mass Spectrometry. Anal. Chem. *85*, 5965–5973.

Hanahan, D., and Weinberg, R.A. (2011). Hallmarks of Cancer: The Next Generation. Cell *144*, 646–674.

Haperen, V.W.T.R. van, Veerman, G., Eriksson, S., Boven, E., Stegmann, A.P.A., Hermsen, M., Vermorken, J.B., Pinedo, H.M., and Peters, G.J. (1994). Development and Molecular

Characterization of a 2′,2′-Difluorodeoxycytidine-resistant Variant of the Human Ovarian Carcinoma Cell Line A2780. Cancer Res. *54*, 4138–4143.

Heinemann, V., Xu, Y.Z., Chubb, S., Sen, A., Hertel, L.W., Grindey, G.B., and Plunkett, W. (1990). Inhibition of ribonucleotide reduction in CCRF-CEM cells by 2',2'-difluorodeoxycytidine. Mol. Pharmacol. *38*, 567–572.

Heinemann, V., Xu, Y.-Z., Chubb, S., Sen, A., Hertel, L.W., Grindey, G.B., and Plunkett, W. (1992). Cellular Elimination of 2′,2′-Difluorodeoxycytidine 5′-Triphosphate: A Mechanism of Self-Potentiation. Cancer Res. *52*, 533–539.

Hill, R., Rabb, M., Madureira, P.A., Clements, D., Gujar, S.A., Waisman, D.M., Giacomantonio, C.A., and Lee, P.W.K. (2013). Gemcitabine-mediated tumour regression and p53-dependent gene expression: implications for colon and pancreatic cancer therapy. Cell Death Dis. *4*, e791.

Hiratsuka, T., Inomata, M., Kono, Y., Yokoyama, S., Shiraishi, N., and Kitano, S. (2013). DHL-TauZnNa, a newly synthesized α-lipoic acid derivative, induces autophagy in human colorectal cancer cells. Oncol. Rep. *29*, 2140–2146.

Hitosugi, T., and Chen, J. (2014). Post-translational modifications and the Warburg effect. Oncogene *33*, 4279–4285.

Hitosugi, T., Fan, J., Chung, T.-W., Lythgoe, K., Wang, X., Xie, J., Ge, Q., Gu, T.-L., Polakiewicz, R.D., Roesel, J.L., et al. (2011). Tyrosine phosphorylation of mitochondrial pyruvate dehydrogenase kinase 1 is important for cancer metabolism. Mol. Cell *44*, 864–877.

Howard, J.M., and Jordan, G.L. (1977). Cancer of the pancreas. Curr. Probl. Cancer *2*, 1–52.

Hruban, R.H., Goggins, M., Parsons, J., and Kern, S.E. (2000). Progression Model for Pancreatic Cancer. Clin. Cancer Res. *6*, 2969–2972.

Hu, C., Hart, S.N., Polley, E.C., Gnanaolivu, R., Shimelis, H., Lee, K.Y., Lilyquist, J., Na, J., Moore, R., Antwi, S.O., et al. (2018). Association Between Inherited Germline Mutations in Cancer Predisposition Genes and Risk of Pancreatic Cancer. JAMA *319*, 2401–2409.

Huang, H.-M., Zhang, H., Xu, H., and Gibson, G.E. (2003). Inhibition of the alpha-ketoglutarate dehydrogenase complex alters mitochondrial function and cellular calcium regulation. Biochim. Biophys. Acta *1637*, 119–126.

Hue, L., and Taegtmeyer, H. (2009). The Randle cycle revisited: a new head for an old hat. Am. J. Physiol. - Endocrinol. Metab. *297*, E578–E591.

Humbert, M., Castéran, N., Letard, S., Hanssens, K., Iovanna, J., Finetti, P., Bertucci, F., Bader, T., Mansfield, C.D., Moussy, A., et al. (2010). Masitinib combined with standard gemcitabine chemotherapy: in vitro and in vivo studies in human pancreatic tumour cell lines and ectopic mouse model. PloS One *5*, e9430.

Hung, S.W., Mody, H.R., and Govindarajan, R. (2012). Overcoming nucleoside analog chemoresistance of pancreatic cancer: a therapeutic challenge. Cancer Lett. *320*, 138–149.

Ilkow, C.S., Marguerie, M., Batenchuk, C., Mayer, J., Ben Neriah, D., Cousineau, S., Falls, T., Jennings, V.A., Boileau, M., Bellamy, D., et al. (2015). Reciprocal cellular cross-talk within the tumor microenvironment promotes oncolytic virus activity. Nat. Med. *21*, 530–536.

Izaki, S., Goto, H., and Yokota, S. (2008). Increased chemosensitivity and elevated reactive oxygen species are mediated by glutathione reduction in glutamine deprived neuroblastoma cells. J. Cancer Res. Clin. Oncol. *134*, 761–768.

Jemal, A., Siegel, R., Xu, J., and Ward, E. (2010). Cancer statistics, 2010. CA. Cancer J. Clin. *60*, 277–300.

Jenkins, C.M., Yang, J., Sims, H.F., and Gross, R.W. (2011). Reversible High Affinity Inhibition of Phosphofructokinase-1 by Acyl-CoA. J. Biol. Chem. *286*, 11937–11950.

Jeon, M.J., Kim, W.G., Lim, S., Choi, H.-J., Sim, S., Kim, T.Y., Shong, Y.K., and Kim, W.B. (2016). Alpha lipoic acid inhibits proliferation and epithelial mesenchymal transition of thyroid cancer cells. Mol. Cell. Endocrinol. *419*, 113–123.

Jindal, V. (2018). Immune checkpoint inhibitors in gastrointestinal malignancies. J. Gastrointest. Oncol. *9*, 390–403.

Jonckheere, N., Skrypek, N., Merlin, J., Dessein, A.F., Dumont, P., Leteurtre, E., Harris, A., Desseyn, J.-L., Susini, C., Frénois, F., et al. (2012). The Mucin MUC4 and Its Membrane Partner ErbB2 Regulate Biological Properties of Human CAPAN-2 Pancreatic Cancer Cells via Different Signalling Pathways. PLoS ONE *7*.

Jones, N.P., and Schulze, A. (2012). Targeting cancer metabolism--aiming at a tumour's sweet-spot. Drug Discov. Today *17*, 232–241.

Jordheim, L.P., and Dumontet, C. (2007). Review of recent studies on resistance to cytotoxic deoxynucleoside analogues. Biochim. Biophys. Acta *1776*, 138–159.

Ju, H.-Q., Gocho, T., Aguilar, M., Wu, M., Zhuang, Z.-N., Fu, J., Yanaga, K., Huang, P., and Chiao, P.J. (2015). Mechanisms of Overcoming Intrinsic Resistance to Gemcitabine in Pancreatic Ductal Adenocarcinoma through the Redox Modulation. Am. Assoc. Cancer Res. *14*, 788–798.

Kadaba, R., Birke, H., Wang, J., Hooper, S., Andl, C.D., Di Maggio, F., Soylu, E., Ghallab, M., Bor, D., Froeling, F.E., et al. (2013). Imbalance of desmoplastic stromal cell numbers drives aggressive cancer processes. J. Pathol. *230*, 107–117.

Kafara, P., Icard, P., Guillamin, M., Schwartz, L., and Lincet, H. (2015). Lipoic acid decreases Mcl-1, Bcl-xL and up regulates Bim on ovarian carcinoma cells leading to cell death. J. Ovarian Res. *8*.

Kakuda, T.N. (2000). Pharmacology of nucleoside and nucleotide reverse transcriptase inhibitor-induced mitochondrial toxicity. Clin. Ther. *22*, 685–708.

Kamangar, F., Dores, G.M., and Anderson, W.F. (2006). Patterns of cancer incidence, mortality, and prevalence across five continents: defining priorities to reduce cancer disparities in different geographic regions of the world. J. Clin. Oncol. Off. J. Am. Soc. Clin. Oncol. *24*, 2137–2150.

Kamisawa, T., Wood, L.D., Itoi, T., and Takaori, K. (2016). Pancreatic cancer. The Lancet *388*, 73–85.

Kikuchi, G., Motokawa, Y., Yoshida, T., and Hiraga, K. (2008). Glycine cleavage system: reaction mechanism, physiological significance, and hyperglycinemia. Proc. Jpn. Acad. Ser. B Phys. Biol. Sci. *84*, 246–263.

Kikuchi, L., Oliveira, C.P., and Carrilho, F.J. (2014). Nonalcoholic Fatty Liver Disease and Hepatocellular Carcinoma.

Kim, Y.M., and Cho, M. (2014). Activation of NADPH oxidase subunit NCF4 induces ROS-mediated EMT signaling in HeLa cells. Cell. Signal. *26*, 784–796.

Kim, J., Kim, J., and Bae, J.-S. (2016). ROS homeostasis and metabolism: a critical liaison for cancer therapy. Exp. Mol. Med. *48*, e269.

Kim, M.J., Hwang, J.W., Yun, C.-K., Lee, Y., and Choi, Y.-S. (2018). Delivery of exogenous mitochondria via centrifugation enhances cellular metabolic function. Sci. Rep. *8*, 3330.

Kinnaird, A., and Michelakis, E.D. (2015). Metabolic modulation of cancer: a new frontier with great translational potential. J. Mol. Med. *93*, 127–142.

Kleeff, J., Michalski, C., Friess, H., and Büchler, M.W. (2006). Pancreatic cancer: from bench to 5-year survival. Pancreas *33*, 111–118.

Kleeff, J., Korc, M., Apte, M., Vecchia, C.L., Johnson, C.D., Biankin, A.V., Neale, R.E., Tempero, M., Tuveson, D.A., Hruban, R.H., et al. (2016). Pancreatic cancer. Nat. Rev. Dis. Primer *2*, 16022.

Kleger, A., Perkhofer, L., and Seufferlein, T. (2014). Smarter drugs emerging in pancreatic cancer therapy. Ann. Oncol. *25*, 1260–1270.

Kloos, M., Brüser, A., Kirchberger, J., Schöneberg, T., and Sträter, N. (2015). Crystal structure of human platelet phosphofructokinase-1 locked in an activated conformation. Biochem. J. *469*, 421–432.

Koay, E.J., Truty, M.J., Cristini, V., Thomas, R.M., Chen, R., Chatterjee, D., Kang, Y., Bhosale, P.R., Tamm, E.P., Crane, C.H., et al. (2014). Transport properties of pancreatic cancer describe gemcitabine delivery and response. J. Clin. Invest. *124*, 1525–1536.

Kohan, H.G., and Boroujerdi, M. (2015). Time and concentration dependency of P-gp, MRP1 and MRP5 induction in response to gemcitabine uptake in Capan-2 pancreatic cancer cells. Xenobiotica *45*, 642–652.

Kole, H.K., Resnick, R.J., Van Doren, M., and Racker, E. (1991). Regulation of 6-phosphofructo-1-kinase activity in ras-transformed rat-1 fibroblasts. Arch. Biochem. Biophys. *286*, 586–590.

Kong, X., Li, L., Li, Z., and Xie, K. (2012). Targeted Disruption of Orchestration between Stroma and Tumor Cells in Pancreatic Cancer: Molecular Basis and Therapeutic Implications. Cytokine Growth Factor Rev. *23*, 343–356.

Kopp, J.L., von Figura, G., Mayes, E., Liu, F.-F., Dubois, C.L., Morris, J.P., Pan, F.C., Akiyama, H., Wright, C.V.E., Jensen, K., et al. (2012). Identification of Sox9-dependent acinar-to-ductal reprogramming as the principal mechanism for initiation of pancreatic ductal adenocarcinoma. Cancer Cell *22*, 737–750.

Krempien, R., Muenter, M.W., Harms, W., and Debus, J. (2006). Neoadjuvant chemoradiation in patients with pancreatic adenocarcinoma. HPB *8*, 22–28.

Kroep, J.R., Loves, W.J.P., van der Wilt, C.L., Alvarez, E., Talianidis, I., Boven, E., Braakhuis, B.J.M., van Groeningen, C.J., Pinedo, H.M., and Peters, G.J. (2002). Pretreatment deoxycytidine kinase levels predict in vivo gemcitabine sensitivity. Mol. Cancer Ther. *1*, 371–376.

Lam, W., Chen, C., Ruan, S., Leung, C.-H., and Cheng, Y.-C. (2005). Expression of deoxynucleotide carrier is not associated with the mitochondrial DNA depletion caused by anti-HIV dideoxynucleoside analogs and mitochondrial dNTP uptake. Mol. Pharmacol. *67*, 408–416.

Lee, B., Hutchinson, R., Wong, H.-L., Tie, J., Putoczki, T., Tran, B., Gibbs, P., and Christie, M. (2017a). Emerging biomarkers for immunomodulatory cancer treatment of upper gastrointestinal, pancreatic and hepatic cancers. Semin. Cancer Biol.

Lee, J.-H., Liu, R., Li, J., Zhang, C., Wang, Y., Cai, Q., Qian, X., Xia, Y., Zheng, Y., Piao, Y., et al. (2017b). Stabilization of phosphofructokinase 1 platelet isoform by AKT promotes tumorigenesis. Nat. Commun. *8*.

Lee, K.C., Maturo, C., Perera, C.N., Luddy, J., Rodriguez, R., and Shorr, R. (2014). Translational assessment of mitochondrial dysfunction of pancreatic cancer from in vitro gene microarray and animal efficacy studies, to early clinical studies, via the novel tumor-specific anti-mitochondrial agent, CPI-613. Ann. Transl. Med. *2*.

Li, D., Fu, Z., Chen, R., Zhao, X., Zhou, Y., Zeng, B., Yu, M., Zhou, Q., Lin, Q., Gao, W., et al. (2015a). Inhibition of glutamine metabolism counteracts pancreatic cancer stem cell features and sensitizes cells to radiotherapy. Oncotarget *6*, 31151–31163.

Li, H.-M., Yang, J.-G., Liu, Z.-J., Wang, W.-M., Yu, Z.-L., Ren, J.-G., Chen, G., Zhang, W., and Jia, J. (2017). Blockage of glycolysis by targeting PFKFB3 suppresses tumor growth and metastasis in head and neck squamous cell carcinoma. J. Exp. Clin. Cancer Res. CR *36*.

Li, J., Csibi, A., Yang, S., Hoffman, G.R., Li, C., Zhang, E., Yu, J.J., and Blenis, J. (2015b). Synthetic lethality of combined glutaminase and Hsp90 inhibition in mTORC1-driven tumor cells. Proc. Natl. Acad. Sci. U. S. A. *112*, E21–E29.

Li, W., Saud, S.M., Young, M.R., Chen, G., and Hua, B. (2015c). Targeting AMPK for cancer prevention and treatment. Oncotarget *6*, 7365–7378.

Liebler, D.C., and Ham, A.-J.L. (2009). Spin filter-based sample preparation for shotgun proteomics. Nat. Methods *6*, 785; author reply 785-786.

Lincet, H., and Icard, P. (2015). How do glycolytic enzymes favour cancer cell proliferation by nonmetabolic functions? Oncogene *34*, 3751–3759.

Llovet, J.M., Ricci, S., Mazzaferro, V., Hilgard, P., Gane, E., Blanc, J.-F., de Oliveira, A.C., Santoro, A., Raoul, J.-L., Forner, A., et al. (2008). Sorafenib in Advanced Hepatocellular Carcinoma. N. Engl. J. Med. *359*, 378–390.

Locasale, J.W. (2013). Serine, glycine and the one-carbon cycle: cancer metabolism in full circle. Nat. Rev. Cancer *13*, 572–583.

Lu, J., Tan, M., and Cai, Q. (2015). The Warburg effect in tumor progression: mitochondrial oxidative metabolism as an anti-metastasis mechanism. Cancer Lett. *356*, 156–164.

Lycan, T.W., Pardee, T.S., Petty, W.J., Bonomi, M., Alistar, A., Lamar, Z.S., Isom, S., Chan, M.D., Miller, A.A., and Ruiz, J. (2016). A Phase II Clinical Trial of CPI-613 in Patients with Relapsed or Refractory Small Cell Lung Carcinoma. PloS One *11*, e0164244.

Mackey, J.R., Mani, R.S., Selner, M., Mowles, D., Young, J.D., Belt, J.A., Crawford, C.R., and Cass, C.E. (1998). Functional Nucleoside Transporters Are Required for Gemcitabine Influx and Manifestation of Toxicity in Cancer Cell Lines. Cancer Res. *58*, 4349–4357.

Mackey, J.R., Yao, S.Y., Smith, K.M., Karpinski, E., Baldwin, S.A., Cass, C.E., and Young, J.D. (1999). Gemcitabine transport in xenopus oocytes expressing recombinant plasma membrane mammalian nucleoside transporters. J. Natl. Cancer Inst. *91*, 1876–1881.

Mailloux, R.J., Craig Ayre, D., and Christian, S.L. (2016). Induction of mitochondrial reactive oxygen species production by GSH mediated S-glutathionylation of 2-oxoglutarate dehydrogenase. Redox Biol. *8*, 285–297.

Maksimenko, A., Caron, J., Mougin, J., Desmaële, D., and Couvreur, P. (2015). Gemcitabine-based therapy for pancreatic cancer using the squalenoyl nucleoside monophosphate nanoassemblies. Int. J. Pharm. *482*, 38–46.

Marchiq, I., and Pouysségur, J. (2016). Hypoxia, cancer metabolism and the therapeutic benefit of targeting lactate/H(+) symporters. J. Mol. Med. Berl. Ger. *94*, 155–171.

Marcondes, M.C., Sola-Penna, M., and Zancan, P. (2010). Clotrimazole potentiates the inhibitory effects of ATP on the key glycolytic enzyme 6-phosphofructo-1-kinase. Arch. Biochem. Biophys. *497*, 62–67.

Maréchal, R., Mackey, J.R., Lai, R., Demetter, P., Peeters, M., Polus, M., Cass, C.E., Salmon, I., Devière, J., and Van Laethem, J.-L. (2010). Deoxycitidine kinase is associated with prolonged survival after adjuvant gemcitabine for resected pancreatic adenocarcinoma. Cancer *116*, 5200–5206.

Maréchal, R., Bachet, J.-B., Mackey, J.R., Dalban, C., Demetter, P., Graham, K., Couvelard, A., Svrcek, M., Bardier-Dupas, A., Hammel, P., et al. (2012). Levels of gemcitabine transport and metabolism proteins predict survival times of patients treated with gemcitabine for pancreatic adenocarcinoma. Gastroenterology *143*, 664-674.e6.

Marinho-Carvalho, M.M., Costa-Mattos, P.V., Spitz, G.A., Zancan, P., and Sola-Penna, M. (2009). Calmodulin upregulates skeletal muscle 6-phosphofructo-1-kinase reversing the inhibitory effects of allosteric modulators. Biochim. Biophys. Acta *1794*, 1175–1180.

Martinez-Outschoorn, U.E., Peiris-Pagés, M., Pestell, R.G., Sotgia, F., and Lisanti, M.P. (2017). Cancer metabolism: a therapeutic perspective. Nat. Rev. Clin. Oncol. *14*, 11–31.

Martínez-Reyes, I., Diebold, L.P., Kong, H., Schieber, M., Huang, H., Hensley, C.T., Mehta, M.M., Wang, T., Santos, J.H., Woychik, R., et al. (2016). TCA Cycle and Mitochondrial Membrane Potential Are Necessary for Diverse Biological Functions. Mol. Cell *61*, 199–209.

Martinez-Useros, J., Li, W., Cabeza-Morales, M., and Garcia-Foncillas, J. (2017). Oxidative Stress: A New Target for Pancreatic Cancer Prognosis and Treatment. J. Clin. Med. *6*.

McGuigan, C., Habib, N.A., Wasan, H.S., Gabra, H., Jiao, L.R., Slusarczyk, M., Chabot, J.A., and Saif, M.W. (2011). A phosphoramidate ProTide (NUC-1031) and acquired and intrinsic resistance to gemcitabine. J. Clin. Oncol. *29*, e13540–e13540.

McLain, A.L., Szweda, P.A., and Szweda, L.I. (2011). α-Ketoglutarate dehydrogenase: A mitochondrial redox sensor. Free Radic. Res. *45*, 29–36.

Medina, R.A., and Owen, G.I. (2002). Glucose transporters: expression, regulation and cancer. Biol. Res. *35*, 9–26.

Metallo, C.M., Gameiro, P.A., Bell, E.L., Mattaini, K.R., Yang, J., Hiller, K., Jewell, C.M., Johnson, Z.R., Irvine, D.J., Guarente, L., et al. (2011). Reductive glutamine metabolism by IDH1 mediates lipogenesis under hypoxia. Nature *481*, 380–384.

Mignini, F., Nasuti, C., Fedeli, D., Mattioli, L., Cosenza, M., Artico, M., and Gabbianelli, R. (2013). Protective effect of alpha-lipoic acid on cypermethrin-induced oxidative stress in Wistar rats. Int. J. Immunopathol. Pharmacol. *26*, 871–881.

Mihailidou, C., Papakotoulas, P., Papavassiliou, A.G., and Karamouzis, M.V. (2017). Superior efficacy of the antifungal agent ciclopirox olamine over gemcitabine in pancreatic cancer models. Oncotarget *9*, 10360–10374.

Miller, D.W., Fontain, M., Kolar, C., and Lawson, T. (1996). The expression of multidrug resistance-associated protein (MRP) in pancreatic adenocarcinoma cell lines. Cancer Lett. *107*, 301–306.

Minchenko, O.H., Tsuchihara, K., Minchenko, D.O., Bikfalvi, A., and Esumi, H. (2014). Mechanisms of regulation of PFKFB expression in pancreatic and gastric cancer cells. World J. Gastroenterol. *20*, 13705–13717.

Mislang, A.R., Di Donato, S., Hubbard, J., Krishna, L., Mottino, G., Bozzetti, F., and Biganzoli, L. (2018). Nutritional management of older adults with gastrointestinal cancers: An International Society of Geriatric Oncology (SIOG) review paper. J. Geriatr. Oncol. *9*, 382–392.

Misra, S., Ghatak, S., and Toole, B.P. (2005). Regulation of MDR1 Expression and Drug Resistance by a Positive Feedback Loop Involving Hyaluronan, Phosphoinositide 3-Kinase, and ErbB2. J. Biol. Chem. *280*, 20310–20315.

Mookerjee, S.A., Nicholls, D.G., and Brand, M.D. (2016). Determining Maximum Glycolytic Capacity Using Extracellular Flux Measurements. PLoS ONE *11*.

Mor, I., Cheung, E.C., and Vousden, K.H. (2011). Control of glycolysis through regulation of PFK1: old friends and recent additions. Cold Spring Harb. Symp. Quant. Biol. *76*, 211–216.

Morinaga, S., Nakamura, Y., Watanabe, T., Mikayama, H., Tamagawa, H., Yamamoto, N., Shiozawa, M., Akaike, M., Ohkawa, S., Kameda, Y., et al. (2012). Immunohistochemical Analysis of Human Equilibrative Nucleoside Transporter-1 (hENT1) Predicts Survival in Resected Pancreatic Cancer Patients Treated with Adjuvant Gemcitabine Monotherapy. Ann. Surg. Oncol. *19*, 558–564.

Morris, J.P., Wang, S.C., and Hebrok, M. (2010). KRAS, Hedgehog, Wnt and the twisted developmental biology of pancreatic ductal adenocarcinoma. Nat. Rev. Cancer *10*, 683–695.

Morris, T.W., Reed, K.E., and Cronan, J.E. (1994). Identification of the gene encoding lipoate-protein ligase A of Escherichia coli. Molecular cloning and characterization of the lplA gene and gene product. J. Biol. Chem. *269*, 16091–16100.

Moungjaroen, J., Nimmannit, U., Callery, P.S., Wang, L., Azad, N., Lipipun, V., Chanvorachote, P., and Rojanasakul, Y. (2006). Reactive oxygen species mediate caspase activation and apoptosis induced by lipoic acid in human lung epithelial cancer cells through Bcl-2 down-regulation. J. Pharmacol. Exp. Ther. *319*, 1062–1069.

Moysan, E., Bastiat, G., and Benoit, J.-P. (2013). Gemcitabine versus Modified Gemcitabine: A Review of Several Promising Chemical Modifications. Mol. Pharm. *10*, 430–444.

Mullen, A.R., Wheaton, W.W., Jin, E.S., Chen, P.-H., Sullivan, L.B., Cheng, T., Yang, Y., Linehan, W.M., Chandel, N.S., and DeBerardinis, R.J. (2011). Reductive carboxylation supports growth in tumour cells with defective mitochondria. Nature *481*, 385–388.

Mullen, A.R., Hu, Z., Shi, X., Jiang, L., Boroughs, L.K., Kovacs, Z., Boriack, R., Rakheja, D., Sullivan, L.B., Linehan, W.M., et al. (2014). Oxidation of alpha-ketoglutarate is required for reductive carboxylation in cancer cells with mitochondrial defects. Cell Rep. *7*, 1679–1690.

Murphy, A.M., Besmer, D.M., Moerdyk-Schauwecker, M., Moestl, N., Ornelles, D.A., Mukherjee, P., and Grdzelishvili, V.Z. (2012). Vesicular Stomatitis Virus as an Oncolytic Agent against Pancreatic Ductal Adenocarcinoma. J. Virol. *86*, 3073–3087.

Nakahira, S., Nakamori, S., Tsujie, M., Takahashi, Y., Okami, J., Yoshioka, S., Yamasaki, M., Marubashi, S., Takemasa, I., Miyamoto, A., et al. (2007). Involvement of ribonucleotide reductase M1 subunit overexpression in gemcitabine resistance of human pancreatic cancer. Int. J. Cancer *120*, 1355–1363.

Nakano, K., and Vousden, K.H. (2001). PUMA, a novel proapoptotic gene, is induced by p53. Mol. Cell *7*, 683–694.

Nakano, Y., Tanno, S., Koizumi, K., Nishikawa, T., Nakamura, K., Minoguchi, M., Izawa, T., Mizukami, Y., Okumura, T., and Kohgo, Y. (2007). Gemcitabine chemoresistance and molecular markers associated with gemcitabine transport and metabolism in human pancreatic cancer cells. Br. J. Cancer *96*, 457–463.

Nath, S., Daneshvar, K., Roy, L.D., Grover, P., Kidiyoor, A., Mosley, L., Sahraei, M., and Mukherjee, P. (2013). MUC1 induces drug resistance in pancreatic cancer cells via upregulation of multidrug resistance genes. Oncogenesis *2*, e51.

Neesse, A., Michl, P., Frese, K.K., Feig, C., Cook, N., Jacobetz, M.A., Lolkema, M.P., Buchholz, M., Olive, K.P., Gress, T.M., et al. (2011). Stromal biology and therapy in pancreatic cancer. Gut *60*, 861–868.

Nielsen, M.F.B., Mortensen, M.B., and Detlefsen, S. (2016). Key players in pancreatic cancer-stroma interaction: Cancer-associated fibroblasts, endothelial and inflammatory cells. World J. Gastroenterol. *22*, 2678–2700.

Nomme, J., Murphy, J.M., Su, Y., Sansone, N.D., Armijo, A.L., Olson, S.T., Radu, C., and Lavie, A. (2013). Structural characterization of new deoxycytidine kinase inhibitors rationalizes the affinity-determining moieties of the molecules. Acta Crystallogr. D Biol. Crystallogr. *70*, 68–78.

Ogawa, M., Hori, H., Ohta, T., Onozato, K., Miyahara, M., and Komada, Y. (2005). Sensitivity to gemcitabine and its metabolizing enzymes in neuroblastoma. Clin. Cancer Res. Off. J. Am. Assoc. Cancer Res. *11*, 3485–3493.

Ohhashi, S., Ohuchida, K., Mizumoto, K., Fujita, H., Egami, T., Yu, J., Toma, H., Sadatomi, S., Nagai, E., and Tanaka, M. (2008). Down-regulation of Deoxycytidine Kinase Enhances Acquired Resistance to Gemcitabine in Pancreatic Cancer. Anticancer Res. *28*, 2205–2212.

Oldfield, L.E., Connor, A.A., and Gallinger, S. (2017). Molecular Events in the Natural History of Pancreatic Cancer. Trends Cancer *3*, 336–346.

Ooi, A.T., and Gomperts, B.N. (2015). Molecular Pathways: Targeting Cellular Energy Metabolism in Cancer via Inhibition of SLC2A1 and LDHA. Clin. Cancer Res. Off. J. Am. Assoc. Cancer Res. *21*, 2440–2444.

Osthus, R.C., Shim, H., Kim, S., Li, Q., Reddy, R., Mukherjee, M., Xu, Y., Wonsey, D., Lee, L.A., and Dang, C.V. (2000). Deregulation of Glucose Transporter 1 and Glycolytic Gene Expression by c-Myc. J. Biol. Chem. *275*, 21797–21800.

Pardee, T.S., Lee, K., Luddy, J., Maturo, C., Rodriguez, R., Isom, S., Miller, L.D., Stadelman, K.M., Levitan, D., Hurd, D., et al. (2014a). A Phase I Study of the First-in-Class Anti-Mitochondrial Metabolism Agent, CPI-613, in Patients with Advanced Hematologic Malignancies. Clin. Cancer Res. Off. J. Am. Assoc. Cancer Res. *20*, 5255–5264.

Pardee, T.S., Lee, K., Luddy, J., Maturo, C., Rodriguez, R., Isom, S., Miller, L.D., Stadelman, K.M., Levitan, D., Hurd, D., et al. (2014b). A Phase I Study of the First-in-Class Anti-Mitochondrial Metabolism Agent, CPI-613, in Patients with Advanced Hematologic Malignancies. Clin. Cancer Res. Off. J. Am. Assoc. Cancer Res. *20*, 5255–5264.

Paredes, F., Sheldon, K., Lassègue, B., Williams, H.C., Faidley, E.A., Benavides, G.A., Torres, G., Sanhueza-Olivares, F., Yeligar, S.M., Griendling, K.K., et al. (2018). Poldip2 is an oxygen-sensitive protein that controls PDH and αKGDH lipoylation and activation to support metabolic adaptation in hypoxia and cancer. Proc. Natl. Acad. Sci. *115*, 1789–1794.

Park, K.-G., Min, A.-K., Koh, E.H., Kim, H.S., Kim, M.-O., Park, H.-S., Kim, Y.-D., Yoon, T.-S., Jang, B.K., Hwang, J.S., et al. (2008). Alpha-lipoic acid decreases hepatic lipogenesis through adenosine monophosphate-activated protein kinase (AMPK)-dependent and AMPK-independent pathways. Hepatol. Baltim. Md *48*, 1477–1486.

Patel, M.S., and Roche, T.E. (1990). Molecular biology and biochemistry of pyruvate dehydrogenase complexes. FASEB J. Off. Publ. Fed. Am. Soc. Exp. Biol. *4*, 3224–3233.

Patra, K.C., Bardeesy, N., and Mizukami, Y. (2017). Diversity of Precursor Lesions For Pancreatic Cancer: The Genetics and Biology of Intraductal Papillary Mucinous Neoplasm. Clin. Transl. Gastroenterol. *8*, e86.

Pavlova, N.N., and Thompson, C.B. (2016). THE EMERGING HALLMARKS OF CANCER METABOLISM. Cell Metab. *23*, 27–47.

Pickin, K.A., Alexander, R.L., Morrow, C.S., Morris-Natschke, S.L., Ishaq, K.S., Fleming, R.A., and Kucera, G.L. (2009). Phospholipid/deoxycytidine analogue prodrugs for the treatment of cancer. J. Drug Deliv. Sci. Technol. *19*, 31–36.

Pietrocola, F., Galluzzi, L., Bravo-San Pedro, J.M., Madeo, F., and Kroemer, G. (2015). Acetyl coenzyme A: a central metabolite and second messenger. Cell Metab. *21*, 805–821.

Pompella, A., Visvikis, A., Paolicchi, A., De Tata, V., and Casini, A.F. (2003). The changing faces of glutathione, a cellular protagonist. Biochem. Pharmacol. *66*, 1499–1503.

Poplin, E., Wasan, H., Rolfe, L., Raponi, M., Ikdahl, T., Bondarenko, I., Davidenko, I., Bondar, V., Garin, A., Boeck, S., et al. (2013). Randomized, Multicenter, Phase II Study of CO-101 Versus Gemcitabine in Patients With Metastatic Pancreatic Ductal Adenocarcinoma: Including a Prospective Evaluation of the Role of hENT1 in Gemcitabine or CO-101 Sensitivity. J. Clin. Oncol. *31*, 4453–4461.

Pradelli, L.A., Villa, E., Zunino, B., Marchetti, S., and Ricci, J.-E. (2014). Glucose metabolism is inhibited by caspases upon the induction of apoptosis. Cell Death Dis. *5*, e1406.

Qin, T., Jelinek, J., Si, J., Shu, J., and Issa, J.-P.J. (2009). Mechanisms of resistance to 5-aza-2′-deoxycytidine in human cancer cell lines. Blood *113*, 659–667.

Rahib, L., Smith, B.D., Aizenberg, R., Rosenzweig, A.B., Fleshman, J.M., and Matrisian, L.M. (2014). Projecting Cancer Incidence and Deaths to 2030: The Unexpected Burden of Thyroid, Liver, and Pancreas Cancers in the United States. Cancer Res. *74*, 2913–2921.

Rao, C.V., Asch, A.S., and Yamada, H.Y. (2017). Frequently mutated genes/pathways and genomic instability as prevention targets in liver cancer. Carcinogenesis *38*, 2–11.

Reed, L.J., and Hackert, M.L. (1990). Structure-function relationships in dihydrolipoamide acyltransferases. J. Biol. Chem. *265*, 8971–8974.

Reinhart, G.D., and Lardy, H.A. (1980). Rat liver phosphofructokinase: kinetic activity under near-physiological conditions. Biochemistry *19*, 1477–1484.

Réjiba, S., Reddy, L.H., Bigand, C., Parmentier, C., Couvreur, P., and Hajri, A. (2011). Squalenoyl gemcitabine nanomedicine overcomes the low efficacy of gemcitabine therapy in pancreatic cancer. Nanomedicine Nanotechnol. Biol. Med. *7*, 841–849.

Richards, N.G., Rittenhouse, D.W., Freydin, B., Cozzitorto, J.A., Grenda, D., Rui, H., Gonye, G., Kennedy, E.P., Yeo, C.J., Brody, J.R., et al. (2010). HuR status is a powerful marker for prognosis and response to gemcitabine-based chemotherapy for resected pancreatic ductal adenocarcinoma patients. Ann. Surg. *252*, 499–505; discussion 505-506.

Roche, T.E., and Hiromasa, Y. (2007). Pyruvate dehydrogenase kinase regulatory mechanisms and inhibition in treating diabetes, heart ischemia, and cancer. Cell. Mol. Life Sci. *64*, 830.

Roche, T.E., Baker, J.C., Yan, X., Hiromasa, Y., Gong, X., Peng, T., Dong, J., Turkan, A., and Kasten, S.A. (2001). Distinct regulatory properties of pyruvate dehydrogenase kinase and phosphatase isoforms. In Progress in Nucleic Acid Research and Molecular Biology, (Academic Press), pp. 33–75.

Roth, M.T., and Berlin, J.D. (2018). Current Concepts in the Treatment of Resectable Pancreatic Cancer. Curr. Oncol. Rep. *20*, 39.

Roy, K., Wu, Y., Meitzler, J.L., Juhasz, A., Liu, H., Jiang, G., Lu, J., Antony, S., and Doroshow, J.H. (2015). NADPH oxidases and cancer. Clin. Sci. Lond. Engl. 1979 *128*, 863–875.

Ruiz van Haperen, V.W.T., Veerman, G., Vermorken, J.B., Pinedo, H.M., and Peters, G.J. (1996). Regulation of phosphorylation of deoxycytidine and 2′,2′-difluorodeoxycytidine (gemcitabine); effects of cytidine 5′-triphosphate and uridine 5′-triphosphate in relation to chemosensitivity for 2′,2′-difluorodeoxycytidine. Biochem. Pharmacol. *51*, 911–918.

Saiki, Y., Yoshino, Y., Fujimura, H., Manabe, T., Kudo, Y., Shimada, M., Mano, N., Nakano, T., Lee, Y., Shimizu, S., et al. (2012). DCK is frequently inactivated in acquired gemcitabine-resistant human cancer cells. Biochem. Biophys. Res. Commun. *421*, 98–104.

Samulitis, B.K., Pond, K.W., Pond, E., Cress, A.E., Patel, H., Wisner, L., Patel, C., Dorr, R.T., and Landowski, T.H. (2014). Gemcitabine resistant pancreatic cancer cell lines acquire an invasive phenotype with collateral hypersensitivity to histone deacetylase inhibitors. Cancer Biol. Ther. *16*, 43–51.

Sausen, M., Phallen, J., Adleff, V., Jones, S., Leary, R.J., Barrett, M.T., Anagnostou, V., Parpart-Li, S., Murphy, D., Li, Q.K., et al. (2015). Clinical implications of genomic alterations in the tumour and circulation of pancreatic cancer patients. Nat. Commun. *6*, 7686.

Scarbrough, P.M., Mapuskar, K.A., Mattson, D.M., Gius, D., Watson, W.H., and Spitz, D.R. (2012). Simultaneous inhibition of glutathione- and thioredoxin-dependent metabolism is necessary to potentiate 17AAG-induced cancer cell killing via oxidative stress. Free Radic. Biol. Med. *52*, 436–443.

Schafer, F.Q., and Buettner, G.R. (2001). Redox environment of the cell as viewed through the redox state of the glutathione disulfide/glutathione couple. Free Radic. Biol. Med. *30*, 1191–1212.

Schafer, Z.T., Grassian, A.R., Song, L., Jiang, Z., Gerhart-Hines, Z., Irie, H.Y., Gao, S., Puigserver, P., and Brugge, J.S. (2009). Antioxidant and Oncogene Rescue of Metabolic Defects Caused by Loss of Matrix Attachment. Nature *461*, 109–113.

Schniewind, B., Christgen, M., Kurdow, R., Haye, S., Kremer, B., Kalthoff, H., and Ungefroren, H. (2004). Resistance of pancreatic cancer to gemcitabine treatment is dependent on mitochondria-mediated apoptosis. Int. J. Cancer *109*, 182–188.

Schöneberg, T., Kloos, M., Brüser, A., Kirchberger, J., and Sträter, N. (2013). Structure and allosteric regulation of eukaryotic 6-phosphofructokinases. Biol. Chem. *394*, 977–993.

Schulze, A., and Harris, A.L. (2012). How cancer metabolism is tuned for proliferation and vulnerable to disruption. Nature *491*, 364–373.

Sebastiani, V., Ricci, F., Rubio-Viquiera, B., Kulesza, P., Yeo, C.J., Hidalgo, M., Klein, A., Laheru, D., and Iacobuzio-Donahue, C.A. (2006). Immunohistochemical and Genetic Evaluation of Deoxycytidine Kinase in Pancreatic Cancer: Relationship to Molecular Mechanisms of Gemcitabine Resistance and Survival. Clin. Cancer Res. Off. J. Am. Assoc. Cancer Res. *12*, 2492–2497.

Sen, C.K., Sashwati, R., and Packer, L. (1999). Fas mediated apoptosis of human Jurkat T-cells: intracellular events and potentiation by redox-active alpha-lipoic acid. Cell Death Differ. *6*, 481–491.

Shang, Q.-Y., Wu, C.-S., and Gao, H.-R. (2017a). Effects of DCK knockdown on proliferation, apoptosis and tumorigenicity *in vivo* of cervical cancer HeLa cells. Cancer Gene Ther. *24*, 367–372.

Shang, Q.-Y., Wu, C.-S., and Gao, H.-R. (2017b). Effects of DCK knockdown on proliferation, apoptosis and tumorigenicity in vivo of cervical cancer HeLa cells. Cancer Gene Ther. *24*, 367–372.

Sherrod, A.M., Brufsky, A., and Puhalla, S. (2011). A Case of Late-Onset Gemcitabine Lung Toxicity. Clin. Med. Insights Oncol. *5*, 171–176.

Shi, H., Zhang, C.-J., Chen, G.Y.J., and Yao, S.Q. (2012). Cell-Based Proteome Profiling of Potential Dasatinib Targets by Use of Affinity-Based Probes. J. Am. Chem. Soc. *134*, 3001–3014.

Shipley, L.A., Brown, T.J., Cornpropst, J.D., Hamilton, M., Daniels, W.D., and Culp, H.W. (1992). Metabolism and disposition of gemcitabine, and oncolytic deoxycytidine analog, in mice, rats, and dogs. Drug Metab. Dispos. *20*, 849–855.

Siegel, R., Ma, J., Zou, Z., and Jemal, A. (2014). Cancer statistics, 2014. CA. Cancer J. Clin. *64*, 9–29.

Siegel, R.L., Miller, K.D., and Jemal, A. (2015). Cancer statistics, 2015. CA. Cancer J. Clin. *65*, 5–29.

Siegel, R.L., Miller, K.D., and Jemal, A. (2017). Cancer Statistics, 2017. CA. Cancer J. Clin. *67*, 7–30.

Sies, H. (1999). Glutathione and its role in cellular functions. Free Radic. Biol. Med. *27*, 916–921.

Simbula, G., Columbano, A., Ledda-Columbano, G.M., Sanna, L., Deidda, M., Diana, A., and Pibiri, M. (2007). Increased ROS generation and p53 activation in alpha-lipoic acid-induced apoptosis of hepatoma cells. Apoptosis Int. J. Program. Cell Death *12*, 113–123.

Slusarczyk, M., Lopez, M.H., Balzarini, J., Mason, M., Jiang, W.G., Blagden, S., Thompson, E., Ghazaly, E., and McGuigan, C. (2014). Application of ProTide Technology to Gemcitabine: A Successful Approach to Overcome the Key Cancer Resistance Mechanisms Leads to a New Agent (NUC-1031) in Clinical Development. J. Med. Chem. *57*, 1531–1542.

Sols, A. (1981). Multimodulation of Enzyme Activity. In Current Topics in Cellular Regulation, B.L. Horecker, and E.R. Stadtman, eds. (Academic Press), pp. 77–101.

Son, J., Lyssiotis, C.A., Ying, H., Wang, X., Hua, S., Ligorio, M., Perera, R.M., Ferrone, C.R., Mullarky, E., Shyh-Chang, N., et al. (2013). Glutamine supports pancreatic cancer growth through a KRAS-regulated metabolic pathway. Nature *496*, 101–105.

Song, X., Lorenzi, P.L., Landowski, C.P., Vig, B.S., Hilfinger, J.M., and Amidon, G.L. (2005). Amino Acid Ester Prodrugs of the Anticancer Agent Gemcitabine: Synthesis, Bioconversion, Metabolic Bioevasion, and hPEPT1-Mediated Transport. Mol. Pharm. *2*, 157–167.

Sonveaux, P., Végran, F., Schroeder, T., Wergin, M.C., Verrax, J., Rabbani, Z.N., De Saedeleer, C.J., Kennedy, K.M., Diepart, C., Jordan, B.F., et al. (2008). Targeting lactate-fueled respiration selectively kills hypoxic tumor cells in mice. J. Clin. Invest. *118*, 3930–3942.

Soreze, Y., Boutron, A., Habarou, F., Barnerias, C., Nonnenmacher, L., Delpech, H., Mamoune, A., Chrétien, D., Hubert, L., Bole-Feysot, C., et al. (2013). Mutations in human lipoyltransferase gene LIPT1 cause a Leigh disease with secondary deficiency for pyruvate and alpha-ketoglutarate dehydrogenase. Orphanet J. Rare Dis. *8*, 192.

de Sousa Cavalcante, L., and Monteiro, G. (2014). Gemcitabine: Metabolism and molecular mechanisms of action, sensitivity and chemoresistance in pancreatic cancer. Eur. J. Pharmacol. *741*, 8–16.

Spratlin, J., Sangha, R., Glubrecht, D., Dabbagh, L., Young, J.D., Dumontet, C., Cass, C., Lai, R., and Mackey, J.R. (2004). The absence of human equilibrative nucleoside transporter 1 is associated with reduced survival in patients with gemcitabine-treated pancreas adenocarcinoma. Clin. Cancer Res. Off. J. Am. Assoc. Cancer Res. *10*, 6956–6961.

Starkov, A.A., Fiskum, G., Chinopoulos, C., Lorenzo, B.J., Browne, S.E., Patel, M.S., and Beal, M.F. (2004). Mitochondrial alpha-ketoglutarate dehydrogenase complex generates reactive oxygen species. J. Neurosci. Off. J. Soc. Neurosci. *24*, 7779–7788.

Stathis, A., and Moore, M.J. (2010). Advanced pancreatic carcinoma: current treatment and future challenges. Nat. Rev. Clin. Oncol. *7*, 163–172.

Stincone, A., Prigione, A., Cramer, T., Wamelink, M.M.C., Campbell, K., Cheung, E., Olin-Sandoval, V., Grüning, N.-M., Krüger, A., Tauqeer Alam, M., et al. (2015). The return of metabolism: biochemistry and physiology of the pentose phosphate pathway. Biol. Rev. Camb. Philos. Soc. *90*, 927–963.

Stromnes, I.M., DelGiorno, K.E., Greenberg, P.D., and Hingorani, S.R. (2014). Stromal reengineering to treat pancreas cancer. Carcinogenesis *35*, 1451–1460.

Strumilo, S. (2005). Short-term regulation of the alpha-ketoglutarate dehydrogenase complex by energy-linked and some other effectors. Biochem. Biokhimiia *70*, 726–729.

Stuart, S.D., Schauble, A., Gupta, S., Kennedy, A.D., Keppler, B.R., Bingham, P.M., and Zachar, Z. (2014). A strategically designed small molecule attacks alpha-ketoglutarate dehydrogenase in tumor cells through a redox process. Cancer Metab. *2*, 4.

Stuurman, F.E., Lolkema, M.P., Huitema, A.D.R., Soetekouw, P.M.M.B., Rosing, H., Rolfe, L., Kaur, P., Beijnen, J.H., van Tinteren, H., Voest, E.E., et al. (2013). A phase 1 comparative pharmacokinetic and cardiac safety study of two intravenous formulations of CO-101 in patients with advanced solid tumors. J. Clin. Pharmacol. *53*, 878–883.

Su, G., Burant, C.F., Beecher, C.W., Athey, B.D., and Meng, F. (2011). Integrated metabolome and transcriptome analysis of the NCI60 dataset. BMC Bioinformatics *12 Suppl 1*, S36.

Sultana, A., Smith, C.T., Cunningham, D., Starling, N., Neoptolemos, J.P., and Ghaneh, P. (2007). Meta-Analyses of Chemotherapy for Locally Advanced and Metastatic Pancreatic Cancer. J. Clin. Oncol. *25*, 2607–2615.

Sun, R.C., and Denko, N.C. (2014). Hypoxic regulation of glutamine metabolism through HIF1 and SIAH2 supports lipid synthesis that is necessary for tumor growth. Cell Metab. *19*, 285–292.

Sun, C., Zhang, H., Ma, X., Zhou, X., Gan, L., Liu, Y., and Wang, Z. (2013). Isoliquiritigenin Enhances Radiosensitivity of HepG2 Cells via Disturbance of Redox Status. Cell Biochem. Biophys. *65*, 433–444.

Szucs, Z., and Jones, R.L. (2018). Perspectives on the evolving state of the art management of gastrointestinal stromal tumours. Transl. Gastroenterol. Hepatol. *3*.

Tedeschi, P.M., Markert, E.K., Gounder, M., Lin, H., Dvorzhinski, D., Dolfi, S.C., Chan, L.L.-Y., Qiu, J., DiPaola, R.S., Hirshfield, K.M., et al. (2013). Contribution of serine, folate and glycine metabolism to the ATP, NADPH and purine requirements of cancer cells. Cell Death Dis. *4*, e877.

Teichert, J., Hermann, R., Ruus, P., and Preiss, R. (2003). Plasma kinetics, metabolism, and urinary excretion of alpha-lipoic acid following oral administration in healthy volunteers. J. Clin. Pharmacol. *43*, 1257–1267.

Tejwani, G.A. (1978). The role of phosphofructokinase in the Pasteur effect. Trends Biochem. Sci. *3*, 30–33.

Telang, S., Yalcin, A., Clem, A.L., Bucala, R., Lane, A.N., Eaton, J.W., and Chesney, J. (2006). Ras transformation requires metabolic control by 6-phosphofructo-2-kinase. Oncogene *25*, 7225–7234.

The Lancet (2011). Pancreatic cancer in the UK. The Lancet *378*, 1050.

Tibaldi, C., Giovannetti, E., Tiseo, M., Leon, L.G., D'Incecco, A., Loosekoot, N., Bartolotti, M., Honeywell, R., Cappuzzo, F., Ardizzoni, A., et al. (2012). Correlation of cytidine deaminase polymorphisms and activity with clinical outcome in gemcitabine-/platinum-treated advanced non-small-cell lung cancer patients. Ann. Oncol. Off. J. Eur. Soc. Med. Oncol. *23*, 670–677.

Torre, L.A., Bray, F., Siegel, R.L., Ferlay, J., Lortet-Tieulent, J., and Jemal, A. (2015). Global cancer statistics, 2012. CA. Cancer J. Clin. *65*, 87–108.

Tort, F., Ferrer-Cortès, X., Thió, M., Navarro-Sastre, A., Matalonga, L., Quintana, E., Bujan, N., Arias, A., García-Villoria, J., Acquaviva, C., et al. (2014). Mutations in the lipoyltransferase LIPT1 gene cause a fatal disease associated with a specific lipoylation defect of the 2-ketoacid dehydrogenase complexes. Hum. Mol. Genet. *23*, 1907–1915.

Toy, G., Austin, W.R., Liao, H.-I., Cheng, D., Singh, A., Campbell, D.O., Ishikawa, T., Lehmann, L.W., Satyamurthy, N., Phelps, M.E., et al. (2010). Requirement for deoxycytidine kinase in T and B lymphocyte development. Proc. Natl. Acad. Sci. U. S. A. *107*, 5551–5556.

Trachootham, D., Alexandre, J., and Huang, P. (2009). Targeting cancer cells by ROS-mediated mechanisms: a radical therapeutic approach? Nat. Rev. Drug Discov. *8*, 579–591.

Trivedi, P.P., and Jena, G.B. (2013). Role of α-lipoic acid in dextran sulfate sodium-induced ulcerative colitis in mice: studies on inflammation, oxidative stress, DNA damage and fibrosis. Food Chem. Toxicol. Int. J. Publ. Br. Ind. Biol. Res. Assoc. *59*, 339–355.

Uccello, M., Moschetta, M., Mak, G., Alam, T., Henriquez, C.M., and Arkenau, H.-T. (2018). Towards an optimal treatment algorithm for metastatic pancreatic ductal adenocarcinoma (PDA). Curr. Oncol. *25*, e90–e94.

Usenik, A., and Legiša, M. (2010). Evolution of Allosteric Citrate Binding Sites on 6-phosphofructo-1-kinase. PLOS ONE *5*, e15447.

Van Schaftingen, E., Lederer, B., Bartrons, R., and Hers, H.G. (1982). A kinetic study of pyrophosphate: fructose-6-phosphate phosphotransferase from potato tubers. Application to a microassay of fructose 2,6-bisphosphate. Eur. J. Biochem. *129*, 191–195.

Vander Heiden, M.G., Cantley, L.C., and Thompson, C.B. (2009). Understanding the Warburg effect: the metabolic requirements of cell proliferation. Science *324*, 1029–1033.

Vaquero, E.C., Edderkaoui, M., Pandol, S.J., Gukovsky, I., and Gukovskaya, A.S. (2004). Reactive oxygen species produced by NAD(P)H oxidase inhibit apoptosis in pancreatic cancer cells. J. Biol. Chem. *279*, 34643–34654.

Vatrinet, R., Leone, G., De Luise, M., Girolimetti, G., Vidone, M., Gasparre, G., and Porcelli, A.M. (2017a). The α-ketoglutarate dehydrogenase complex in cancer metabolic plasticity. Cancer Metab. *5*.

Vatrinet, R., Leone, G., De Luise, M., Girolimetti, G., Vidone, M., Gasparre, G., and Porcelli, A.M. (2017b). The α-ketoglutarate dehydrogenase complex in cancer metabolic plasticity. Cancer Metab. *5*, 3.

Vazquez, A., Markert, E.K., and Oltvai, Z.N. (2011). Serine Biosynthesis with One Carbon Catabolism and the Glycine Cleavage System Represents a Novel Pathway for ATP Generation. PLoS ONE *6*.

Velpula, K.K., Bhasin, A., Asuthkar, S., and Tsung, A.J. (2013). Combined targeting of PDK1 and EGFR triggers regression of glioblastoma by reversing the Warburg effect. Cancer Res. *73*, 7277–7289.

Viale, A., Pettazzoni, P., Lyssiotis, C.A., Ying, H., Sánchez, N., Marchesini, M., Carugo, A., Green, T., Seth, S., Giuliani, V., et al. (2014). Oncogene ablation-resistant pancreatic cancer cells depend on mitochondrial function. Nature *514*, 628–632.

Von Hoff, D.D., Ervin, T., Arena, F.P., Chiorean, E.G., Infante, J., Moore, M., Seay, T., Tjulandin, S.A., Ma, W.W., Saleh, M.N., et al. (2013). Increased survival in pancreatic cancer with nab-paclitaxel plus gemcitabine. N. Engl. J. Med. *369*, 1691–1703.

Vora, S., Oskam, R., and Staal, G.E. (1985). Isoenzymes of phosphofructokinase in the rat. Demonstration of the three non-identical subunits by biochemical, immunochemical and kinetic studies. Biochem. J. *229*, 333–341.

Vyas, S., Zaganjor, E., and Haigis, M.C. (2016). Mitochondria and Cancer. Cell *166*, 555–566.

Waddell, N., Pajic, M., Patch, A.-M., Chang, D.K., Kassahn, K.S., Bailey, P., Johns, A.L., Miller, D., Nones, K., Quek, K., et al. (2015). Whole genomes redefine the mutational landscape of pancreatic cancer. Nature *518*, 495–501.

Walker, E.J., and Ko, A.H. (2014). Beyond first-line chemotherapy for advanced pancreatic cancer: An expanding array of therapeutic options? World J. Gastroenterol. WJG *20*, 2224–2236.

Wang, Q., and Beck, W.T. (1998). Transcriptional Suppression of Multidrug Resistance-associated Protein (MRP) Gene Expression by Wild-Type p53. Cancer Res. *58*, 5762–5769.

Wang, C., Zhang, W., Fu, M., Yang, A., Huang, H., and Xie, J. (2015). Establishment of human pancreatic cancer gemcitabine-resistant cell line with ribonucleotide reductase overexpression. Oncol. Rep. *33*, 383–390.

WANG, G., XU, Z., WANG, C., YAO, F., LI, J., CHEN, C., and SUN, S. (2013). Differential phosphofructokinase-1 isoenzyme patterns associated with glycolytic efficiency in human breast cancer and paracancer tissues. Oncol. Lett. *6*, 1701–1706.

Wang, L., Meng, L., Wang, X., Ma, G., and Chen, J. (2014). Expression of RRM1 and RRM2 as a novel prognostic marker in advanced non-small cell lung cancer receiving chemotherapy. Tumour Biol. J. Int. Soc. Oncodevelopmental Biol. Med. *35*, 1899–1906.

Warburg, O. (1956). On the origin of cancer cells. Science *123*, 309–314.

Warburg, O., Wind, F., and Negelein, E. (1927). THE METABOLISM OF TUMORS IN THE BODY. J. Gen. Physiol. *8*, 519–530.

Warshaw, A.L., and Castillo, C.F. (1992). Pancreatic Carcinoma. N. Engl. J. Med. *326*, 455–465.

Waters, A.M., and Der, C.J. (2018). KRAS: The Critical Driver and Therapeutic Target for Pancreatic Cancer. Cold Spring Harb. Perspect. Med. *8*.

Watson, J. (2013). Oxidants, antioxidants and the current incurability of metastatic cancers. Open Biol. *3*, 120144.

Weinberg, F., Hamanaka, R., Wheaton, W.W., Weinberg, S., Joseph, J., Lopez, M., Kalyanaraman, B., Mutlu, G.M., Budinger, G.R.S., and Chandel, N.S. (2010). Mitochondrial

metabolism and ROS generation are essential for Kras-mediated tumorigenicity. Proc. Natl. Acad. Sci. U. S. A. *107*, 8788–8793.

Weizman, N., Krelin, Y., Shabtay-Orbach, A., Amit, M., Binenbaum, Y., Wong, R.J., and Gil, Z. (2014). Macrophages mediate gemcitabine resistance of pancreatic adenocarcinoma by upregulating cytidine deaminase. Oncogene *33*, 3812–3819.

Whitaker-Menezes, D., Martinez-Outschoorn, U.E., Flomenberg, N., Birbe, R.C., Witkiewicz, A.K., Howell, A., Pavlides, S., Tsirigos, A., Ertel, A., Pestell, R.G., et al. (2011). Hyperactivation of oxidative mitochondrial metabolism in epithelial cancer cells in situ: visualizing the therapeutic effects of metformin in tumor tissue. Cell Cycle Georget. Tex *10*, 4047–4064.

White, E. (2012). Deconvoluting the context-dependent role for autophagy in cancer. Nat. Rev. Cancer *12*, 401–410.

Williams, T.K., Costantino, C.L., Bildzukewicz, N.A., Richards, N.G., Rittenhouse, D.W., Einstein, L., Cozzitorto, J.A., Keen, J.C., Dasgupta, A., Gorospe, M., et al. (2010). pp32 (ANP32A) Expression Inhibits Pancreatic Cancer Cell Growth and Induces Gemcitabine Resistance by Disrupting HuR Binding to mRNAs. PLoS ONE *5*.

Wise, D.R., Ward, P.S., Shay, J.E.S., Cross, J.R., Gruber, J.J., Sachdeva, U.M., Platt, J.M., DeMatteo, R.G., Simon, M.C., and Thompson, C.B. (2011). Hypoxia promotes isocitrate dehydrogenase-dependent carboxylation of α-ketoglutarate to citrate to support cell growth and viability. Proc. Natl. Acad. Sci. U. S. A. *108*, 19611–19616.

Witkiewicz, A.K., McMillan, E.A., Balaji, U., Baek, G., Lin, W.-C., Mansour, J., Mollaee, M., Wagner, K.-U., Koduru, P., Yopp, A., et al. (2015). Whole-exome sequencing of pancreatic cancer defines genetic diversity and therapeutic targets. Nat. Commun. *6*.

Wu, W., Sigmond, J., Peters, G.J., and Borch, R.F. (2007). Synthesis and Biological Activity of a Gemcitabine Phosphoramidate Prodrug. J. Med. Chem. *50*, 3743–3746.

Xu, H., Faber, C., Uchiki, T., Racca, J., and Dealwis, C. (2006). Structures of eukaryotic ribonucleotide reductase I define gemcitabine diphosphate binding and subunit assembly. Proc. Natl. Acad. Sci. U. S. A. *103*, 4028–4033.

Yachida, S., Jones, S., Bozic, I., Antal, T., Leary, R., Fu, B., Kamiyama, M., Hruban, R.H., Eshleman, J.R., Nowak, M.A., et al. (2010). Distant metastasis occurs late during the genetic evolution of pancreatic cancer. Nature *467*, 1114–1117.

Yalcin, A., Clem, B.F., Imbert-Fernandez, Y., Ozcan, S.C., Peker, S., O'Neal, J., Klarer, A.C., Clem, A.L., Telang, S., and Chesney, J. (2014). 6-Phosphofructo-2-kinase (PFKFB3) promotes cell cycle progression and suppresses apoptosis via Cdk1-mediated phosphorylation of p27. Cell Death Dis. *5*, e1337.

Yamada, T., Hashida, K., Takarada-Iemata, M., Matsugo, S., and Hori, O. (2011). α-Lipoic acid (LA) enantiomers protect SH-SY5Y cells against glutathione depletion. Neurochem. Int. *59*, 1003–1009.

Yeaman, S.J. (1989). The 2-oxo acid dehydrogenase complexes: recent advances. Biochem. J. *257*, 625–632.

Yi, W., Clark, P.M., Mason, D.E., Keenan, M.C., Hill, C., Goddard, W.A., Peters, E.C., Driggers, E.M., and Hsieh-Wilson, L.C. (2012). Phosphofructokinase 1 glycosylation regulates cell growth and metabolism. Science *337*, 975–980.

Yu, X., and Li, S. (2017). Non-metabolic functions of glycolytic enzymes in tumorigenesis. Oncogene *36*, 2629–2636.

Yu, G., Liu, J., Xu, K., and Dong, J. (2015). Uncoupling protein 2 mediates resistance to gemcitabine-induced apoptosis in hepatocellular carcinoma cell lines. Biosci. Rep. *35*.

Yu, G., Wang, J., Xu, K., and Dong, J. (2016). Dynamic regulation of uncoupling protein 2 expression by microRNA-214 in hepatocellular carcinoma. Biosci. Rep. *36*.

Zachar, Z., Marecek, J., Maturo, C., Gupta, S., Stuart, S.D., Howell, K., Schauble, A., Lem, J., Piramzadian, A., Karnik, S., et al. (2011). Non-redox-active lipoate derivates disrupt cancer cell mitochondrial metabolism and are potent anticancer agents in vivo. J. Mol. Med. Berl. Ger. *89*, 1137–1148.

Zancan, P., Almeida, F.V.R., Faber-Barata, J., Dellias, J.M., and Sola-Penna, M. (2007). Fructose-2,6-bisphosphate counteracts guanidinium chloride-, thermal-, and ATP-induced dissociation of skeletal muscle key glycolytic enzyme 6-phosphofructo-1-kinase: A structural mechanism for PFK allosteric regulation. Arch. Biochem. Biophys. *467*, 275–282.

Zancan, P., Marinho-Carvalho, M.M., Faber-Barata, J., Dellias, J.M.M., and Sola-Penna, M. (2008). ATP and fructose-2,6-bisphosphate regulate skeletal muscle 6-phosphofructo-1-kinase by altering its quaternary structure. IUBMB Life *60*, 526–533.

Zeitouni, D., Pylayeva-Gupta, Y., Der, C.J., and Bryant, K.L. (2016). KRAS Mutant Pancreatic Cancer: No Lone Path to an Effective Treatment. Cancers *8*.

Zhang, C., Cao, S., Toole, B.P., and Xu, Y. (2015a). Cancer may be a pathway to cell survival under persistent hypoxia and elevated ROS: a model for solid-cancer initiation and early development. Int. J. Cancer *136*, 2001–2011.

Zhang, S.-J., Ge, Q.-F., Guo, D.-W., Hu, W.-X., and Liu, H.-Z. (2010). Synthesis and anticancer evaluation of alpha-lipoic acid derivatives. Bioorg. Med. Chem. Lett. *20*, 3078–3083.

Zhang, Y.-K., Wang, Y.-J., Gupta, P., and Chen, Z.-S. (2015b). Multidrug Resistance Proteins (MRPs) and Cancer Therapy. AAPS J. *17*, 802–812.

Zhang, Z., Duan, Q., Zhao, H., Liu, T., Wu, H., Shen, Q., Wang, C., and Yin, T. (2016). Gemcitabine treatment promotes pancreatic cancer stemness through the Nox/ROS/NF-κB/STAT3 signaling cascade. Cancer Lett. *382*, 53–63.

Zhu, W., Ye, L., Zhang, J., Yu, P., Wang, H., Ye, Z., and Tian, J. (2016). PFK15, a Small Molecule Inhibitor of PFKFB3, Induces Cell Cycle Arrest, Apoptosis and Inhibits Invasion in Gastric Cancer. PLoS ONE *11*.

Zhu, X., Shen, X., Qu, J., Straubinger, R.M., and Jusko, W.J. (2018). Proteomic Analysis of Combined Gemcitabine and Birinapant in Pancreatic Cancer Cells. Front. Pharmacol. *9*.

Ziegler, D., Hanefeld, M., Ruhnau, K.J., Mei\ner, H.P., Lobisch, M., Schütte, K., Gries, F.A., and The ALADIN Study Group (1995). Treatment of symptomatic diabetic peripheral neuropathy with the anti-oxidant α-lipoic acid. Diabetologia *38*, 1425–1433.

Zijlstra, M., Bernards, N., Hingh, I.H.J.T. de, Wouw, A.J. van de, Goey, S.H., Jacobs, E.M.G., Lemmens, V.E.P.P., and Creemers, G.-J. (2016). Does long-term survival exist in pancreatic adenocarcinoma? Acta Oncol. *55*, 259–264.

Zucman-Rossi, J., Villanueva, A., Nault, J.-C., and Llovet, J.M. (2015). Genetic Landscape and Biomarkers of Hepatocellular Carcinoma. Gastroenterology *149*, 1226-1239.e4.

Canadian Cancer Statistics Advisory Committee. *Canadian Cancer Statistics 2018.* Toronto, ON: Canadian Cancer Society; 2018. Available at: cancer.ca/Canadian-Cancer-Statistics-2018-EN (accessed February 2019).